UNIVERSIDADE ESTADUAL DE CAMPINAS
FACULDADE DE ODONTOLOGIA DE PIRACICABA

JAIRO MATOZINHO CORDEIRO

DESENVOLVIMENTO DE BIOMATERIAIS ANTIMICROBIANOS FUNCIONALIZADOS COM COBRE PARA APLICAÇÃO ODONTOLÓGICA

DEVELOPMENT OF ANTIMICROBIAL BIOMATERIALS FUNCTIONALIZED WITH COPPER FOR DENTAL APPLICATION

Piracicaba
2021

JAIRO MATOZINHO CORDEIRO

DESENVOLVIMENTO DE BIOMATERIAIS ANTIMICROBIANOS FUNCIONALIZADOS COM COBRE PARA APLICAÇÃO ODONTOLÓGICA

DEVELOPMENT OF ANTIMICROBIAL BIOMATERIALS FUNCTIONALIZED WITH COPPER FOR DENTAL APPLICATION

Tese apresentada à Faculdade de Odontologia de Piracicaba da Universidade Estadual de Campinas como parte dos requisitos exigidos para obtenção do título de Doutor em Clínica Odontológica, na Área de Prótese Dental.

Thesis presented to the Piracicaba Dental School of the University of Campinas in partial fulfillment of the requirements for the degree of Doctor in Clinical Dentistry, in Prosthodontics area.

Orientador: Prof. Dr. Valentim Adelino Ricardo Barão

Este exemplar corresponde à versão final da tese defendida pelo aluno Jairo Matozinho Cordeiro e orientada pelo Prof. Dr. Valentim Adelino Ricardo Barão.

Piracicaba

2021

Ficha catalográfica
Universidade Estadual de Campinas
Biblioteca da Faculdade de Odontologia de Piracicaba
Marilene Girello - CRB 8/6159

C811d

Cordeiro, Jairo Matozinho, 1991-
Desenvolvimento de biomateriais antimicrobianos funcionalizados com cobre para aplicação odontológica / Jairo Matozinho Cordeiro. – Piracicaba, SP : [s.n.], 2021.

Orientador: Valentim Adelino Ricardo Barão.
Tese (doutorado) – Universidade Estadual de Campinas, Faculdade de Odontologia de Piracicaba.

1. Biomateriais. 2. Implantes dentários. 3. Ossos - Regeneração. 4. Biofilmes. I. Barão, Valentim Adelino Ricardo, 1983-. II. Universidade Estadual de Campinas. Faculdade de Odontologia de Piracicaba. III. Título.

Informações para Biblioteca Digital

Título em outro idioma: Development of antimicrobial biomaterials functionalized with copper for dental application
Palavras-chave em inglês:
Biomaterials
Dental implants
Bone regeneration
Biofilms
Área de concentração: Prótese Dental
Titulação: Doutor em Clínica Odontológica
Banca examinadora:
Valentim Adelino Ricardo Barão [Orientador]
Jamil Awad Shibli
Heloísa Fonseca Marão
Diana Gabriela Soares dos Passos
Renata Cunha Matheus Rodrigues Garcia
Data de defesa: 21-12-2021
Programa de Pós-Graduação: Clínica Odontológica

Identificação e informações acadêmicas do(a) aluno(a)
- ORCID do autor: https://orcid.org/0000-0003-0591-9270
- Currículo Lattes do autor: http://lattes.cnpq.br/6478593835162986

UNIVERSIDADE ESTADUAL DE CAMPINAS
Faculdade de Odontologia de Piracicaba

A Comissão Julgadora dos trabalhos de Defesa de Tese de Doutorado, em sessão pública realizada em 21 de dezembro de 2021, considerou o candidato JAIRO MATOZINHO CORDEIRO aprovado.

PROF. DR. VALENTIM ADELINO RICARDO BARÃO

PROF. DR. JAMIL AWAD SHIBLI

PROFª. DRª. HELOÍSA FONSECA MARÃO

PROFª. DRª. DIANA GABRIELA SOARES DOS PASSOS

PROFª. DRª. RENATA CUNHA MATHEUS RODRIGUES GARCIA

A Ata da defesa, assinada pelos membros da Comissão Examinadora, consta no SIGA/Sistema de Fluxo de Dissertação/Tese e na Secretaria do Programa da Unidade.

Dedicatória

Dedico esta tese à minha família, cujo amor, carinho e educação foram a base da minha formação. Aos meus pais, **Eva** e **Pedro**, às minhas irmãs, **Jeans** e **Julvani**, e ao meu cunhado, **Delcino**, por me protegerem e ampararem mesmo na distância, permitindo a concretização deste sonho. Aos meus sobrinhos, **Maria Luiza** e **Bernardo**, que vejam em mim um exemplo para seguirem os seus anseios.

Muito obrigado por serem uma inspiração contínua em minha vida.

Agradecimento Especial

Ao **Prof. Dr. Valentim Adelino Ricardo Barão**, agradeço à orientação inestimável. A sua confiança em minha capacidade de crescer e estímulo constante permitiram meu amadurecimento pessoal e profissional. Estou certo de que não sou mais o mesmo. Aprendi e ainda tenho muito a aprender com você. Que eu possa, no exercício da academia, repassar aos meus alunos e pacientes um pouco do que tenho guardado em mim de você: o respeito, a generosidade, a disponibilidade, a honestidade, o pensamento crítico e a vontade de sempre fazer o melhor. Sou profundamente grato por ter tido a oportunidade de tê-lo como orientador e exemplo nesta fase da minha vida. Muito obrigado!

Agradecimentos

A Deus, por ter me fornecido sabedoria e me guiado pelas escolhas corretas.

À Universidade Estadual de Campinas, na pessoa do Magnífico Reitor **Prof. Dr. Antonio José de Almeida Meirelles.**

À Faculdade de Odontologia de Piracicaba da Universidade Estadual de Campinas, na pessoa de seu Diretor, **Prof. Dr. Francisco Haiter Neto**, e de seu Diretor Associado, **Prof. Dr. Flávio Henrique Baggio Aguiar.**

À Coordenadora dos Cursos de Pós-Graduação e do Programa de Pós-Graduação em Clínica Odontológica da Faculdade de Odontologia de Piracicaba, **Prof.ª Dr.ª Karina Gonzales Silvério Ruiz.**

Aos docentes da área de Prótese Total da Faculdade de Odontologia de Piracicaba, **Prof. Dr. Marcelo Ferraz Mesquita** e **Prof. Dr. Rafael Leonardo Xediek Consani**, e aos professores da área de Prótese Parcial Removível, **Profa. Dra. Altair Del Bel Cury, Profa. Dra. Renata Cunha Matheus Rodrigues Garcia, Prof. Dr. Wander José da Silva**, agradeço à disponibilidade, inspiração e por todo conhecimento transmitido ao longo destes anos.

Aos professores da Universidade Estadual Paulista, **Dr. Nilson Cristino da Cruz, Dra. Elidiane Cipriano Rangel, Dr. Leonardo Perez Faverani** e **Dra. Érica Dorigatti de Avila**, pela parceria no desenvolvimento destes trabalhos e ensinamentos compartilhados.

Ao **Prof. Dr. Jeroen van den Beucken** e à **Profa. Dra. Fang Yang**, da Radboudumc, pela orientação durante o período de estágio no exterior. Agradeço a disponibilidade em transmitir tanto conhecimento, pelas oportunidades e confiança depositada.

À **Sra. Eliete A. Ferreira Lima Marim**, secretária do Departamento de Prótese e Periodontia da FOP-UNICAMP, ao **Sr. Eduardo Pinez**, técnico do Laboratório de Prótese Total da FOP-UNICAMP, aos técnicos do Laboratório de Plasmas Tecnológicos da UNESP-Sorocaba, pela competência e solicitude constantes.

Àqueles que tive o prazer de compartilhar esta jornada de perto, **Bruna Egumi, Raphael Costa, Guilherme Borges, Caroline Dini, Heloísa Pantaroto** e **João Gabriel,** pela amizade e apoio que foram fundamentais para a realização deste trabalho e obtenção deste

título. Vocês foram esteio na exaustão, ânimo nas incertezas, fonte de alegria diária e impulso em busca de novas conquistas. Nos méritos desta conquista, há muito de vocês.

Aos grandes amigos conquistados deste o início desta jornada, **Rodrigo Lins**, **Mariana Barbosa** e **Camilla Fraga**, agradeço a disponibilidade, paciência, inspiração e amparo incondicional. Vocês se fizeram presentes e se tornaram minha família em Piracicaba, compartilhando momentos especiais que levarei para sempre comigo. Neste momento, olho para trás e vejo a importância de cada abraço e sorriso dividido com vocês.

Aos amigos de longa data, **Bianca Rodrigues, Bruno Rodrigues**, **Comphúcio Fraga**, **Herick Fernando** e **Luziany Sene,** que torceram por mim a cada nova conquista e me encorajaram a persistir este sonho. Os laços que nos unem são impossíveis de se explicar, nos reconhecemos uns nos outros e cativamos uma amizade verdadeira que perdura por anos. Muito obrigado pelo companheirismo e carinho constantes.

Aos amigos conquistados durante o estágio no exterior, **Fabrício Stocker**, **Myrna Lima**, **Rafaela Bürger** e, em especial, **Verônica Lima**, que me acolheram durante um momento desafiador e me fizeram sentir estar em família. Muito obrigado por continuarem presentes, fazendo a diferença nessa trajetória. Serei para sempre grato por cada experiência e sonhos compartilhados. A amizade de vocês é a prova de que independentemente de onde estivermos, sempre haverá alguém perto para ajudar, somar e dividir.

Aos amigos de laboratório, **Thais Barbin**, **Letícia Del Rio**, **Daniele Valente**, **Anna Presotto**, **Halina Berejuk**, **Ricardo Caldas**, **Luís Fernando** e **Maria Helena**, agradeço a convivência que tornaram os dias mais leves. Aos amigos feitos durante os quase sete anos de pós-graduação, em especial, **Amanda Bandeira**, **André Rabelo, Catharina Sacramento**, **Elis Lira**, **Edmara Bergamo**, **Gercino Ferreira, Giancarlo De La Torre, Ingrid Andrade, João Júlio, Júlia Marques, Louise Dornelas, Loyse Martorano, Mariana Marinho, Mayara Abreu**, **Marina Xavier, Olívia Figueredo, Rahyza Freire, Talita Malini**, **Tamires Dutra**, **Tatiane Eufrásio** e **Vinícius Aguiar**, sou grato pelos momentos e apoio partilhados que facilitaram a concretização dessa etapa.

O presente trabalho foi realizado com apoio da **Coordenação de Aperfeiçoamento de Pessoal de Nível Superior – Brasil (CAPES)** - Código de Financiamento 001 e da **Fundação de Amparo à Pesquisa do Estado de São Paulo (FAPESP)**, processos nº 2017/01320-0 e 2018/14117-0.

A todos que contribuíram para que este trabalho e esta etapa fossem concluídos, muito obrigado!

RESUMO

O acúmulo de biofilme é um dos principais fatores envolvidos na falha das reabilitações com implantes dentários. Tratamentos de superfícies para implantes e membranas para regeneração óssea guiada (ROG) usadas clinicamente não apresentam capacidade antimicrobiana. Ainda existe a necessidade de desenvolver biomateriais que possam prevenir infecções e auxiliar no recrutamento de células endógenas, suportando e estimulando a osseointegração e regeneração óssea. Diante disso, este trabalho teve como objetivos: (1) sintetizar e caracterizar revestimentos antimicrobianos e bioativos no titânio (Ti) para o emprego como superfícies de implantes dentários produzidas pela oxidação por plasma eletrolítico (PEO) e diferentes fontes de cobre (Cu): acetato de cobre (CuAc), sulfato de cobre (CuS) e óxido de cobre (CuO); (2) desenvolver e avaliar membranas contendo óxido de Cu (CuO 1%, CuO 0,5%, CuO 0,1% e CuO 0,05% em peso) para ROG formadas por meio da técnica de eletrofiação. Foram avaliadas as propriedades morfológicas, estruturais, químicas e mecânicas dos biomateriais. Experimentos de citocompatibilidade *in vitro* foram realizados com células-tronco mesenquimais de osso humano e células endoteliais da veia umbilical humana. O potencial antibacteriano dos biomateriais foi testado pela formação de biofilme de *Streptococcus sanguinis* para os revestimentos por PEO e *Staphylococcus aureus* para as membranas para ROG. One-way ANOVA e teste de Tukey foram usados para comparações múltiplas ($p < 0,05$). Os revestimentos para implantes dentários contendo Cu foram desenvolvidos por PEO empregando diferentes fontes de Cu, as quais foram capazes de afetar a morfologia e composição dos revestimentos, também influenciando seu efeito em células humanas e bactérias. A formação de biofilme bacteriano nos revestimentos experimentais dependeu da rugosidade superficial gerada e liberação de íons de Cu pelas diferentes fontes utilizadas para funcionalizar o Ti. Uma topografia otimizada do revestimento produzida com CuAc levou à inibição na formação de biofilme e aumento da resposta celular. As membranas para ROG contendo Cu em diferentes concentrações foram sintetizadas com sucesso pela técnica de eletrofiação. A concentração de Cu foi crucial para as respostas biológicas, em que altas concentrações demonstraram melhor atividade antimicrobiana, mas baixa citocompatibilidade. As membranas com baixa concentração de Cu apresentaram boas propriedades mecânicas, suportando e estimulando a adesão e proliferação de células humanas, bem como a angiogênese. Os resultados deste estudo são promissores no que diz respeito ao emprego do Cu como um agente de funcionalização para dois biomateriais diferentes. Ambas as estratégias apresentadas neste trabalho podem ser alternativas valiosas para diminuir o risco de infecções e melhorar o processo de osseointegração e regeneração tecidual, consequentemente, acelerando o tratamento reabilitador com implantes dentários.

Palavras-chave: Biomateriais. Implante Dentário. Regeneração Óssea. Biofilme.

ABSTRACT

Biofilm accumulation is one of the main factors involved in the failure of dental implant rehabilitation. Surface treatments for implants and membranes for guided bone regeneration (GBR) in current clinical use do not have antimicrobial capacity. Thus, the need to develop biomaterials that could assist in recruiting endogenous stem cells, supporting and stimulating the innate bone regeneration is still ongoing. Therefore, this work aimed: (1) to synthesize and characterize antimicrobial and bioactive coatings onto titanium (Ti) to be applied as surfaces for dental implants produced by plasma electrolytic oxidation (PEO) and using different copper (Cu) sources: copper acetate (CuAc), copper sulfate (CuS), and copper oxide (CuO); (2) to develop and evaluate membranes containing Cu oxide (CuO 1%, CuO 0.5%, CuO 0.1%, and CuO 0.05%; wt. %) for GBR formed by electrospinning technique. The morphological, structural, chemical and mechanical properties of the biomaterials were evaluated. *In vitro* cytocompatibility experiments were performed with human bone mesenchymal stem cells and human umbilical vein endothelial cells. The antibacterial potential of biomaterials was tested by biofilm formation of *Streptococcus sanguinis* for PEO coatings and *Staphylococcus aureus* for GBR membranes. One-way ANOVA and Tukey test was used for multiple comparisons ($p < 0.05$). Cu-containing coatings for dental implants were successfully developed by PEO using different Cu sources, which were able to affect the morphology and composition of the coatings, also influencing their effect on human cells and bacteria. The surface roughness of the coating and Cu ions release generated by distinct sources used to functionalize the Ti influenced the biofilm formation. An optimized topography of the coating produced with CuAc led to biofilm formation inhibition and an increase in cellular responses. Cu-loaded GBR membranes with different concentrations were successfully synthesized by the electrospinning technique. Cu concentration was crucial for biological responses, in which higher concentrations showed better antimicrobial activity, but decreased cytocompatibility. Membranes with a lower concentration of Cu showed good mechanical properties, supporting and stimulating human cell adhesion and proliferation, as well as angiogenesis. The use of Cu as a functionalizing agent for two different biomaterials seems to be promising. Both strategies presented in this study may be valuable alternatives to reduce the risk of infections and improve the process of osseointegration and tissue regeneration, consequently, accelerating the rehabilitation treatment with dental implants.

Keywords: Biomaterials. Dental implant. Bone Regeneration. Biofilm.

SUMÁRIO

1 INTRODUÇÃO

A reabilitação com implantes dentários de pacientes desdentados, total ou parcialmente, tornou-se um padrão ouro de atendimento em odontologia nos últimos 20 anos para repor dentes perdidos (Bornstein et al., 2008). Apesar da previsibilidade dos tratamentos com implantes dentários, as falhas podem acontecer pela associação de alguns fatores, tais como: história pregressa de doença periodontal, bruxismo, tabagismo, diabetes mal controlada, radioterapia (Kullar and Miller, 2019), envelhecimento (Howe et al., 2019), qualidade e volume ósseo deficiente (Van Steenberghe et al., 2002). Outro fator que pode comprometer o sucesso do tratamento é a presença de deficiências ósseas, um dos cenários clínicos mais desafiadores devido às dificuldades nas técnicas de regeneração e presença de limitações anatômicas decorrentes de atrofia óssea, trauma, ressecção tumoral ou doença periodontal (D'Mello et al., 2015). Neste contexto, um estudo retrospectivo demonstrou que cerca de 52% dos implantes instalados (939) necessitam de aumento ósseo como parte da reabilitação do paciente (Bornstein et al., 2008).

Diversas abordagens têm sido exploradas para aprimorar o processo de osseointegração e garantir o sucesso e a sobrevivência do implante em situações desafiadoras. A utilização de biomateriais com o objetivo restabelecer a integridade estrutural do osso ou substituí-lo (Kumar et al., 2020) é uma estratégia cada vez mais presente na prática clínica. Por exemplo, nos casos de defeitos verticais e/ou horizontais, nos quais é necessário a regeneração óssea para colocação de implantes dentários, algumas técnicas têm se mostrado eficazes quanto ao ganho ósseo e sobrevivência do implante. A regeneração óssea guiada (ROG) tem sido considerada a técnica mais previsível em termos de estabilidade óssea, garantindo menor reabsorção óssea e baixo número de complicações após sua aplicação (Clementini et al., 2012; Elangovan et al., 2013).

A ROG tem sido estudada desde o final dos anos 1980 e é baseada no uso de uma membrana não reabsorvível ou reabsorvível para estabilizar o coágulo sanguíneo e criar um espaço isolado no local da ferida, evitando a invasão de células dos tecidos moles e favorecendo a proliferação de células envolvidas na formação de osso (Castro et al., 2018; Clementini et al., 2012). Embora uma alta taxa de sucesso (90 a 100%) tem sido observado para os implantes colocados em cristas ósseas aumentadas por ROG (Clementini et al., 2012; Elnayef et al., 2017), essa técnica não é isenta de complicações. Uma revisão sistemática mostrou que as complicações dos tecidos moles (por exemplo, exposição da membrana,

deiscência dos tecidos moles e infecção aguda) estão presentes em 16,5% dos casos (Lim et al., 2018).

Para se alcançar o sucesso do tratamento, além de um sítio favorável, a superfície do implante também precisa estimular a osseointegração e controlar possíveis infecções que podem levar ao insucesso do tratamento. Os tratamentos de superfície são usados na implantodontia para criar revestimentos bioativos semelhantes ao osso, que podem melhorar as respostas celulares, promover uma maior e mais rápida diferenciação celular, mineralização e aposição óssea, bem como acelerar a osseointegração (Hu et al., 2019; Kunrath et al., 2021; Spriano et al., 2018). Além disso, modificações e revestimentos de superfície para implantes dentários têm sido propostos como uma promessa para aumentar a sobrevivência de implantes dentários pela criação de superfícies antimicrobianas, prevenindo infecções relacionadas ao acúmulo de biofilme. No entanto, não há consenso quanto ao melhor tratamento de superfície disponível para reduzir o acúmulo de bactérias orais e prevenir infecções microbianas (Costa et al., 2021).

Considerando este cenário, seria válido desenvolver biomateriais que apresentassem potencial regenerativo e que pudessem atuar clinicamente recrutando células endógenas e estimulando a regeneração óssea e osseointegração, bem como evitando infecções bacterianas. Sendo assim, a funcionalização dos tratamentos de superfície para implantes dentários e membranas para ROG apresentariam como vantagem a possibilidade de induzir o efeito biológico desejado pela ativação de constituintes moleculares e células envolvidas no processo de regeneração/osseointegração. Proteínas orgânicas, produtos naturais e íons inorgânicos tem sido incorporados a biomateriais com essa finalidade (O'Neill et al., 2018; Xu et al., 2018a). Íons inorgânicos, como boro (B^{3+}), cálcio (Ca^{2+}), cobalto (Co^{2+}), cobre (Cu^{2+}), fluoreto (F^{-}), lítio (Li^{+}), magnésio (Mg^{2+}), nióbio (Nb^{5+}), fosfato ($PO4^{3-}$), silicato (Si^{4-}), prata (Ag^{+}), estrôncio (Sr^{2+}), vanádio (V^{5+}) e zinco (Zn^{2+}), tem chamado a atenção devido aos custos de tratamento reduzidos e menor risco de efeitos colaterais biológicos quando comparados ao uso de fatores de crescimento ou abordagens de engenharia genética (Wang et al., 2014), apresentando maior simplicidade, maior estabilidade e maior eficácia em baixas concentrações (Hoppe et al., 2011; O'Neill et al., 2018). Em geral, a liberação de íons inorgânicos estáveis para um ambiente fisiológico impulsiona sua função como cofatores enzimáticos (Gérard et al., 2010) e induz a sinalização de vias bioquímicas envolvidas na diferenciação de células, resultando na estimulação da osteogênese e angiogênese e, consequentemente, o crescimento e regeneração do tecido ósseo (Gérard et al., 2010; Hoppe et al., 2011; O'Neill et al., 2018).

Dentre os íons metálicos citados acima, o cobre (Cu) é um oligoelemento de alta abundância e baixo custo, apresentando aplicações que abrangem os mais diversos campos da pesquisa eletroquímica, biotecnologia e medicina (Ojha et al., 2017; Tamayo et al., 2016; Zhou et al., 2019). Na Odontologia, Cu tem sido utilizado em sistemas adesivos (Gutiérrez et al., 2019), tratamentos de superfície (Prinz et al., 2017; Wojcieszak et al., 2017), ligas para implantes (Luo et al., 2018; Wang et al., 2019; Xu et al., 2018a), substitutos ósseos (Zhang et al., 2019), "*scaffolds*" (Bari et al., 2017; Wang et al., 2014; Wu et al., 2013) e barreiras metálicas usadas na ROG (Xu et al., 2018b). Especificamente para a regeneração óssea, a ampla aplicação do Cu está relacionada aos seus múltiplos estados de oxidação (Cu, Cu_2O, CuO) que apresentam capacidade angiogênica, osteoestimuladora, atividade antibacteriana e biocompatibilidade em uma concentração adequada (Tamayo et al., 2016; Wang et al., 2014; Wu et al., 2013; Zhang et al., 2019). Estudos *in vivo* mostraram que implantes e "*scaffolds*" dopados com Cu são opções favoráveis para a prevenção de infecção bacteriana e estimulação de processos regenerativos (Prinz et al., 2017; Wang et al., 2014). Dessa forma, a incorporação do Cu pode ser crucial em aplicações clínicas não só pelo seu potencial em estimular a formação óssea, mas também pela sua excelente resposta antibacteriana, uma vez que a cavidade oral é uma área com alta acessibilidade de micro-organismos que podem aumentar o risco de infecções (ex.: osteomielite e peri-implantite) e resultar na falha da regeneração tecidual e reabilitação com implantes dentários (Bari et al., 2017; He et al., 2015; Jin et al., 2018; Wu et al., 2013; Xu et al., 2018b).

Para garantir o comportamento biológico desejado, é importante que as técnicas utilizadas para confeccionar o revestimento do implante e a membrana utilizada na ROG sejam suficientemente versáteis para permitir a incorporação e liberação sustentada dos íons em função do tempo (O'Neill et al., 2018). Dentre as técnicas disponíveis para incorporação de íons metálicos, permitindo sua posterior liberação, pode-se destacar a oxidação por plasma eletrolítico ou oxidação por microarcos (PEO ou MAO, respectivamente) para o tratamento de superfícies de implantes e a eletrofiação para o desenvolvimento de membranas.

O plasma eletrolítico é eficaz para a confecção de tratamentos de superfície pela oxidação anódica de alta tensão de um substrato metálico imerso em soluções eletrolíticas sem a necessidade de equipamentos altamente complexos (Fig. 1a). O PEO permite a criação de revestimentos duráveis, espessos, uniformes, rugosos e fortemente aderentes (Clyne & Troughton, 2019). Além disso, esta técnica permite a incorporação de elementos bioativos (Ca e P) e antimicrobianos (Cu, Ag, Bi e Zn) na camada de óxido de metais como o titânio (Ti) pela sua adição ao eletrólito (Lu et al., 2016; Marques et al., 2015; Nagay et al., 2019; Yao et

al., 2014). Geralmente, os revestimentos por PEO fornecem uma área de superfície maior para fixação do implante ao osso, melhor resistência à corrosão, excelente biocompatibilidade e maior contato osso-implante (Beline et al., 2016; Liu et al., 2015; Polo et al., 2020). Estudos que incorporaram Cu ao substrato de Ti por meio de PEO ainda são escassos (Huang et al., 2018; Sedelnikova et al., 2019; Zhang et al., 2018) e nenhum deles avaliou a influência de diferentes fontes de Cu nas propriedades superficiais e biológicas do revestimento.

A eletrofiação é uma tecnologia simples e robusta desenvolvida para gerar micro e nanofibras usando soluções poliméricas (Fig. 1b). Estas soluções são sujeitas a altas tensões para superar sua tensão superficial e criar um jato eletricamente carregado que ejetará através de uma agulha de pequeno diâmetro em direção a um coletor (condutor de carga oposta) (Lim et al., 2004; O'Neill et al., 2018; Patil et al., 2017; Zou et al., 2018). Antes de chegar ao coletor, o jato de solução evapora e se solidifica, sendo coletado como uma rede interconectada de fibras finas (Lim et al., 2004). As nanofibras produzidas por eletrofiação tem porosidade, topografia e área de superfície diferentes, sendo densamente coletadas para formar uma membrana que pode limitar a infiltração celular (Lian et al., 2019). Trabalhos anteriores com nanofibras contendo Cu foram focados em "*scaffolds*" (Weng et al., 2017) ou delineados para diferentes propósitos biomédicos (Ahire et al., 2016; Amna et al., 2014; Gönen et al., 2016; Kharaghani et al., 2018; Li et al., 2016). Além disso, estes estudos não realizaram uma avaliação completa das nanofibras contendo Cu com relação ao comportamento mecânico e à resposta biológica considerando a aplicação na ROG.

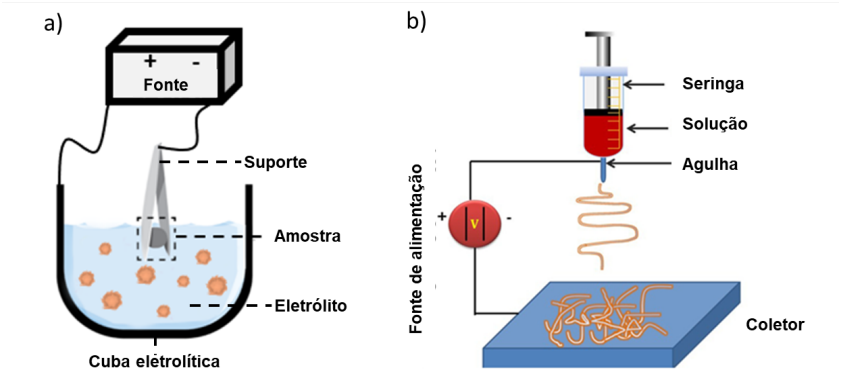

Figure 1. Ilustração das tecnologias usadas para a obtenção de biomateriais: a) oxidação a plasma eletrolítico, consistindo em uma fonte de alta tensão, suporte para amostra e cuba eletrolítica; b) eletrofiação, consistindo em uma fonte de alimentação, seringa e placa coletora. Reimpresso com modificações de Nagay et al., 2019 e Patil et al., 2017.

Recentemente, os implantes dentários e as membranas para ROG em uso clínico não apresentam efeito intencional na regulação funcional das células que participam da osseointegração e regeneração óssea. Mais esforços devem ser dedicados à criação de implantes bioativos e membranas funcionais para ROG que possam estimular simultaneamente a osteogênese e a angiogênese, e minimizar a atividade bacteriana (Lian et al., 2019; Shao et al., 2017). Portanto, este trabalho teve como objetivos: (1) sintetizar e caracterizar revestimentos antimicrobianos e bioativos no Ti para o emprego como superfícies de implantes dentários produzidas por PEO e diferentes fontes de Cu; (2) desenvolver e avaliar membranas contendo óxido de Cu para ROG formadas por meio da técnica de eletrofiação. É esperado que a incorporação de íons Cu na superfície de Ti e na membrana para ROG fornecerá ação antibacteriana e melhores comportamentos biológicos no que diz respeito às células ósseas e endoteliais.

2 ARTIGOS

2.1 Copper source determines chemistry and topography of implant coatings to optimally couple cellular responses and antibacterial activity#

Jairo M. Cordeiro[ae*], Bruna E. Nagay[a], Caroline Dini[a], João G. S. Souza[bc], Elidiane C. Rangel[d], Nilson C. da Cruz[d], Fang Yang[e], Jeroen J. J. P. van den Beucken[e*], Valentim A. R. Barão[a*]

[a]*Department of Prosthodontics and Periodontology, Piracicaba Dental School, University of Campinas (UNICAMP), Piracicaba, São Paulo 13414-903, Brazil*

[b]*Faculdade de Ciências Odontológicas (FCO), Montes Claros, Minas Gerais 39401-303, Brazil*

[c]*Dental Research Division, Guarulhos University, Guarulhos, São Paulo 07023-070, Brazil*

[d]*Laboratory of Technological Plasmas, Institute of Science and Technology, São Paulo State University (UNESP), Sorocaba, São Paulo 18087-180, Brazil*

[e]*Regenerative Biomaterials, Dentistry, Radboudumc, 6500 HB Nijmegen, The Netherlands*

Note: Valentim A. R. Barão and Jeroen J. J. P. van den Beucken should be considered a joint senior author.

***Corresponding author:**

E-mail addresses: vbarao@unicamp.br (Valentim A. R. Barão), jeroen.vandenbeucken@radboudumc.nl (Jeroen J. J. P. van den Beucken), jairocordeirom@hotmail.com (Jairo M. Cordeiro).

#Artigo publicado na revista *Materials Science and Engineering C (IF = 7.328)* (Anexo 1). Reprinted from Mater Sci Eng C, 2021; 112550, https://doi.org/10.1016/j.msec.2021.112550., with permission from Elsevier.

Abstract

Implant-related infections at the early healing period are considered one of the main risk factors in implant failure. Designing coatings that control bacterial adhesion and have cell stimulatory behavior remains a challenging strategy for dental implants. Here, we used plasma electrolytic oxidation (PEO) to produce antimicrobial coatings on commercially pure titanium (cpTi) using bioactive elements (calcium and phosphorus) and different copper (Cu) sources: copper acetate (CuAc), copper sulfate (CuS), and copper oxide (CuO); coatings containing only Ca and P (CaP) served as controls. Cu sources drove differential physical and chemical surface features of PEO coatings, resulting in tailorable release kinetics with a sustained Cu ion release over 10 weeks. The antibacterial effects of Cu-containing coatings were roughness-dependent. CuAc coating exhibited optimal properties in terms of its hydrophilicity, pores density, and limited surface roughness, which provided the most robust antibacterial activity combined with appropriate responses of human primary stem cells and angiogenic cells. Our data indicate that Cu source selection largely determines the functionality of Cu-containing PEO coatings regarding their antibacterial efficacy and cytocompatibility.

Keywords: Titanium, Microarc oxidation, Dental implant, Biomimetic Material, Osseointegration, Biofilm

Highlights

- The best source of Cu to create an antimicrobial and bioactive PEO coating was defined.
- Surface morphology and chemistry were altered by increased electrolyte conductivity.
- Coatings produced with copper acetate and copper oxide improved cell responses.
- The bacterial adhesion of Cu-containing coatings was roughness-dependent.
- Cu-containing coatings can be a valuable strategy to prevent or diminish implant infection.

Graphical abstract

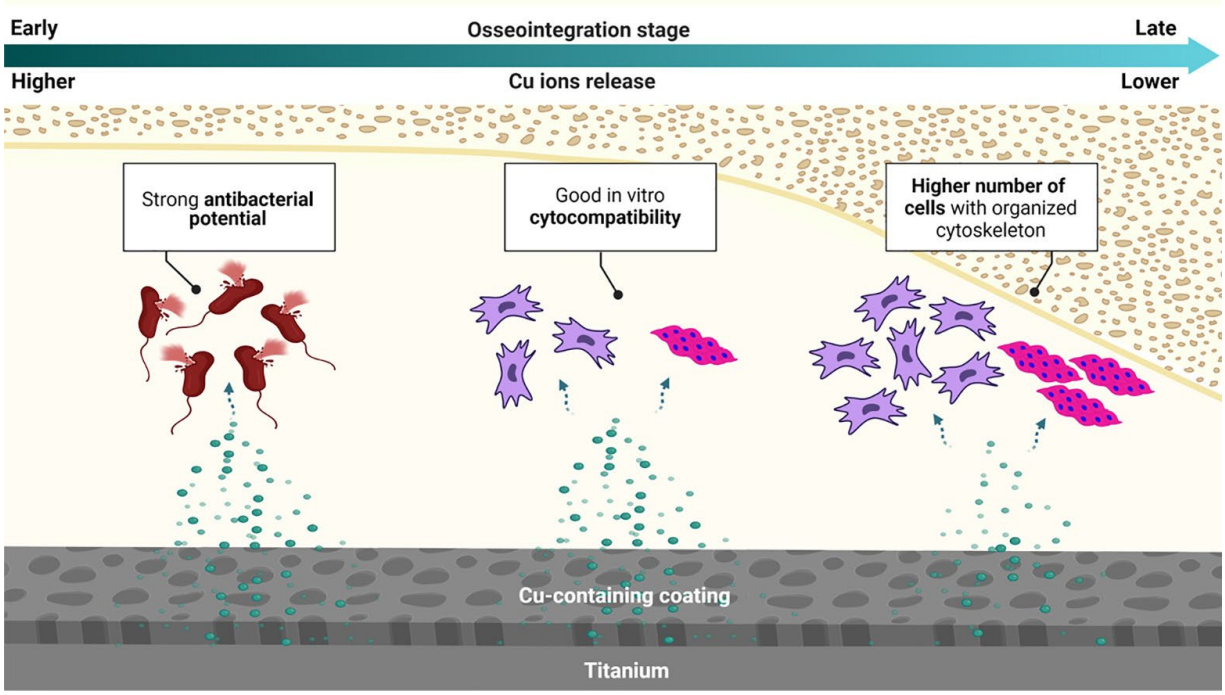

1 Introduction

Designing implants with specific biology-related physical and chemical surface properties has attracted attention for the application in the biomedical field. Coating technologies have been applied in dental implantology to create bioactive surfaces similar to the bone in terms of topography and composition, which can improve cellular responses or the growth of new natural bone on and around the implant surface, increasing implant stability and osseointegration [1–3]. In fact, surface modifications for dental implants enable steering desired biological responses by activating specific molecular pathways and cells involved in bone healing and remodeling. For example, several biomaterials have aimed at stimulating angiogenesis due to their key roles in repairing tissues, supporting the delivery of nutrients and signaling factors, and removing bioproducts, thus promoting neo-tissue formation [4].

Even with the ongoing advances in the biomedical field, titanium (Ti) implants still undergo some undesirable biological responses and treatment failure, such as implant-related infections, which also impair the osseointegration due to the challenging physiological environment established by the biofilm accumulation and inflammatory process [5]. Commercially available implants have shown improved osseointegration and success rates by tuning their surface chemistry and topography [1,6]. On the other hand, no Ti dental implants currently exist in the market with proven reliable antimicrobial properties for clinical use [7]. In this context, designing coatings with combined cell stimulatory capacity and antibacterial potential remains a feasible but challenging strategy for implantable materials.

Surface coatings for dental implants can be achieved by various techniques, which may be physical, chemical, mechanical, or a combination of these [8]. When designing an antimicrobial coating, three major strategies can be considered: antimicrobial agent release, bacteria repelling/non-adhering surface properties, and contact-killing surfaces [2]. Several methods can be applied to achieve these outcomes: from dipping/soaking the implant into an antibacterial solution for drug immobilization to surface modifications based on chemical reactions and physical alterations (e.g., ion implantation, magnetron sputtering, plasma electrolytic oxidation, electrophoresis, plasma spraying, electrospinning, sol-gel, covalent immobilization, hydrothermal method, vapor deposition, polyelectrolyte, and so on) [9–11].

Among the current techniques used for coating production, plasma electrolytic oxidation (PEO), also known as microarc oxidation, is an effective technique that allows the incorporation of bioactive and antimicrobial elements to Ti-based alloys [12,13]. Furthermore, PEO forms a porous, rough TiO_2 layer on Ti surface [14–16] with strong bonding to the substrate owing to the localized high energy given by spark discharges that create a fusing

effect of the oxide films produced on the metallic substrate [17]. PEO coatings have a favorable surface area for implant bonding to the bone and are highly biocompatible for bone formation and maturation [18,19]. Moreover, earlier work [13] showed that PEO coating has the potential to promote a positive oral biofilm modulation with decreased pathogenic potential. However, due to their increased surface area, these rough implant surfaces increase the risks of microbial adhesion and, hence require additional surface functionalization to reduce microbial loads [14,20].

The possibility to incorporate several functional compounds into PEO coatings to boost their antibacterial efficacy evidence this technology as a promising strategy for dental implant manufacturing. Inorganic ions have attracted attention because of their low costs and diminished risk of biological side effects compared to growth factors or genetic engineering approaches [21], presenting greater simplicity, higher stability, and more efficacy at low concentrations [22,23]. Among metal ions, copper (Cu) is a highly abundant trace element with low cost that has been used in a broad range of dental applications: adhesive systems [24], implant surface treatments [25,26], alloys design [27], metallic barriers used in guided bone regeneration [27], bone grafting biomaterials, and scaffolds [21,28].

The broad application of Cu is related to its multiple oxidation states (Cu, Cu^{2+}, Cu^{+}) that have demonstrated effective antibacterial capacity combined with cell compatibility in scaffolds [21]. In coatings, Cu has presented long-term antibacterial ability and antifouling property by ROS generation and down-regulation of genes involved in the biofilm formation of both gram-positive (e.g., *Staphylococcus aureus*) [29–33] and gram-negative bacteria (e.g., *Escherichia coli* and *Porphyromonas gingivalis*) [30,32,34,35]. Regarding the effect of Cu on cells, it has been tested in several cell lines, such as osteosarcoma [30,36], fibroblast [29], bone marrow stem cells [34,37], macrophages [33], osteoblast [5,35,38,39], and endothelial cells [5,38], stimulating their metabolic activity, adhesion, and proliferation, as well as the expression of specific proteins and genes in a Cu-dependent manner.

Cu has been incorporated into coatings on Ti-based materials employing PEO [29,30,36] or as an additional layer using hydrothermal [33,39] or galvanic [37] treatment after PEO. Those studies have demonstrated that Cu effectively increases angiogenesis, favoring osteoblastic responses, modulating inflammation responses, and minimizing bacterial adhesion. Studies incorporating Cu ions within PEO coatings focused on concentration-dependent effects [29,30,38] or the association of different metal ions [5,20,40,41] on surface features and their biological behavior. Remarkably, the influence of different Cu sources on PEO coating functionalization and efficacy has been neglected. Since the electrolyte solution used during

PEO treatment significantly affects the nature of the discharge and resultant coating [18,42–44], it is straightforward to assume that altering the Cu source will affect the physico-chemical properties of the coating, and hence its biological function. Consequently, it is crucial to investigate how different Cu sources affect key features of PEO surfaces toward developing a bioactive coating that combines optimal osseointegration with minimizing implant-related infections. Here, we show for the first time that tailoring Cu-containing coatings with suitable features by changing the Cu source during coating production differentially affects coating physicochemical properties and functional efficacy.

2 Material and Methods

2.1 Synthesis of PEO coatings

Commercially pure titanium (cpTi) grade 2 discs (Ø10 mm ×1 mm; Realum Ind. e Com. de Metais Puros e Ligas Ltd., Brazil) were submitted to grinding with #320- and #400-grit SiC abrasive papers (Buehler, USA) [14] to standardize the surface finishing (Ra 0.24 ± 0.01 μm). Samples were randomly divided into four groups according to the composition of the electrolytic solution used for PEO treatment (Table 1). Cu-containing coatings were obtained by using different Cu sources: copper(II) acetate (CuAc; 99.99% purity), copper(II) sulfate (CuS; 98.9% purity), and copper(II) oxide (CuO; 99.6% purity), all from Dinâmica Ltd. (Brazil). The concentration of each source was defined after a pilot study that considered the incorporation of ~1 at.% of Cu for all groups, which has been reported to exhibit antibacterial properties without being cytotoxic [38,45]. This standardization was adopted to focus on the major effect of Cu sources on response variables and exclude the possible influence of their concentration. PEO treatment was carried out in a glass beaker with the cpTi disc as the anode and a steel cylinder as the cathode. The electrolytic solution (1 L) was prepared following two steps. First, Na_2(EDTA) [$Na_2(C_{10}H_{14}N_2O_8)_2H_2O$] (99.8% purity; Química Moderna Ltd., Brazil) was dissolved in 500 mL of distilled water followed by the addition of the copper source, which was kept under agitation for 30 min at room temperature. Separately, calcium acetate [$Ca(CH_3CO_2)_2$] (99.5% purity; Dinâmica Ltd., Brazil) and glycerophosphate disodium ($C_3H_7Na_2O_6P$) (99.0% purity; Sigma-Aldrich, USA) were dissolved in 500 mL of distilled water. Then, both solutions were mixed and used during PEO deposition. PEO process was conducted by a pulsed AC power supply (PlasmaTechnology Ltd., China) [12,46,47] for 10 min with a negative and positive pulse voltage (-100 V/+500 V), unipolar frequency (600 Hz), and alternate duty cycle: 10% (+) and 20% (-). Calcium and phosphorus (CaP) coating was

used as a control. The PEO-treated discs were washed with deionized water and air-dried. Samples were sterilized in an autoclave (121 °C for 15 min) before the experiments.

Table 1. Experimental groups and electrolyte composition used for PEO treatment.

Group	$Na_2(EDTA)$ (M)	$C_3H_7Na_2O_6P$ (M)	$Ca(CH_3CO_2)_2$ (M)	$Cu(CH_3COO)_2$ (M)	$CuSO_4$ (M)	CuO (M)	Electrolyte conductivity (mS cm^{-1})*
CaP	0.15	0.01	0.05	-	-	-	14.81 ± 0.05
CuAc	0.15	0.01	0.05	0.04	-	-	18.38 ± 0.09
CuS	0.15	0.01	0.05	-	0.03	-	17.14 ± 0.03
CuO	0.15	0.01	0.05	-	-	0.1	15.24 ± 0.01

* Data are expressed as mean ±standard deviation.

2.2 Characterization of coatings topography

Surface morphology was observed by scanning electron microscopy (SEM; ZEISS Sigma 300, Carl Zeiss Microscopy GmbH, Germany) under an accelerating voltage of 3.0 kV (n = 1). ImageJ 1.53e software (NIH, USA) was used to verify pore counts, area, and length of five random regions. Three-dimensional images, roughness line profiles, coatings surface roughness, and area were assessed using confocal laser scanning microscopy (CLSM; VK-X200 series, Keyence, Japan) (n = 3). After obtaining images from each sample, it was processed with the VK Analyzer v3.3.0.0 software (Keyence) to obtain the surface area and roughness (average roughness - Ra parameter) that was presented as a mean value of the three samples [16,48].

2.3 Coatings thickness measurement

To measure coating thickness, additional samples (n =1) were included in poly(methyl methacrylate) resin (PMMA; Sigma-Aldrich, The Netherlands) and cross-sectioned using a microtome (Leica RM2165, Germany). SEM images were acquired from five random regions and then analyzed by ImageJ.

2.4 Surface wettability

The wettability (distilled water) of PEO coatings was evaluated via a goniometer (Ramé-Hart 100-00; Ramé-Hart Instrument Co., USA) by the sessile drop (2 μL) method (n = 5) [46].

2.5 Elemental and crystalline phases detection

The oxidation state of the elements composing the PEO coatings was investigated by X-ray photoelectron spectroscopy (XPS) in a UNI-SPECS UHV Surface Analysis System using the Al Kα line (1254.6 eV) and pass energy for high-resolution spectra of 10 eV (n = 1). The composition was determined from the peak intensities using Scofield's atomic sensitivity factors of the corresponding elements. Energy-dispersive X-ray spectrometry (EDS; Bruker, Germany) was performed in the order of 1 μm^3 to verify the semi-quantitative composition of coatings surfaces (n = 1). Elements distribution through coating was observed via the mapping technique of cross-sectional images (n = 1). X-ray diffraction (XRD; X'pert3 powder, PANalytical, The Netherlands) was used to identify PEO coating crystalline phases (n = 1) [49].

2.6 Compositional analysis of PEO coatings

Since EDS is a semiquantitative method, coatings were digested to precisely quantify the chemical composition by inductively coupled plasma optical emission spectrometry (ICP-OES; iCAP 6000, Thermo Fischer Scientific Inc., USA). PEO coatings were digested using 45% HNO_3 to measure elements concentration. Samples (n = 3) were placed in hermetically closed glass tubes with 20 mL of HNO_3 and kept under continuous stirring for 24 h. After the completed digestion of the coating, the solution was diluted in deionized water, and Ca, Cu, Ti, and P concentrations were determined by ICP-OES. Digested samples (n = 1) were analyzed using SEM and EDS (both sides) to confirm whether the digestion process was effective in dissolving the coating completely.

2.7 Cu ion release

To access Cu ions release from coatings, sterilized samples (n = 3) were placed in hermetically closed tubes containing 3 mL of phosphate-buffered saline (PBS) pH 7.4 (Gibco™, Life Technologies, The Netherlands). The tubes were maintained under agitation (90 rpm) at 37 °C, and samples were moved to another tube with 3 mL of fresh solution in defined periods (2 h, 6 h, 24 h, 48 h, 72 h, 96 h, 7 days, 14 days, 28 days, 56 days, and 70 days). Aliquots were diluted in HNO_3 65%, and the Cu release content was measured using ICP-OES [13].

2.8 Cell culture experiments

Two cell lines that have been extensively investigated for their role in the regenerative and wound healing properties were used to assess the biocompatibility of PEO surfaces. Firstly, human bone mesenchymal cells (hBMSC) were isolated and cultured from bone fragments according to an approved ethical protocol (CMO Radboudumc; dossier# 2017-3252), while human umbilical vein endothelial cells (HUVEC-2) were purchased from Becton Dickinson Biosciences (The Netherlands). The hBMSCs were cultured in minimum essential medium eagle – alpha modification (Alpha MEM; Gibco™) supplemented with 10% fetal bovine serum (FBS; Gibco™) and 1% penicillin/streptomycin. HUVECs were cultured in medium 200 (Gibco™) supplemented with 1% penicillin/streptomycin (Gibco™) and a low serum growth supplement (LSGS; Gibco™). Cells were kept in a humidified incubator at 37 °C and 5% CO_2 atmosphere. After cell expansion, a low passage of hBMSCs and HUVECs were counted and seeded on autoclaved discs in triplicate (n = 3) at 2×10^4 and 4×10^4 cells/mL, respectively. Cells were incubated for 1 and 3 days. Then, the cell counting kit 8 (CCK-8; Abcam plc, China) assay was performed according to the manufacturer's protocol. Cells from the same original culture growth on a 24-well plate and culture medium served as a positive and negative control, respectively, and it was used for data calculation. The cell metabolic activity (%) was expressed using the following formula (equation 1):

$$\text{Metabolic Activity \%} = (100 \times OD_{experimental})/OD_{control} \qquad (1)$$

Cell viability was assessed via LIVE/DEAD™ Cell Imaging Kit (Invitrogen™, Life Technologies) following the manufacturer's instructions. The assessment was carried out after a 1-day culture of hBMSCs and HUVECs. Four images from each PEO surface were acquired using a fluorescence microscope (Zeiss AxioImager Z.1, Carl Zeiss Microscopy GmbH). The percentage of live and dead cells was quantified using ImageJ software.

The hBMSCs adhesion to coatings was observed by fluorescence staining as previously described [50]. Briefly, cells were washed twice in PBS and fixed for 20 min with 4% formaldehyde after 1 and 4 days. Alexa Fluor® 568 phalloidin (1:200 dilution; Thermo Fischer Scientific Inc., The Netherlands) was used for the cell cytoskeleton staining (20 min) and 5 mg/mL of 4,6-diamidino-2-phenylindole (DAPI; Sigma-Aldrich) for the nucleus staining (10 min). Samples were washed twice in PBS before analysis. Then, cells were imaged with a fluorescence microscope. Additionally, the number of nuclei was counted

using ImageJ software in four different images, and the quantification of nuclei/mm^2 was calculated.

To check the non-cytotoxicity effect of Cu concentration used, an additional experiment was carried out with different Cu^{2+} concentrations for reference purposes and to understand the dose-response relationship of Cu ions on hBMSC metabolic activity. Copper acetate was chosen as the source due to its ease of dissolution in distilled water and the absence of secondary elements that can influence the results. Thus, copper acetate was used to prepare a 0.1 M stock solution that was filtered with 0.22 μm filter and serially diluted in alpha MEM at final concentrations of 0 μM, 25 μM, 50 μM, 250 μM, and 500 μM. The hBMSC were seeded at a density of 5×10^3 cells/well in a 96–well plate (n = 4). After incubation for 24 h, the culture medium was removed and replaced with the Cu-containing medium. Then, the CCK-8 assay (Tokyo Chemical Industry Co., Japan) was executed as above mentioned after 6 h, 24 h, 48 h, and 72 h.

2.9 Antibacterial assay

The antibacterial activity of PEO coatings was tested against *Streptococcus sanguinis* (strain IAL 1832). *S. sanguinis* is considered an initial colonizer of oral surfaces and dental implant materials [51], presenting an important role in the co-adhesion process of other micro-organisms [52] and has been found in health and disease implant sites [53]. For this investigation, the study was approved by the University Research and Ethics Committee (79224917.0.0000.5418/2017). The experiments were performed following a previous protocol [16]. Briefly, discs (2 independent experiments, n = 3/experiment) were coated with human saliva collected from 3 volunteers to allow protein adsorption and promote microbial adhesion mimicking in vivo conditions. Firstly, the collected saliva was previously centrifuged (10,000g for 10 min at 4 °C) and filter-sterilized to remove microorganism and keep only proteins. Then, discs were transferred to wells containing *S. sanguinis* inoculum (10^7 cells/mL). Samples were incubated for 24 h (10% CO_2 at 37 °C) to form biofilm. Then, samples were vigorously vortexed and sonicated. Finally, solutions were serially diluted and plated to count colony-forming units (CFU). Biofilms were visualized by confocal microscopy. Live/dead cells, biovolume measurements, and three-dimensional (3D) structure analyses of 24 h biofilms were evaluated using CLSM (DMI 6000, Leica Microsystems, Germany) [13,14]. Viable cells were stained using SYTO-9 green-fluorescent nucleic acid (480−500 nm; Thermo Fischer Scientific Inc.), and the nonviable cells were stained with propidium iodide solution (490−635 nm; Sigma-Aldrich). At least 3 random regions were

selected to acquire stacks of the z-plane. Then, 3D images were reconstructed with the IMARIS software (Oxford Instruments plc, UK), and biovolumes (in μm^3) of biofilms were calculated.

2.10 Statistical analyses

Data were analyzed with IBM SPSS Statistics for Windows (IBM SPSS Statistics for Windows, v.21.0., IBM Corp.; USA). The normality of all response variables was tested by the Shapiro-Wilk method. Statistical analyses were performed using one-way ANOVA followed by Tukey's HSD test as a post-hoc technique for multiple comparisons. A mean significant difference at the 0.05 level was adopted for all tests. Final graphs were prepared using GraphPad Prism version 8.0.0 for Windows (GraphPad Software, USA).

3 Results and discussion

Dental implants have faced great advances in the last years regarding surface functionalization aiming to improve cellular responses, osseointegration process, and long-term treatment stability. Studies have focused on achieving the best combination of surface features and function when modifying implants, considering their biocompatibility and antimicrobial efficacy. Herein, we adopted a well-established technique to incorporate bioactive elements with recognized cell-stimulatory and antibacterial effects at cpTi surfaces. We demonstrated that Cu source is a crucial factor influencing physicochemical properties of PEO coatings, which provides a facile way to construct implant coating for desired cell responses and antimicrobial efficacy.

3.1 Cu sources affect structural and chemical features of PEO coatings

The PEO technique used in this study has been widely applied in the biomedical field [19,54] due to the favorable structural properties of resultant coatings. PEO can be utilized for metallic devices with complex geometries such as implants, forming a highly porous, rough, and thick surface modification that is wear-resistant and strongly adherent to the substrate [18]. Herein, coatings were produced by PEO and characterized to verify whether different Cu sources affect coating surface morphology. A porous surface was formed for all groups (Fig. 1a), regardless of the electrolyte composition and Cu source. The pore structures are produced by plasma micro-discharges that lead to substrate melting, eruption, and solidification [43]. As observed, PEO pores can vary regarding shape, size, and density depending on the discharge process.

Three-dimensional images obtained by CLSM (Fig. 1b) show more prominent vertical discrepancies for CuS (8.3 μm) and CuO (7.9 μm), which can be noted by the larger areas in black and dark blue or red and orange color that represent deeper valleys and higher peaks, respectively. In fact, roughness line profiles assessed from the 3D images (Fig. 1c) display a more homogeneous delineation with smaller vertical and horizontal distances between peaks for CuAc and CaP. Confirming these findings, CuS and CuO presented significantly higher surface roughness (Fig. 1d) and area (Fig. 1e) than CuAc and CaP ($p < 0.01$). Whereas CaP and CuAc showed a minimally rough (0.5–1.0 μm) surface, CuO and CuS exhibited a moderately rough (1.0–2.0 μm) profile [55,56]. CuS also exhibited the highest water contact angle among the groups ($p < 0.01$), but all groups displayed hydrophilic properties because of high numbers of hydroxyl (OH^-) groups present in PEO coatings, which makes the surface more wettable [14,16]. Both roughness and wettability are relevant properties to consider in the design of implants due to their role in the first phase of cell-material interactions, especially protein adsorption and bone anchorage [57–59].

Fig. 2 shows micrographs and EDS maps from samples after cross-sectioning. PEO coatings showed a uniform bonding with Ti substrate. All chemical elements were distributed homogeneously along with coating thickness (Fig. 2b). The average coating thickness obtained from micrographs of cross-sectioned samples varied from 4.09 ± 0.41 μm to 7.4 ± 0.82 μm (Fig. 3a). CaP and CuO presented the highest coating thickness across the groups ($p < 0.001$), as suggested by SEM images (Fig. 2a and 2b). Pore features (count, length, and area) were evaluated from SEM micrographs (Fig. S1). Micro-cracks can be observed for PEO coatings as a result of residual stress caused by the fast solidification of the molten substrate. CuAc had statistically significant more pores/cm^2 compared to the other groups ($p < 0.01$; Fig. 3c). This difference is mainly due to a higher number of small pores in the order of 1-2 μm^2 (Fig. 3b). On the other hand, CaP and CuO showed fewer but larger pores, reaching sizes exceeding 6 μm^2. Pores in PEO coatings are known to vary substantially in size and distribution, typically becoming larger and more dispersed as the coating thickness increases [18].

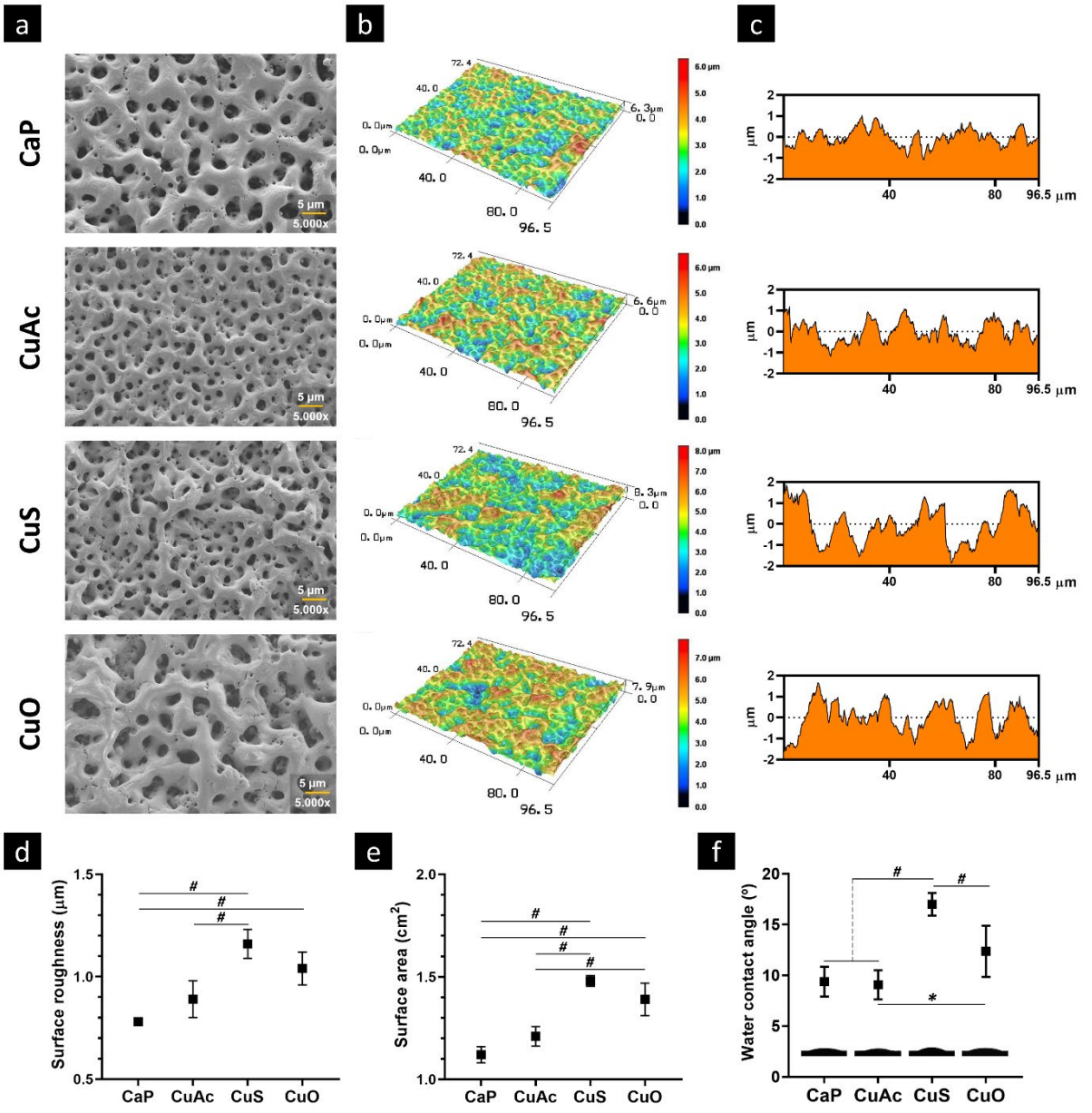

Fig. 1. Topographic characterization of PEO coatings. The surface morphology was inspected by (a) scanning electron microscopy (bar = 5 µm, 5000× magnification, WD = 12 mm, 3 kV). (b) Representative three-dimensional images and (c) roughness profile from each group obtained by confocal laser scanning microscopy (CLSM; 150× of magnification). (d) Surface roughness and (e) surface area were calculated from CLSM two-dimensional images (n = 3). (f) Water contact angle (n = 5) values and water drops onto PEO surfaces. Data are expressed as mean ±standard deviation. Statistically significant differences between groups are indicated by symbols: *$p < 0.05$, $^{\#}p < 0.01$.

Several factors may influence coating morphology, particularly electrolyte composition and conductivity. Herein, the high concentration of salts from CuAc and CuS sources enhanced the electrical conductivity of treatment solutions (Table 1), which affected the growth of PEO coatings and pore count and size (Fig. 3d). It is known that in solutions with high electrical conductivity, the applied voltage drops across the electrolyte due to an insulating barrier action, reducing the potential to create the (breakdown) field across the oxide layer and form the coating [18]. In line with this, CuAc and CuS led to higher values of electrolyte conductivity and hence thinner coatings because of the lower effectiveness of the applied potential. During the PEO process, a 'bubble' of water vapor grows at the top of the pore channel, where the discharge current is forced to flow through. The number of plasma discharges increases along with the increase of the electrolyte concentration, but the size of the gas bubble reduces, as well as the applied potential falls across the solution, as its conductivity increases [43]. Thus, a higher number of plasma micro-discharges with lower intensities may be observed for CuAc and CuS, forming a higher number of pores of smaller sizes [30,60]. On the other hand, as the discharge intensity becomes higher, more coating and substrate will be melted, and more gases will be generated, forming larger pore structures as found for CaP and CuO. Also, the temperature and the yield of the melt increase as the discharge intensity rises, which increases the reflux ability of the melt that can refill and block the discharge channels, lowering the porosity of the coating [43].

The pores formed in PEO coatings and their surface chemistry are known to enhance protein adsorption [14,16,46,61], which is a fundamental step in the interaction of implantable biomaterials with the biological environment guiding the following biologic and molecular processes [58]. Even though bigger pore structures can provide favorable space for cell migration and growth [5], a higher pore count may be capable of increasing the adsorption of proteins due to an enhanced number of active sites [58] and a larger surface area. Correlating with roughness, CuS showed a moderately rough surface with a higher area that can improve bone-material interactions by biomechanical interlocking [62] and, consequently, provides high primary stability that creates possibilities for early loading [55,63]. On the other hand, the less rough surfaces observed for CuAc may mediate the best combinatory activity of cells involved in the bone formation and remodeling around the implant [64].

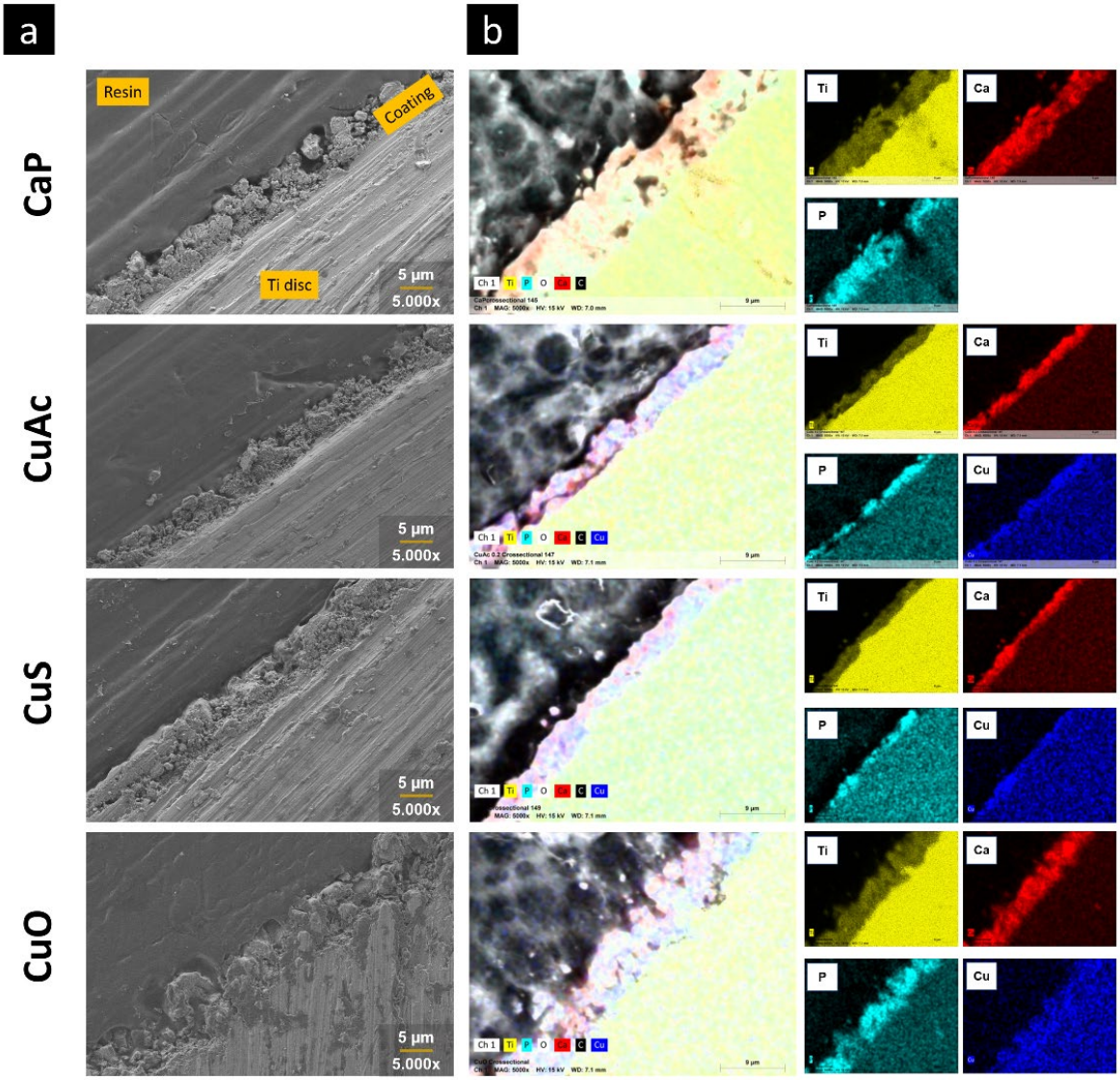

Fig. 2. Cross-sectional analyses of PEO coatings. (a) SEM micrographs (bar = 5 µm, 5000× magnification, WD = 7 mm, 3 kV) and (b) EDS maps of cross-sectioned samples, merged (left) and individual elements (right) (n = 1).

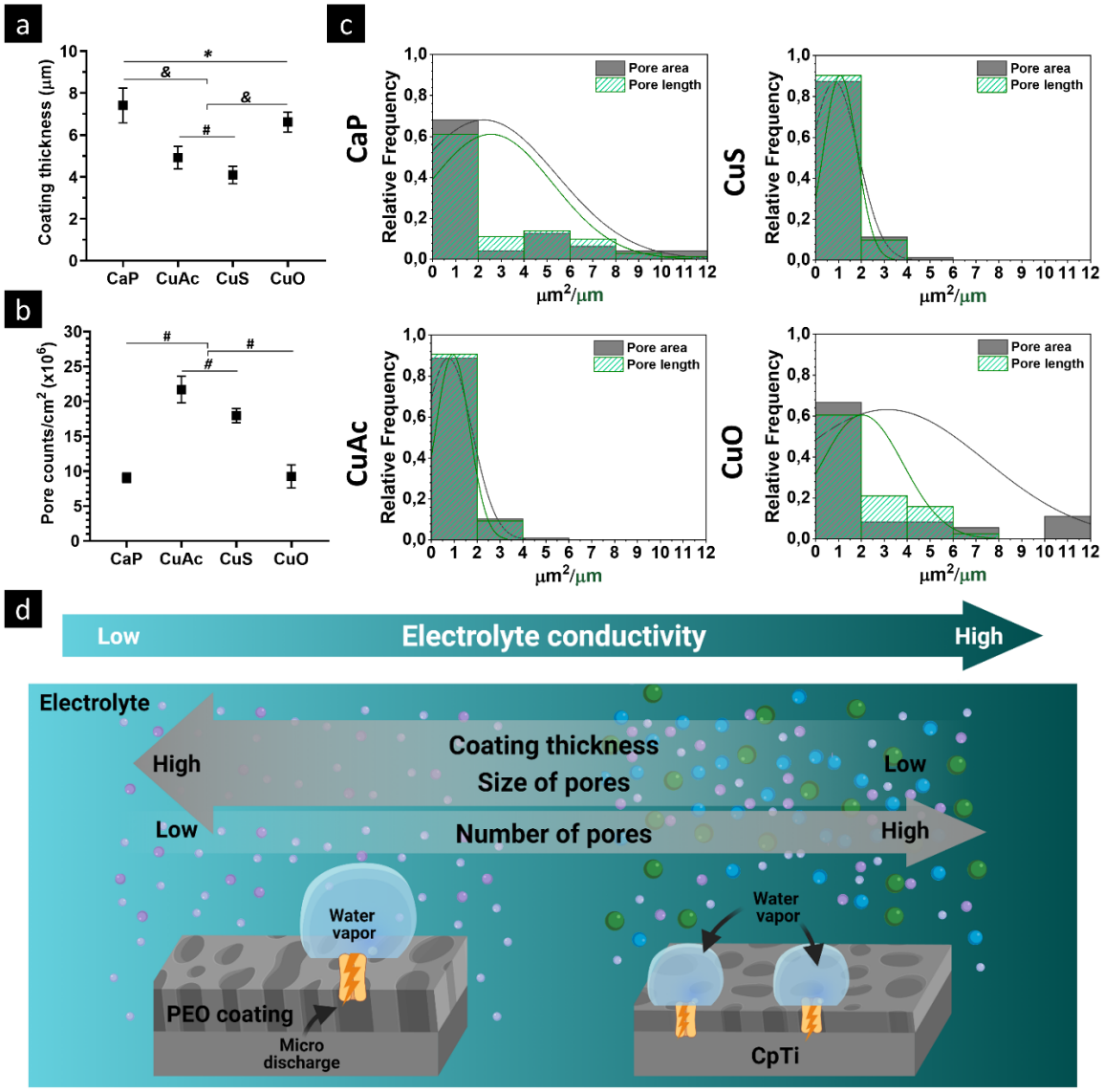

Fig. 3. PEO coating features. (a) Coating thickness was measured from SEM cross-sectional micrographs (n = 5) from Fig. 2a. (b) Pores area, length, and (c) count were calculated from micrographs of 10,000× magnification (Fig. S1; n = 5). (d) Schematic representation of pores formation considering the electrolyte conductivity: higher solutes element concentration (colored spheres) and hence increased electrical conductivity of the electrolyte forms an insulating barrier around the sample. The electrical resistance of this barrier decreases the applied voltage and micro-discharge intensity and, consequently, impairs the growth (thickness) of the coating. In electrolytes with higher conductivity, a higher frequency of micro-discharges with a lower intensity may be generated, creating a higher number of pores but with smaller sizes. Data are expressed as mean ± standard deviation. Statistically significant differences between groups are indicated by symbols: *$p < 0.05$, $^{\#}p < 0.01$, $^{\S}p < 0.001$.

Besides altering the topography, the electrolyte composed of different Cu sources may influence the coating chemical composition. XPS analysis (Fig. 4, Table 2) was used to access the oxidation states of the elements composing the PEO coating, while the EDS technique was employed to confirm their element composition (Table S1; Fig. 5a). Besides the elements added to the electrolyte (Ca, P, Cu, and S), Ti was also incorporated within the coating. Fig. 4 represents the deconvoluted O1s, Ti2p, Cu2p, Ca2p, P2p, and C1s spectra from each group, and Table 2 shows the atomic concentration (%) of the elements composing the coatings. The band S2p was also found for the CuS group (Fig. S2). The presence of approximately 65 at.% of oxygen in both techniques confirms the complete oxidation of the surface layer by the PEO process [12], which can be verified by the absence of metallic peaks of Ti. The oxide states were formed by Ti (TiO_2 at 458.7 eV), Cu (Cu_2O at 931.5 eV and CuO at 933.4), Ca (CaO at 347.1 eV), and P (PO_4 at 14.4 eV). Moreover, two shake-up satellite peaks of Cu(II) from CuO phase were detected at ≈ 939 eV and 942 eV. A similar distribution of the elements and oxide states can be observed among the coatings, but a higher proportion of the CuO phase, from 5% to 13%, was displayed by the CuS group. Other components detected are related to calcium phosphate, surface hydroxyl and O-C, O-C=O, and C-H derived from environmental contamination.

Herein, Ca and P elements were chosen to compose the electrolyte to create a coating that has similarities with bone mineral in terms of chemical composition (hydroxyapatite and/or calcium phosphates) and structure (hierarchical topography), which are known to have osteoconductive properties and facilitate the integration between the material and tissue, respectively [42]. Accordingly, these elements may compensate the negative effects of Cu while maintaining the optimum antibacterial activity [5]. Few PEO coatings containing Cu have incorporated concomitantly Ca as a bioactive element due to their competitive reactions in the electrolyte and on the anode. To avoid this behavior, EDTA was employed as a chelating agent since it can combine with cations in the solution and turn them negatively charged for entering into the coating by diffusion and electromigration [65].

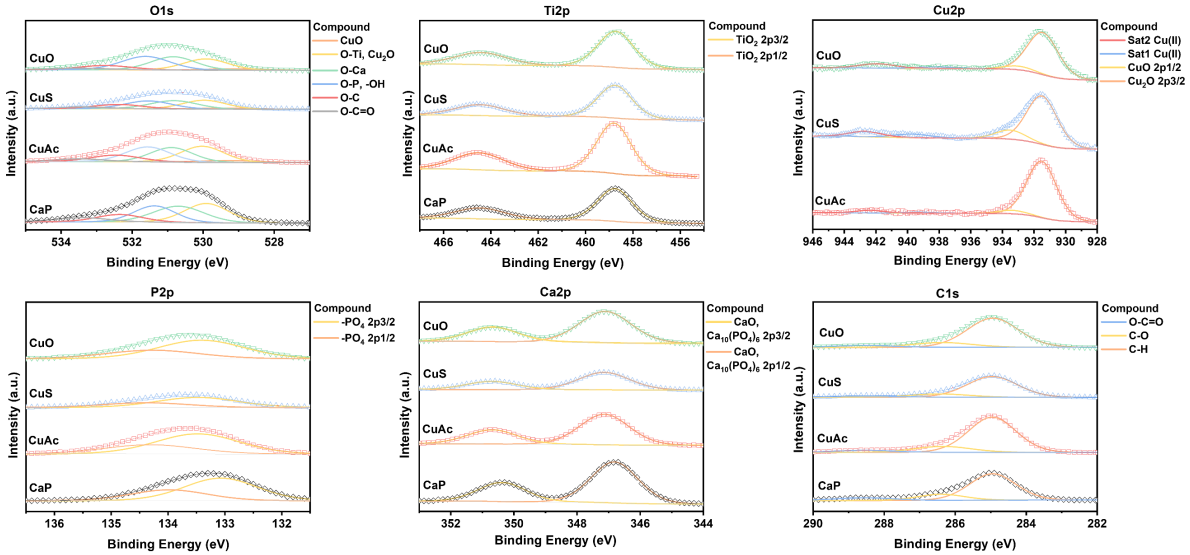

Fig. 4. XPS spectra of PEO coatings (n = 1).

Table 2. Atomic concentration (%) of the elements composing the PEO coatings obtained by X-ray photoelectron spectroscopy (n = 1) after correction using the C1s spectrum.

Peak	CaP	CuAc	CuS	CuO
O1s	67.4	65.2	62.5	63.7
Ti2p	12.5	11.6	12.4	9.9
Ca2p	10.5	9.2	8.8	11.3
P2p	9.6	10.9	8.8	11.9
Cu2p	-	3.1	5.6	3.2
S2p	-	-	2.0	-
Ca/P	1.1	0.8	1.0	0.9

Note: Data extracted from high resolution spectra. Error: ±5%.

Since EDS is a semiquantitative method and XPS only represents the outmost oxide layer of the sample, coatings were digested to quantify their full chemical composition by ICP-OES (Fig. 5b). Fig. S3 shows the micrographs after coating digestion. It is apparent that the pores produced during the micro-discharges grew into the substrate, but the remaining Cu in the surface was extremely low (0.02-0.03 at.%), confirming the near-complete dissolution of coatings. Although Cu was incorporated to achieve ~1 at.% for all groups (Table S1), CuO had a significantly lower Cu concentration (83.77 ± 2.27 μg) in its composition compared to CuS (118.92 ± 5.74 μg) and CuAc (108.50 ± 8.75 μg; $p < 0.001$). Considering that in the PEO process, an electric field between the anode and the cathode pushes the negatively charged

complexes toward the anode where the oxidation reaction takes place [60], the high Cu concentration in CuS and CuAc may be related to higher amounts of Cu ions in the electrolyte and their superior conductivity that promotes the electromigration of Cu ions into the coating. In addition, the presence of SO_4^{2-} and CH_3COO^- complexes associated with EDTA as a chelating agent in the electrolyte may participate in reactions with Cu species to form a complex anion that could promote its migration towards the anode, consequently increasing Cu content [40,43]. The same can be stated for the higher Ca content incorporated in the CuS group and, hence, its higher Ca/P ratio ($p < 0.001$; Fig. 5c). The differences found between EDS/XPS data and ICP-OES quantification are related to the fact that the first techniques consider only a small order of the coating, and the atomic element weight of all elements influences their proportion on the surface. On the other hand, the ICP-OES assessment contemplated the whole coating and identifies elements individually.

Concerning PEO crystalline composition, all surfaces exhibited similar diffraction peaks for anatase (~25°; JCPDS 83-2243) and rutile (~27°; JCPDS 73-1765) TiO_2 phases (Fig. 5d). The presence of both phases simultaneously in coatings for dental implants has shown to be the best strategy to improve the physico-chemical and biological properties of cpTi surfaces [66]. While the anatase phase has been associated with superior biocompatibility [59], rutile is strongly related to increasing coating resistance [15,49]. It seems that Ca, P, and Cu may exist only in amorphous states since no specific peak was identified. CaP and CuO coating present the highest intensity for the rutile phase, while CuAc showed larger peaks for anatase. The rutile to anatase ratio depends on several factors, such as the discharge strength and the temperatures and pressures generated by the sparks that could transform anatase to rutile. The coating thickness is another factor that influences TiO_2 crystallinity since as the oxide becomes thicker, its resistivity increases, therefore a more powerful driven voltage is needed to keep the high current [67] and, therefore, a higher level of anatase to rutile transformation occurs. CuS seems to have the lowest degree of crystallinity, probably due to its reduced coating thickness [65] and increased amorphous Ca-P phases that present insulating properties that may inhibit TiO_2 crystallinity.

Fig. 5e shows the cumulative release profile of Cu in PBS over 70 days. Cu ions into the sample surface may diffuse into the solution upon immersion by gradual dissolution and/or reaction with OH^- in the solution [35]. Cu-containing coatings showed similar Cu release profiles in PBS, but with a higher absolute release for CuS followed by CuAc and CuO. This result may be related to the larger surface area of the CuS group that already has a higher Cu concentration. In general, a high Cu^{2+} release was observed in the first hours, keeping sharp

until 4 days, but not in the general "burst" way that may evoke cytotoxicity in the short term [5]. Less than 3% of Cu was released from the coatings for 7 days (Fig. S4). After that, the release continued steadily increasing without a clear plateau, proving that PEO coatings provide a sustained Cu^{2+}release for at least 10 weeks. This release profile may guarantee continued antibacterial action and stimulation of cells during and after the remodeling phase, which represents the best scenario for the long-term success of an implant [57].

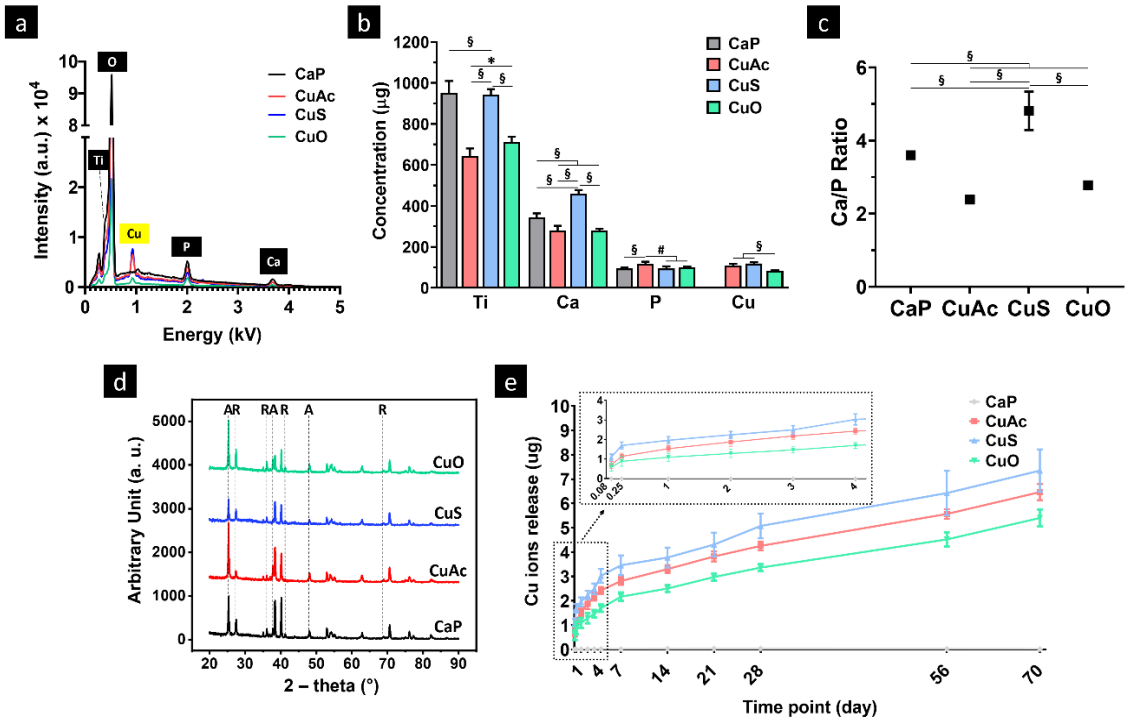

Fig. 5. Chemical composition and Cu release profile of PEO coating. (a) EDS spectra (n = 1). (b) Chemical elements concentration and (c) Ca/P ratio quantified by ICP-OES after coating digestion (n = 3). (d) XRD diffraction (n = 1) and (e) Cu ions release in PBS over 10 weeks (n = 3). A = anatase, and R = rutile. Data are expressed as mean ±standard deviation. Please note that some standard deviations are too small to be seen. Statistically significant differences between groups are indicated by symbols: *$p < 0.05$, $^{\#}p < 0.01$, $^{\S}p < 0.001$.

3.2 Cu sources influence cells response of PEO coatings

The effect of Cu-containing coatings on cell behavior was assessed with hBMSCs (Fig. 6) and HUVECs (Fig. 7). Cu-containing coatings did not significantly affect the metabolic activity of hBMSC compared to CaP on days 1 and 3, except for the CuS group that slightly decreased cell activity (86.00 ± 2.52 %) compared to CaP (100.00 ± 7.42 %) after day 1 of

culture ($p < 0.05$; Fig. 6a). Although CuS continued evoking lower cell metabolic activity (75.65 ± 4.53) among groups on day 3, it cannot be considered cytotoxic. The Live/Dead assay (Fig. 6b) also suggests acceptable in vitro cytocompatibility of all coatings. Besides not affecting cell metabolic activity, CuAc had considerably fewer dead cells on the surface after day 1 (Fig. 6c). None of the surfaces impaired cell adhesion and spreading after 1 and 4 days (Fig. 6d). Cells cultured on the surfaces also displayed an organized cytoskeleton with well-developed stress actin fibers that turned a more elongated spindle shape after day 4 [5], reflecting adequate cell behavior. In general, cells might extend across the microporous structure to be anchored on the surface, forming a bridge structure, and then spread out in the region between pores or directly into the pores through the filamentous and tabular pseudopodia [5]. After day 4, a significantly higher number of cells was observed for CuAc and CuO ($p < 0.05$; Fig. 6e), demonstrating that these coatings provide an appropriate surface (chemistry, roughness, and Cu release) for cellular adhesion and proliferation.

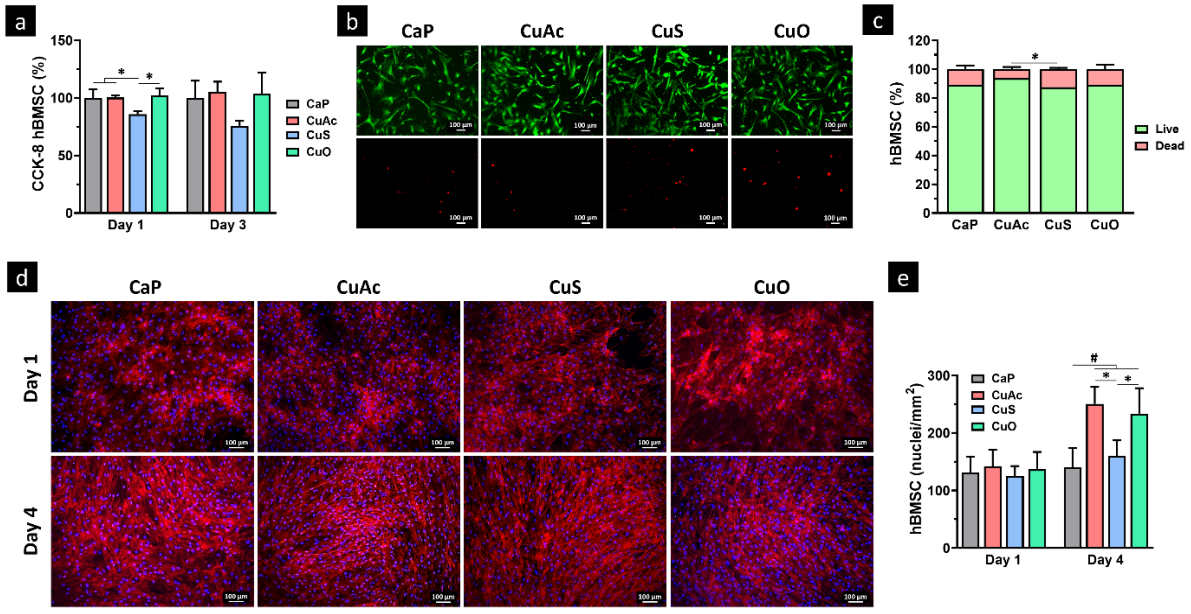

Fig. 6. Effect of PEO surfaces on hBMSCs. (a) Cell metabolic activity (%) evaluated by CCK- 8 assay (n = 3). (b) Cell viability (n = 1) after 1 day of culture via live/dead analysis (green for live cells, red for dead cells). (c) Percentage of live and dead cells on surfaces after 1 day of culture assessed from fluorescence images (n = 3). (d) hBMSC adhesion on coating surfaces after days 1 and 4 (cell nuclei are stained in blue and the cell cytoskeleton in red). (e) Quantification of nuclei from fluorescence images (n = 3). Data are expressed as mean ±standard deviation. Statistically significant differences between groups are indicated by symbols: *$p < 0.05$, #$p < 0.01$.

Cu-containing surfaces had a noticeable effect on HUVECs metabolism. After day 1, all experimental groups reduced cell metabolic activity compared to CaP, but strong recovery at the third day of culture, except for CuS that continued showing a statistically significant difference with controls ($p < 0.05$; Fig. 7a), possibly due to the higher Cu^{2+} concentration in this group. Regardless of metabolism reduction, the experimental surfaces were not cytotoxic to HUVECs after day 1, meaning that the Cu levels released from coatings are within a safe concentration for endothelial cell growth [5]. Actually, CuAc and CuO showed a higher number of cells on their surface (Fig. 7b) and significantly fewer dead cells (Fig. 7c; $p < 0.05$), showing that their surface and Cu^{2+} concentration may be more favorable to HUVECs. These outcomes may be predictive for their ability to stimulate angiogenesis and wound-healing processes since Cu ions have been found to bind and interact with several growth factors involved in blood vessel formation [68]. Besides, the surfaces developed in this study display innate characteristics (tailoring pore structure and physico-chemical properties) favorable for angiogenic responses [4].

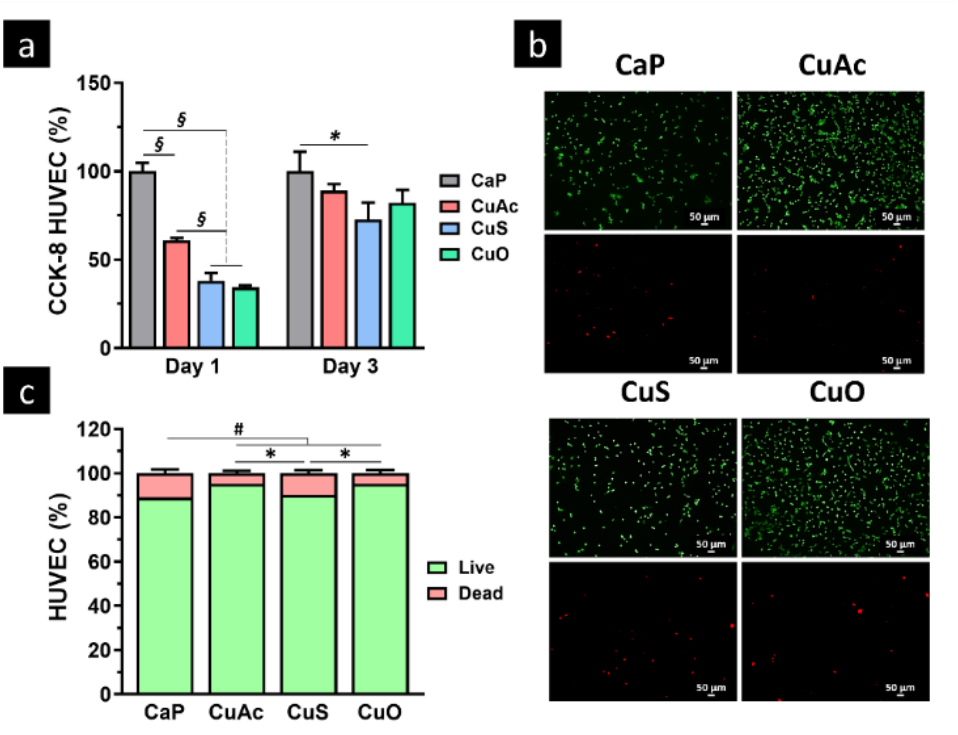

Fig. 7. Effect of PEO surfaces on HUVECs. (a) Cell metabolic activity (%) evaluated by CCK- 8 assay (n = 3). (b) Cell viability (n = 1) after 1 day of culture via live/dead analysis (green for live cells, red for dead cells). (c) Percentage of live and dead cells on surfaces after 1 day of culture assessed from fluorescence images (n = 3). Data are expressed as mean

±standard deviation. Statistically significant differences are indicated by symbols: *$p < 0.05$, $^{\#}p < 0.01$, $^{\S}p < 0.001$.

Besides surface topography, the results obtained with the cell culture experiments can be related to the slight difference in Cu concentration at the surface among groups, since it has been reported that PEO surfaces with lower concentrations of Cu can promote the adhesion and proliferation of cells, while surfaces with higher Cu content may be cytotoxic [5,29,35,38]. As reported previously [37], the role of Cu on hBMSCs proliferation and expression of osteogenic markers only was detected at a narrow concentration range (50 μM to 300 μM). In general, the release of Cu^{2+} observed in this study is not cytotoxic for hBMSCs, considering the experiment evaluating different levels of copper acetate in a culture medium (Fig. S5). The metabolic activity of hBMSCs started to reduce from 500 μM, which only could be reached with the total release of Cu present in the PEO coating. However, the sensitivity of hBMSCs to Cu may depend on the culture medium [37], since the presence of proteins can stimulate coating dissolution and Cu release. Nevertheless, it is important to point out that the Cu ion release here is not the only factor affecting cell behavior since Cu's mere presence on the surface might also present a robust cytotoxic effect. Additionally, we expect similar behavior of developed coatings on cell viability for more extended periods, since the highest amount of copper was released on the first day after incubation, and the release after 3 days is lower and very stably, suggesting that after 3 days, the concentration of Cu in the medium would not cause any harm to cells.

3.3 Antibacterial efficacy of PEO coatings are optimized by Cu sources

Cu-containing coatings demonstrated effective antibacterial activity against an important early colonizer of dental implants and oral surfaces (*S. sanguinis*) compared to CaP control. Inhibiting the adhesion of early colonizers might limit or weaken the attachment of late colonizers and co-aggregation processes and, thereby, the biofilm accumulation and maturation. CuAc significantly reduced almost 2 logs of CFU counts after 24 h of biofilm formation ($p < 0.001$), while CuO and CuS showed ~ 1.2-log reduction ($p < 0.01$; Fig. 8a). These results follow the CLSM images of the live/dead assay, in which a denser *S. sanguinis* biofilm can be observed on CaP after 24 h. In fact, all Cu containing experimental groups presented significantly lower live biovolume on their surface compared to control ($p < 0.05$), which can be related to the release- and contact-killing mechanism of Cu^{2+} [5,29]. *S.*

sanguinis is a gram-positive bacteria with a negatively charged cell surface due to the peptidoglycan layer (20–80 nm), which can easily absorb foreign material [28]. On the other hand, Cu^{2+} is a positively charged ion and thus attracted to negatively charged surfaces. Therefore, the mechanism behind Cu^{2+} antibacterial action may be associated with its release and entering into microbial cells or attachment to the charged outer surfaces by electrostatic attraction, resulting in cell membrane disruption, loss of cytoplasmic content, or production of reactive oxygen species (ROS) that leads to apoptosis via protein denaturation and DNA damage [30,68]. Also, Cu ions might impair the activity of respiratory chains and disturb the process of gene replication of the bacteria [35].

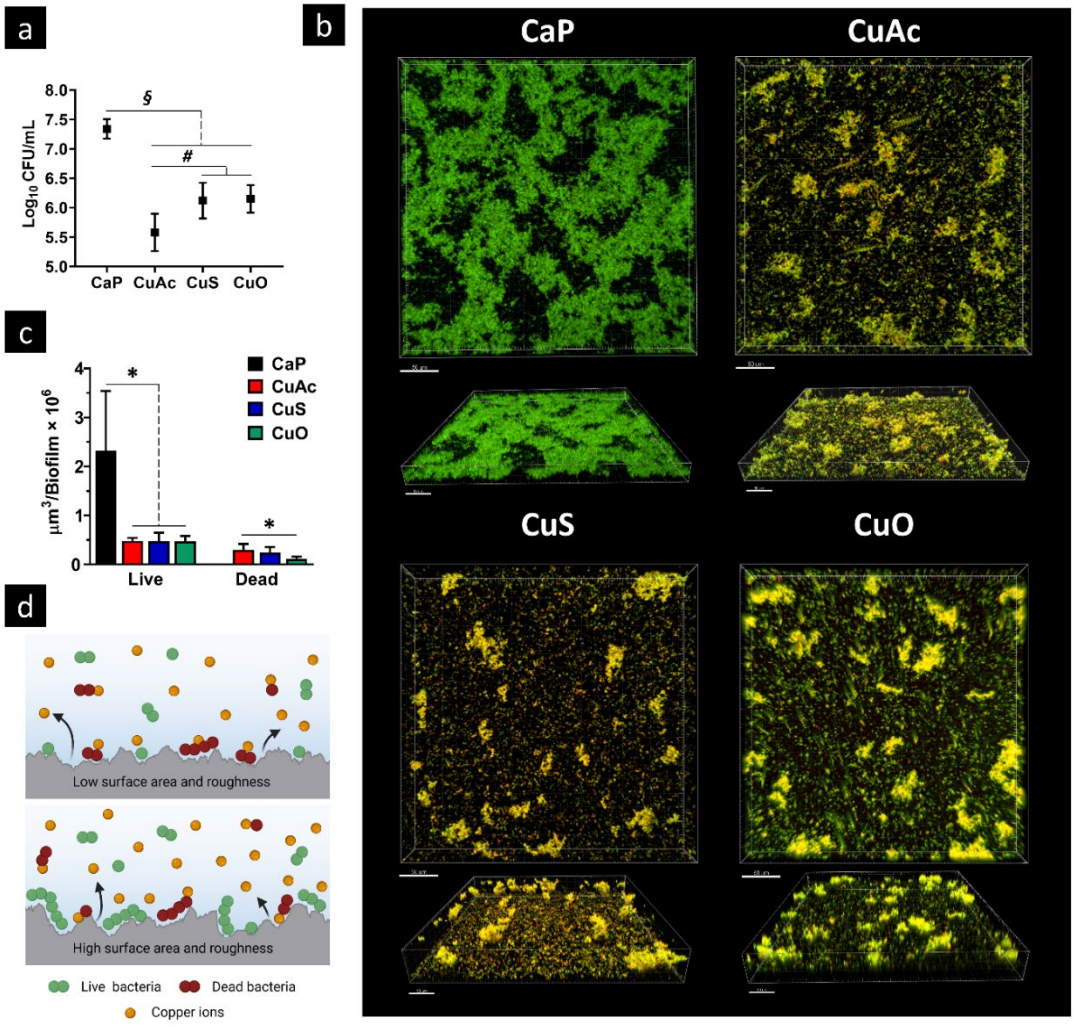

Fig. 8. Antibacterial activity of PEO coatings on *Streptococcus sanguinis* biofilm. (a) Colony-forming units count (Log_{10} CFU/mL) of *S. sanguinis* after 24 h of biofilm formation. (b) Two- (top) and three-dimensional images reconstructions (bottom) of live/dead bacteria after 24 h of *S. sanguinis* biofilm formation. Images were obtained by fluorescence staining (green for

live bacteria, red for dead bacteria) and merge of green and red channels. Scale bars are 50 μm for X–Y surfaces and 70 μm for three-dimensional reconstructions. (c) Biovolume (μm^3) of live and dead cells after 24 h of *S sanguinis* biofilm quantified from fluorescence images. (d) Schematic representation of bacteria adhesion to Cu-containing coatings with different surface areas and roughness. Data are expressed as mean ±standard deviation. Statistically significant differences between groups are indicated by symbols: *$p < 0.05$, #$p < 0.01$, §$p < 0.001$.

Among the experimental coatings, CuAc showed more dead bacterial cells than CuO by viable counts ($p < 0.05$). The difference in antibacterial effects among groups may be attributed to differences in surface chemistry, morphology, and roughness that are able to influence biofilm formation. For instance, a strong difference in contact killing behavior has been shown between CuO and Cu_2O with higher antimicrobial efficacy for Cu_2O [69]. This can be one of the reasons the CuS group showed lower antibacterial activity, even presenting a higher Cu content in its composition, which is mainly due to a higher concentration of CuO phase compared to CuAc as observed by XPS analysis. The higher tendency of bacterial adhesion to CuS and CuO surfaces due to a higher roughness and contact area between the coating and cells might be the other reason for the diminished antibacterial activity for these groups compared to CuAc (Fig. 8d). A previous study showed that smaller pores (15-25 nm) can even reduce bacterial attachment [70]. In this study, CuAc showed the highest number of pores smaller than 1 μm. Specifically, pores dimension does not seem to influence considerable the bacteria attachment once it presents a smaller size than the pore (Fig. S6). But the general complex geometry with increased roughness found for the CuS group tends to increase the formation of bacteria clusters. Generally, an increase in surface roughness can affect the *in vivo* rate of biofilm formation by protecting the bacteria against shear forces and facilitating it to reach an irreversible attachment (firm anchorage) on the material [71]. Roughness has been the most evaluated surface property to affect microbial adhesion to Ti surfaces [7], being one of the major factors underlying the adherence of bacteria to the samples in the initial phases of biofilm formation [14].

3.4 Implications and future perspectives

Several approaches to designing biocompatible surfaces with an antimicrobial activity or limited microbial adhesion have been focused on how human cells and bacteria interact with

the material surface characteristics, such as electrostatic interaction, surface energy, wettability, composition, pH, and topography [6,7]. Tailoring surface properties may be a strategy to control or affect biofilm accumulation or even microbial composition, and in turn, avoiding peri-implant infections [72], essentially when considering that the fabrication of bioactive and antimicrobial coatings cannot only lead to bacteria-killing but also induce the growth and proliferation of cells at the site of implantation, improving the tissue integration.

In this study, we applied a feasible and straightforward one-step technique to produce an implant surface that mimics some of the inherent features of native bone minerals. Based on our findings, altering the electrolyte composition of the PEO process when incorporating functional elements can change coating features and hence affect coating effects on the biological environment. Thus, the selection of the right functional elements and source should be considered comprehensively by researchers that are developing and/or optimizing novel PEO coatings for implant surfaces.

CuAc coatings showed promising results compared to the other groups by increasing hBMSCs and HUVECs adhesion and proliferation to the material surface. Both cell types are involved in the bone healing process after implantation through the secretion of factors that stimulate endogenous repair processes or through direct contribution to vascularization, which is essential to form new bone [37,63,73]. This finding is not only due to the chemical composition of the coating, but also related to its physical properties, such as hydrophilic profile, which enhances cell attachment. Evaluations of how these surfaces work, activating molecular constituents and cells involved in the regeneration/osseointegration process still need to be addressed in future studies.

Concerning the intrinsic antibacterial activity of Cu-containing coatings, the release mechanism of Cu^{2+} presented in this study could minimize two critical periods associated with implants' biological complications. First, the substantial Cu release below the cytotoxic level in the first days is crucial for dental implant rehabilitation to effectively control microbial adhesion and accumulation at the initial stage of osseointegration, then the sustained release over 10 weeks is also essential to prevent the bacterial infection along with the gradual improvement of host defense ability [5]. Although minimally instead of moderately rough surfaces would not help prevent peri-implantitis [74], our data indicate that optimizing the surface chemistry and topography of coatings presenting antibacterial components is a straightforward alternative to reduce the biofilm formation and possibly to avoid implant-related infections. Despite the Cu-containing coatings having confirmed antimicrobial effects, most studies follow methodologies only useful for initial screening

purposes. In order to validate these results and make this coating clinically available, comprehensive investigations are necessary that consider co-culture models, the long-term results, and reusability of the coating, as well as the diversity of the oral microbiome and, especially, *in vivo* models and clinical trials [2,7].

4 Conclusions

Cu-containing PEO coatings were developed employing different Cu sources and systematically characterized to further understand how the PEO process can be controlled to optimize biological responses and antibacterial function. Cu sources were capable of affecting PEO coatings morphology and composition, also influencing their effect on human cells and bacteria. Although Cu-containing coatings seem to decrease cell metabolic activity on the first day, they do not evoke cytotoxic effects. Actually, CuAc and CuO groups improved hBMSC and HUVECs interaction with the substrate compared to CuS. The bacteria number and biovolume of Cu-containing coatings were concentration- and roughness-dependent. The surface formed by CuAc exhibited an optimized topography that led to an optimal outcome in terms of antimicrobial activity, which could prevent early implant infections that are known to compromise treatment success. Overall, choosing the appropriate functional source to form PEO biomimetic coatings represents a valuable strategy to reduce biofilm development and enhance cell response to dental implant surfaces.

Acknowledgments

This work was supported by the São Paulo Research Foundation (FAPESP) – Brazil (grant numbers 2017/01320-0 and 2018/14117-0), the Conselho Nacional de Desenvolvimento Científico e Tecnológico – Brazil (CNPq) (grant number 304853/2018-60), and the Coordenação de Aperfeiçoamento de Pessoal de Nível Superior – Brasil (CAPES) (Finance Code 001). The authors also express their gratitude to the Laboratory of Technological Plasmas at the Univ. Estadual Paulista (UNESP), the Oral Biochemistry Lab at Piracicaba Dental School (UNICAMP) for the microbiology facility, the Regenerative Biomaterials Lab at the Radboud University Medical Center (Radboudumc), Prof. Peter Hammer from the Laboratory of Photoelectron Spectroscopy (LEFE) at the UNESP for the XPS facility, and the LNNano – Brazilian Nanotechnology National Laboratory (CNPEM/MCTI) for the use of the CLSM open-access facility. We also thank Dra. Martinna Bertolini for her contribution to the

3D reconstruction of the live/dead images with the IMARIS software. Graphical abstract, Fig. 4d and Fig. 8d were created with BioRender®.

Supplementary material

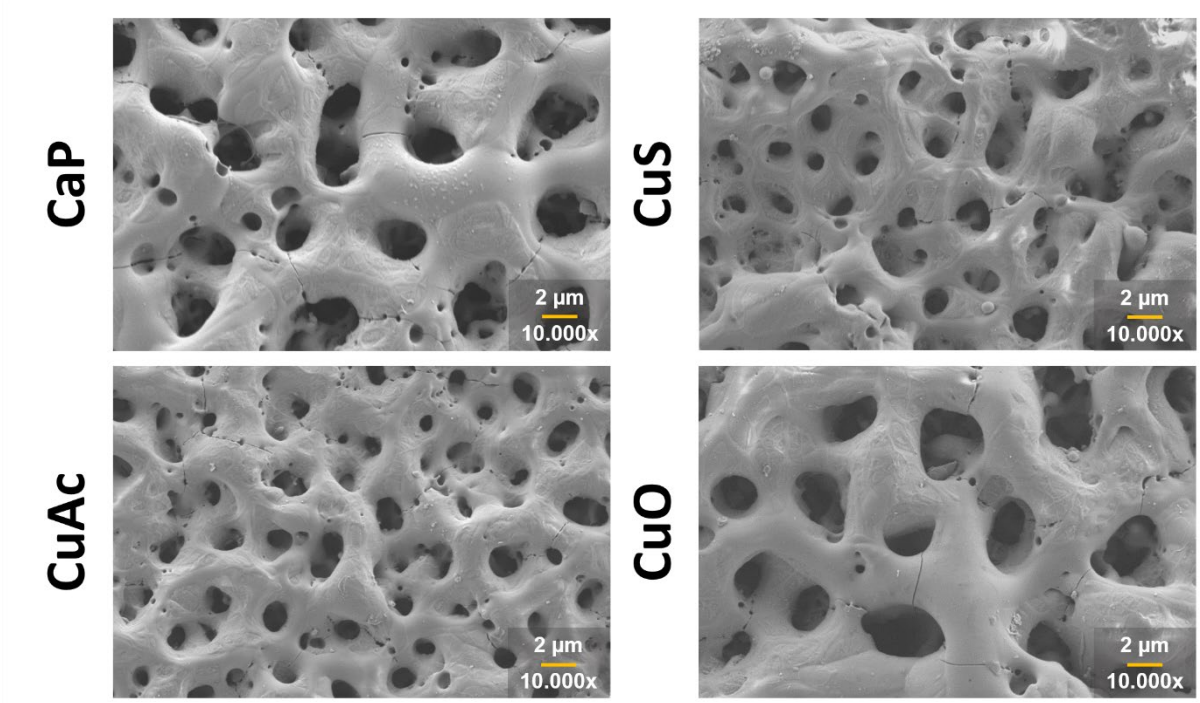

Fig. S1. Scanning electron micrographs of PEO surfaces (10.000 ×).

Table S1. Semiquantitative element concentration (at.%) of PEO coatings measured by energy-dispersive X-ray spectroscopy (EDS).

Element	Groups			
	CaP	**CuAc**	**CuS**	**CuO**
Ti	20.51 ± 0.15	18.99 ± 0.11	22.52 ± 0.59	14.08 ± 1.59
O	66.83 ± 0.28	67.65 ± 0.10	66.09 ± 0.37	67.76 ± 0.17
Ca	8.99 ± 0.16	7.88 ± 0.19	7.16 ± 0.15	10.12 ± 0.79
P	3.68 ± 0.06	4.45 ± 0.12	3.08 ± 0.19	7.03 ± 0.63
Cu	-	1.02 ± 0.06	1.01 ± 0.01	1.00 ± 0.05
S	-	-	0.14 ± 0.02	-
Ca/P	2.45 ± 0.06	1.77 ± 0.02	2.33 ± 0.15	1.44 ± 0.04

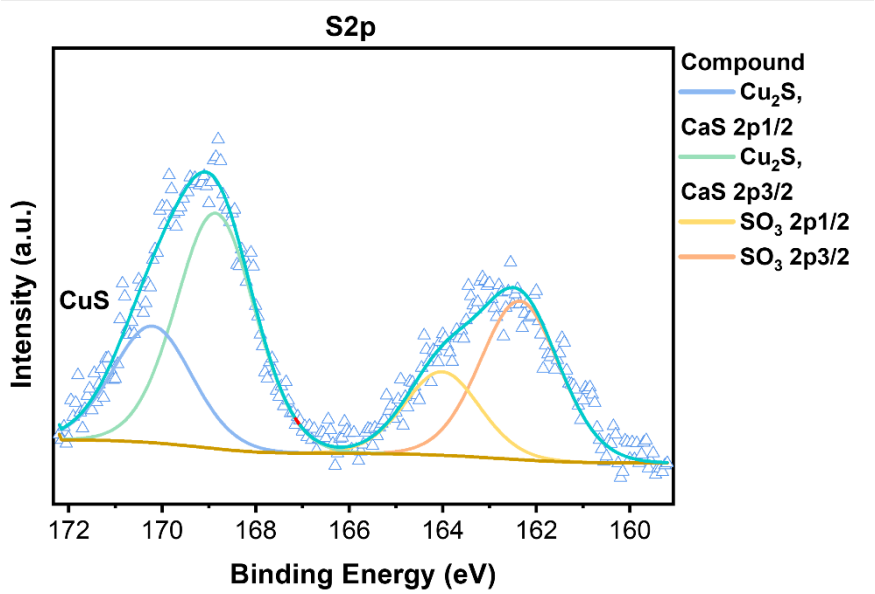

Fig. S3. XPS spectra of S2p band from the CuS group.

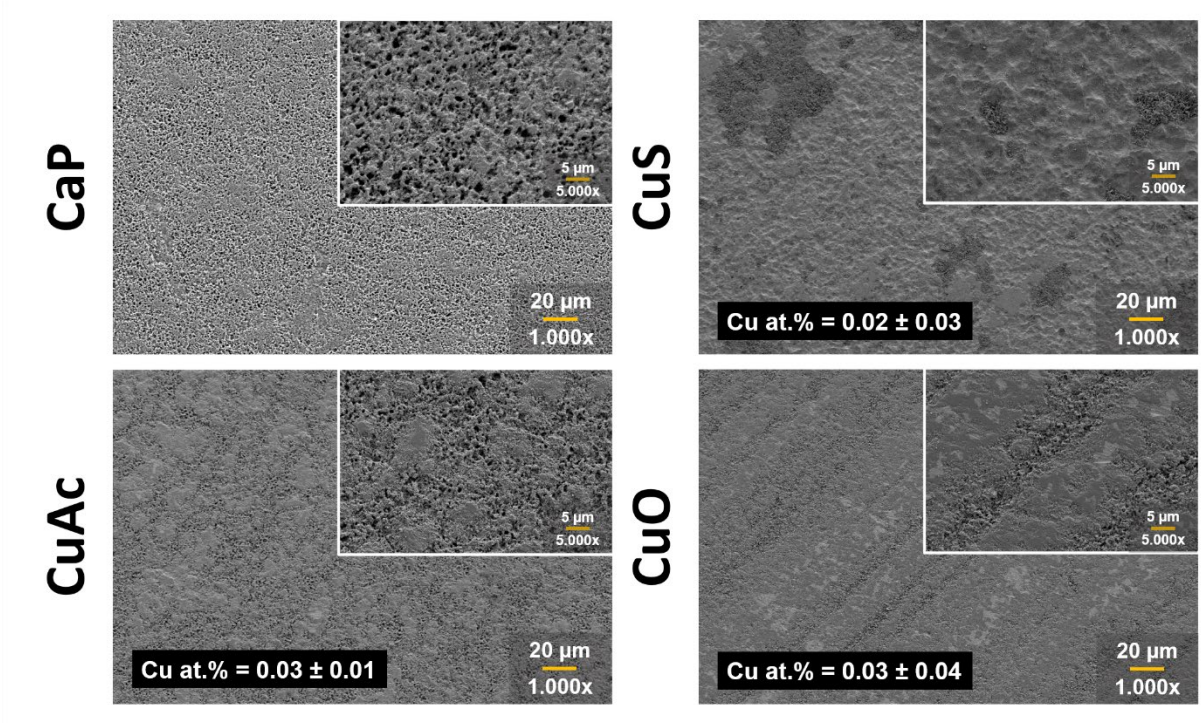

Fig. S3. Scanning electron micrographs of samples and Cu concentration (at.%) obtained by EDS after coating dissolution process.

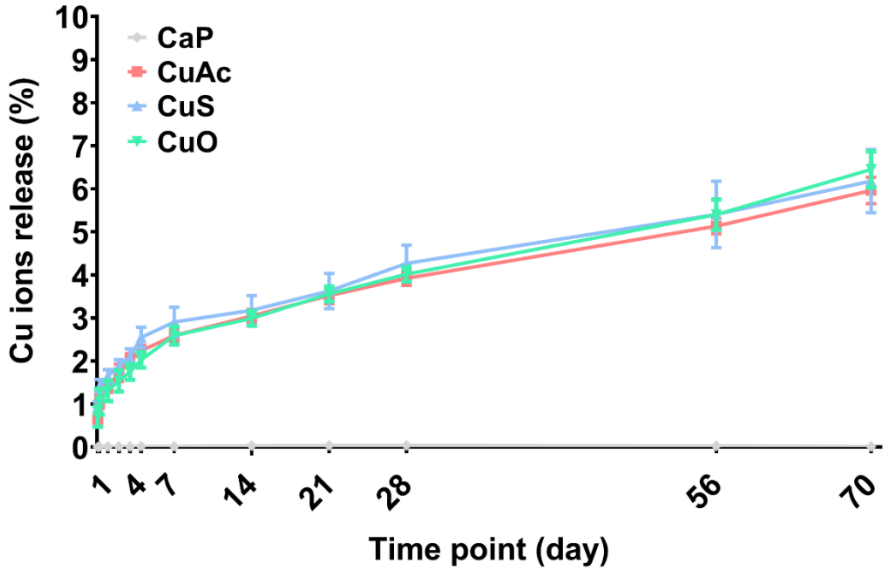

Fig. S4. Cu ions release in PBS over 10 weeks expressed in percentage to the total Cu concentration in the coatings. Data are expressed as mean ±standard deviation.

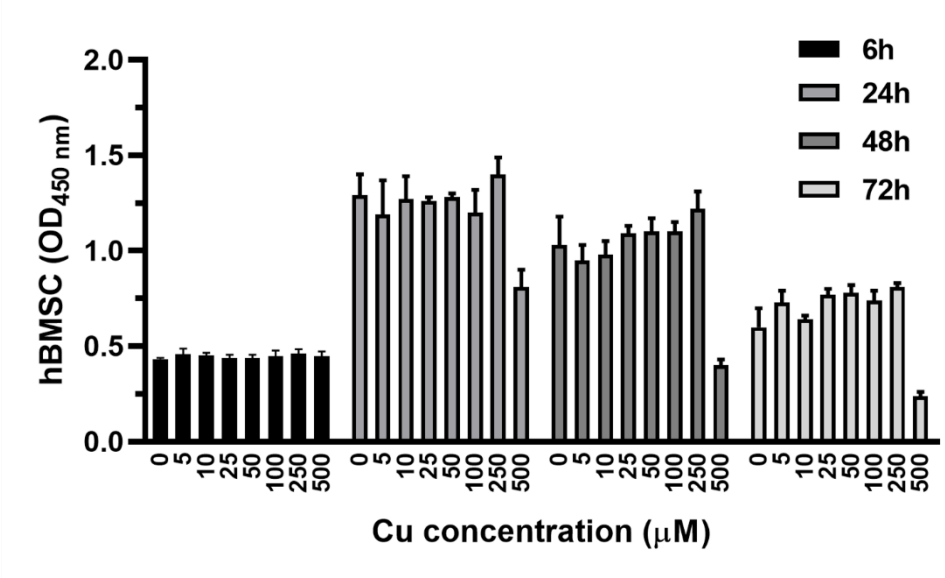

Fig. S5. CCK-8 assessment of hBMSC cultured with different concentrations of copper acetate in culture medium. Data are expressed as mean ±standard deviation.

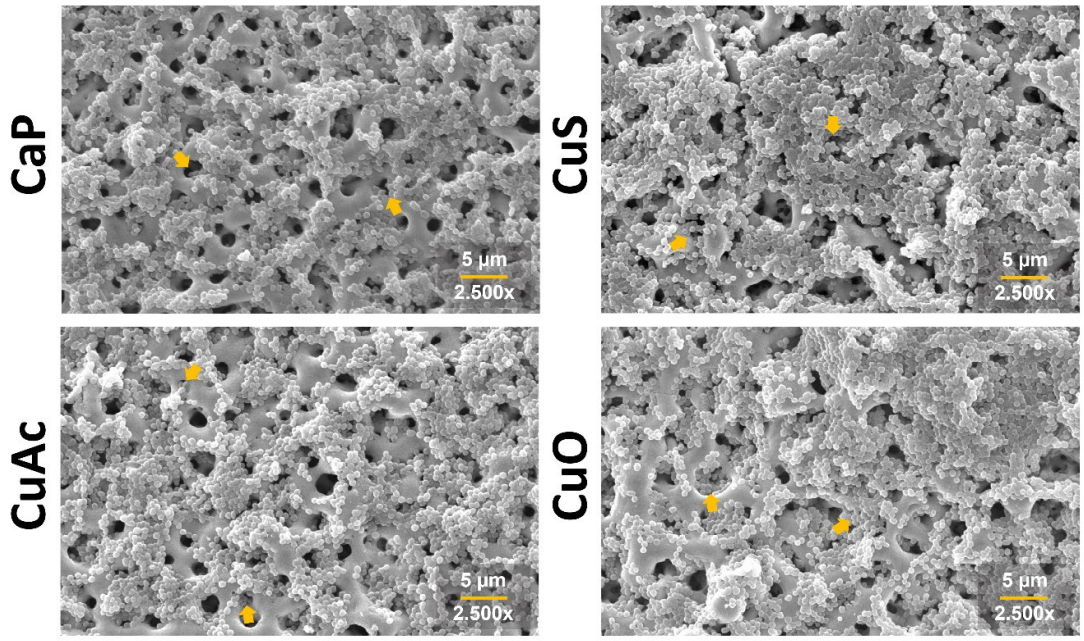

Fig. S6. Micrographs of *S. sanguinis* biofilm formed on top of the samples after 24 h. Arrows indicate the interaction of the bacteria with the coating pores.

References

[1] J.M. Cordeiro, V.A.R. Barão, Is there scientific evidence favoring the substitution of commercially pure titanium with titanium alloys for the manufacture of dental implants?, Mater. Sci. Eng. C. 71 (2017) 1201–1215. https://doi.org/10.1016/j.msec.2016.10.025.

[2] D.A. Florea, D. Albuleț, A.M. Grumezescu, E. Andronescu, Surface modification – A step forward to overcome the current challenges in orthopedic industry and to obtain an improved osseointegration and antimicrobial properties, Mater. Chem. Phys. 243 (2020) 122579. https://doi.org/10.1016/j.matchemphys.2019.122579.

[3] C. Stewart, B. Akhavan, S.G. Wise, M.M.M. Bilek, A review of biomimetic surface functionalization for bone-integrating orthopedic implants: Mechanisms, current approaches, and future directions, Prog. Mater. Sci. 106 (2019) 100588. https://doi.org/10.1016/j.pmatsci.2019.100588.

[4] J.H. Lee, P. Parthiban, G.Z. Jin, J.C. Knowles, H.W. Kim, Materials roles for promoting angiogenesis in tissue regeneration, Prog. Mater. Sci. (2020) 100732.

https://doi.org/10.1016/j.pmatsci.2020.100732.

[5] X. He, G. Zhang, H. Zhang, R. Hang, X. Huang, X. Yao, X. Zhang, Cu and Si co-doped microporous TiO2 coating for osseointegration by the coordinated stimulus action, Appl. Surf. Sci. 503 (2020) 144072. https://doi.org/10.1016/j.apsusc.2019.144072.

[6] V. Kumaravel, K.M. Nair, S. Mathew, J. Bartlett, J.E. Kennedy, H.G. Manning, B.J. Whelan, N.S. Leyland, S.C. Pillai, Antimicrobial TiO2 nanocomposite coatings for surfaces, dental and orthopaedic implants, Chem. Eng. J. 416 (2021) 129071. https://doi.org/10.1016/j.cej.2021.129071.

[7] J.G.S. Souza, M.M. Bertolini, R.C. Costa, B.E. Nagay, A. Dongari-Bagtzoglou, V.A.R. Barão, Targeting implant-associated infections: titanium surface loaded with antimicrobial, IScience. 24 (2021) 102008. https://doi.org/10.1016/j.isci.2020.102008.

[8] J. Alipal, N.A.S. Mohd Pu'ad, N.H.M. Nayan, N. Sahari, H.Z. Abdullah, M.I. Idris, T.C. Lee, An updated review on surface functionalisation of titanium and its alloys for implants applications, Mater. Today Proc. 42 (2021) 270–282. https://doi.org/10.1016/j.matpr.2021.01.499.

[9] M. Godoy-Gallardo, U. Eckhard, L.M. Delgado, Y.J.D. de Roo Puente, M. Hoyos-Nogués, F.J. Gil, R.A. Perez, Antibacterial approaches in tissue engineering using metal ions and nanoparticles: From mechanisms to applications, Bioact. Mater. 6 (2021) 4470–4490. https://doi.org/10.1016/j.bioactmat.2021.04.033.

[10] H. Chouirfa, H. Bouloussa, V. Migonney, C. Falentin-Daudré, Review of titanium surface modification techniques and coatings for antibacterial applications, Acta Biomater. 83 (2019) 37–54. https://doi.org/10.1016/j.actbio.2018.10.036.

[11] Z. Liu, X. Liu, S. Ramakrishna, Surface engineering of biomaterials in orthopedic and dental implants: Strategies to improve osteointegration, bacteriostatic and bactericidal activities, Biotechnol. J. 16 (2021) 2000116. https://doi.org/10.1002/biot.202000116.

[12] J.M. Cordeiro, B.E. Nagay, A.L.R. Ribeiro, N.C. da Cruz, E.C. Rangel, L.M.G. Fais, L.G. Vaz, V.A.R. Barão, Functionalization of an experimental Ti-Nb-Zr-Ta alloy with a biomimetic coating produced by plasma electrolytic oxidation, J. Alloys Compd. 770 (2019) 1038–1048. https://doi.org/10.1016/j.jallcom.2018.08.154.

[13] R.C. Costa, J.G.S. Souza, J.M. Cordeiro, M. Bertolini, E.D. de Avila, R. Landers, E.C. Rangel, C.A. Fortulan, B. Retamal-Valdes, N.C. da Cruz, M. Feres, V.A.R. Barão, Synthesis of bioactive glass-based coating by plasma electrolytic oxidation: Untangling a new deposition pathway toward titanium implant surfaces, J. Colloid Interface Sci. 579 (2020) 680–698. https://doi.org/10.1016/j.jcis.2020.06.102.

[14] B.E. Nagay, C. Dini, J.M. Cordeiro, A.P. Ricomini-Filho, E.D. de Avila, E.C. Rangel, N.C. da Cruz, V.A.R. Barão, Visible-Light-Induced Photocatalytic and Antibacterial Activity of TiO 2 Codoped with Nitrogen and Bismuth: New Perspectives to Control Implant-Biofilm-Related Diseases, ACS Appl. Mater. Interfaces. 11 (2019) 18186–18202. https://doi.org/10.1021/acsami.9b03311.

[15] I. da S.V. Marques, M.F. Alfaro, M.T. Saito, N.C. da Cruz, C. Takoudis, R. Landers, M.F. Mesquita, F.H. Nociti Junior, M.T. Mathew, C. Sukotjo, V.A.R. Barão, Biomimetic coatings enhance tribocorrosion behavior and cell responses of commercially pure titanium surfaces, Biointerphases. 11 (2016) 031008. https://doi.org/10.1116/1.4960654.

[16] J.M. Cordeiro, H.N. Pantaroto, E.M. Paschoaleto, E.C. Rangel, N.C. d. Cruz, C. Sukotjo, V.A.R. Barão, Synthesis of biofunctional coating for a TiZr alloy: Surface, electrochemical, and biological characterizations, Appl. Surf. Sci. 452 (2018) 268–278. https://doi.org/10.1016/j.apsusc.2018.05.044.

[17] Y.-J. Park, K.-H. Shin, H.-J. Song, Effects of anodizing conditions on bond strength of anodically oxidized film to titanium substrate, Appl. Surf. Sci. 253 (2007) 6013–6018. https://doi.org/10.1016/j.apsusc.2006.12.112.

[18] T.W. Clyne, S.C. Troughton, A review of recent work on discharge characteristics during plasma electrolytic oxidation of various metals, Int. Mater. Rev. 64 (2019) 127–162. https://doi.org/10.1080/09506608.2018.1466492.

[19] T.O.B. Polo, W.P. da Silva, G.A.C. Momesso, T.J. Lima-Neto, S. Barbosa, J.M. Cordeiro, J.S. Hassumi, N.C. da Cruz, R. Okamoto, V.A.R. Barão, L.P. Faverani, Plasma Electrolytic Oxidation as a Feasible Surface Treatment for Biomedical Applications: an in vivo study, Sci. Rep. 10 (2020) 10000. https://doi.org/10.1038/s41598-020-65289-2.

[20] I.A.J.J. van Hengel, M.W.A.M.A.M. Tierolf, V.P.M.M. Valerio, M. Minneboo, A.C. Fluit, L.E. Fratila-Apachitei, I. Apachitei, A.A. Zadpoor, Self-defending additively manufactured bone implants bearing silver and copper nanoparticles, J. Mater. Chem. B. 8 (2020) 1589–1602. https://doi.org/10.1039/C9TB02434D.

[21] H. Wang, S. Zhao, J. Zhou, Y. Shen, W. Huang, C. Zhang, M.N. Rahaman, D. Wang, Evaluation of borate bioactive glass scaffolds as a controlled delivery system for copper ions in stimulating osteogenesis and angiogenesis in bone healing, J. Mater. Chem. B. 2 (2014) 8547–8557. https://doi.org/10.1039/c4tb01355g.

[22] A. Hoppe, N.S. Güldal, A.R. Boccaccini, A review of the biological response to ionic dissolution products from bioactive glasses and glass-ceramics, Biomaterials. 32 (2011) 2757–2774. https://doi.org/10.1016/j.biomaterials.2011.01.004.

[23] E. O'Neill, G. Awale, L. Daneshmandi, O. Umerah, K.W.H. Lo, The roles of ions on bone regeneration, Drug Discov. Today. 23 (2018) 879–890. https://doi.org/10.1016/j.drudis.2018.01.049.

[24] M.F. Gutiérrez, L.F. Alegría-Acevedo, L. Méndez-Bauer, J. Bermudez, A. Dávila-Sánchez, S. Buvinic, N. Hernández-Moya, A. Reis, A.D. Loguercio, P. V. Farago, J. Martin, E. Fernández, Biological, mechanical and adhesive properties of universal adhesives containing zinc and copper nanoparticles, J. Dent. 82 (2019) 45–55. https://doi.org/10.1016/j.jdent.2019.01.012.

[25] D. Wojcieszak, M. Mazur, M. Kalisz, M. Grobelny, Influence of Cu, Au and Ag on structural and surface properties of bioactive coatings based on titanium, Mater. Sci. Eng. C. 71 (2017) 1115–1121. https://doi.org/10.1016/j.msec.2016.11.091.

[26] C. Prinz, M. Elhensheri, J. Rychly, H.G. Neumann, Antimicrobial and bone-forming activity of a copper coated implant in a rabbit model, J. Biomater. Appl. 32 (2017) 139–149. https://doi.org/10.1177/0885328217713356.

[27] X. Xu, Y. Lu, S. Li, S. Guo, M. He, K. Luo, J. Lin, Copper-modified Ti6Al4V alloy fabricated by selective laser melting with pro-angiogenic and anti-inflammatory properties for potential guided bone regeneration applications, Mater. Sci. Eng. C. 90 (2018) 198–210. https://doi.org/10.1016/j.msec.2018.04.046.

[28] A. Bari, N. Bloise, S. Fiorilli, G. Novajra, M. Vallet-Regí, G. Bruni, A. Torres-Pardo,

J.M. González-Calbet, L. Visai, C. Vitale-Brovarone, Copper-containing mesoporous bioactive glass nanoparticles as multifunctional agent for bone regeneration, Acta Biomater. 55 (2017) 493–504. https://doi.org/10.1016/j.actbio.2017.04.012.

[29] L. Zhang, J. Guo, X. Huang, Y. Zhang, Y. Han, The dual function of Cu-doped TiO 2 coatings on titanium for application in percutaneous implants, J. Mater. Chem. B. 4 (2016) 3788–3800. https://doi.org/10.1039/C6TB00563B.

[30] T. Liang, Y. Wang, L. Zeng, Y. Liu, L. Qiao, S. Zhang, R. Zhao, G. Li, R. Zhang, J. Xiang, F. Xiong, A. Shanaghi, H. Pan, Y. Zhao, Copper-doped 3D porous coating developed on Ti-6Al-4V alloys and its in vitro long-term antibacterial ability, Appl. Surf. Sci. 509 (2020) 144717. https://doi.org/10.1016/j.apsusc.2019.144717.

[31] X. Zhang, Z. Peng, X. Lu, Y. Lv, G. Cai, L. Yang, Z. Dong, Microstructural evolution and biological performance of Cu-incorporated TiO2 coating fabricated through one-step micro-arc oxidation, Appl. Surf. Sci. 508 (2020) 144766. https://doi.org/10.1016/j.apsusc.2019.144766.

[32] S. Durdu, Characterization, bioactivity and antibacterial properties of copper-based TiO2 bioceramic coatings fabricated on titanium, Coatings. 9 (2019) 1. https://doi.org/10.3390/coatings9010001.

[33] Q. Huang, Z. Ouyang, Y. Tan, H. Wu, Y. Liu, Activating macrophages for enhanced osteogenic and bactericidal performance by Cu ion release from micro/nano-topographical coating on a titanium substrate, Acta Biomater. 100 (2019) 415–426. https://doi.org/10.1016/j.actbio.2019.09.030.

[34] Q. Wu, J. Li, W. Zhang, H. Qian, W. She, H. Pan, J. Wen, X. Zhang, X. Liu, X. Jiang, Antibacterial property, angiogenic and osteogenic activity of Cu-incorporated TiO 2 coating, J. Mater. Chem. B. 2 (2014) 6738–6748. https://doi.org/10.1039/C4TB00923A.

[35] D. Zhang, Q. Han, K. Yu, X. Lu, Y. Liu, Z. Lu, Q. Wang, Antibacterial activities against Porphyromonas gingivalis and biological characteristics of copper-bearing PEO coatings on magnesium, J. Mater. Sci. Technol. 61 (2021) 33–45. https://doi.org/10.1016/j.jmst.2020.05.025.

[36] W. Zhu, Z. Zhang, B. Gu, J. Sun, L. Zhu, Biological Activity and Antibacterial

Property of Nano-structured TiO2 Coating Incorporated with Cu Prepared by Micro-arc Oxidation, J. Mater. Sci. Technol. 29 (2013) 237–244. https://doi.org/10.1016/j.jmst.2012.12.015.

[37] I. Burghardt, F. Lüthen, C. Prinz, B. Kreikemeyer, C. Zietz, H.G. Neumann, J. Rychly, A dual function of copper in designing regenerative implants, Biomaterials. 44 (2015) 36–44. https://doi.org/10.1016/j.biomaterials.2014.12.022.

[38] X. Zhang, J. Li, X. Wang, Y. Wang, R. Hang, X. Huang, B. Tang, P.K. Chu, Effects of copper nanoparticles in porous TiO2 coatings on bacterial resistance and cytocompatibility of osteoblasts and endothelial cells, Mater. Sci. Eng. C. 82 (2018) 110–120. https://doi.org/10.1016/j.msec.2017.08.061.

[39] Q. Huang, X. Liu, R. Zhang, X. Yang, C. Lan, Q. Feng, Y. Liu, The development of Cu-incorporated micro/nano-topographical bio-ceramic coatings for enhanced osteoblast response, Appl. Surf. Sci. 465 (2019) 575–583. https://doi.org/10.1016/j.apsusc.2018.09.208.

[40] Y. Wang, S. Zhao, G. Li, S. Zhang, R. Zhao, A. Dong, R. Zhang, Preparation and in vitro antibacterial properties of anodic coatings co-doped with Cu, Zn, and P on a Ti–6Al–4V alloy, Mater. Chem. Phys. 241 (2020) 122360. https://doi.org/10.1016/j.matchemphys.2019.122360.

[41] L. Zhang, J. Guo, T. Yan, Y. Han, Fibroblast responses and antibacterial activity of Cu and Zn co-doped TiO2 for percutaneous implants, Appl. Surf. Sci. 434 (2018) 633–642. https://doi.org/10.1016/j.apsusc.2017.10.169.

[42] S. Kyrylenko, F. Warchoł, O. Oleshko, Y. Husak, A. Kazek-Kęsik, V. Korniienko, V. Deineka, M. Sowa, A. Maciej, J. Michalska, A. Jakóbik-Kolon, I. Matuła, M. Basiaga, V. Hulubnycha, A. Stolarczyk, M. Pisarek, O. Mishchenko, M. Pogorielov, W. Simka, Effects of the sources of calcium and phosphorus on the structural and functional properties of ceramic coatings on titanium dental implants produced by plasma electrolytic oxidation, Mater. Sci. Eng. C. 119 (2021) 111607. https://doi.org/10.1016/j.msec.2020.111607.

[43] D. dong Wang, X. tong Liu, Y. Wang, Q. Zhang, D. long Li, X. Liu, H. Su, Y. Zhang, S. xue Yu, D. Shen, Role of the electrolyte composition in establishing plasma

discharges and coating growth process during a micro-arc oxidation, Surf. Coatings Technol. 402 (2020) 126349. https://doi.org/10.1016/j.surfcoat.2020.126349.

[44] X. Zhang, C. Li, Y. Yu, X. Lu, Y. Lv, D. Jiang, Z. Peng, J. Zhou, X. Zhang, S. Sun, Z. Dong, Characterization and property of bifunctional Zn-incorporated TiO2 micro-arc oxidation coatings: The influence of different Zn sources, Ceram. Int. 45 (2019) 19747–19756. https://doi.org/10.1016/j.ceramint.2019.06.228.

[45] H. Wu, X. Zhang, Z. Geng, Y. Yin, R. Hang, X. Huang, X. Yao, B. Tang, Preparation, antibacterial effects and corrosion resistant of porous Cu-TiO 2 coatings, Appl. Surf. Sci. 308 (2014) 43–49. https://doi.org/10.1016/j.apsusc.2014.04.081.

[46] C. Dini, B.E. Nagay, J.M. Cordeiro, N.C. da Cruz, E.C. Rangel, A.P. Ricomini-Filho, E.D. de Avila, V.A.R. Barão, UV-photofunctionalization of a biomimetic coating for dental implants application, Mater. Sci. Eng. C. 110 (2020) 110657. https://doi.org/10.1016/j.msec.2020.110657.

[47] T. Beline, C.S. Garcia, E.S. Ogawa, I.S.V. Marques, A.O. Matos, C. Sukotjo, M.T. Mathew, M.F. Mesquita, R.X. Consani, V.A.R. Barão, Surface treatment influences electrochemical stability of cpTi exposed to mouthwashes, Mater. Sci. Eng. C. 59 (2016) 1079–1088. https://doi.org/10.1016/j.msec.2015.11.045.

[48] J.M. Cordeiro, J.M. Pires, J.G.S.S. Souza, C. V. Lima, M.M. Bertolini, E.C. Rangel, V.A.R.R. Barão, Optimizing citric acid protocol to control implant-related infections: An in vitro and in situ study, J. Periodontal Res. (2021) jre.12855. https://doi.org/10.1111/jre.12855.

[49] I. da S.V. Marques, V.A.R. Barão, N.C. da Cruz, J.C.-C. Yuan, M.F. Mesquita, A.P. Ricomini-Filho, C. Sukotjo, M.T. Mathew, Electrochemical behavior of bioactive coatings on cp-Ti surface for dental application, Corros. Sci. 100 (2015) 133–146. https://doi.org/10.1016/j.corsci.2015.07.019.

[50] E. Lamers, X. Frank Walboomers, M. Domanski, J. te Riet, F.C.M.J.M. van Delft, R. Luttge, L.A.J.A. Winnubst, H.J.G.E. Gardeniers, J.A. Jansen, The influence of nanoscale grooved substrates on osteoblast behavior and extracellular matrix deposition, Biomaterials. 31 (2010) 3307–3316. https://doi.org/10.1016/j.biomaterials.2010.01.034.

[51] G. Nakazato, H. Tsuchiya, M. Sato, M. Yamauchi, In vivo plaque formation on implant materials., Int. J. Oral Maxillofac. Implants. 4 (1989) 321–6. http://www.ncbi.nlm.nih.gov/pubmed/2561743.

[52] V. Fröjd, L. Chávez de Paz, M. Andersson, A. Wennerberg, J.R. Davies, G. Svensäter, In situ analysis of multispecies biofilm formation on customized titanium surfaces, Mol. Oral Microbiol. 26 (2011) 241–252. https://doi.org/10.1111/j.2041-1014.2011.00610.x.

[53] J.A. Shibli, L. Melo, D.S. Ferrari, L.C. Figueiredo, M. Faveri, M. Feres, Composition of supra- and subgingival biofilm of subjects with healthy and diseased implants, Clin. Oral Implants Res. 19 (2008) 975–982. https://doi.org/10.1111/j.1600-0501.2008.01566.x.

[54] G.A.C. Momesso, T.O.B. Polo, W.P.P. da Silva, S. Barbosa, G.P. Freitas, H.B. Lopes, A.L. Rosa, J.M. Cordeiro, L.F. Toro, F.Y. Chiba, D.H. Matsushita, M.J.Q. Louzada, N.C. da Cruz, V.A.R. Barão, L.P. Faverani, Miniplates coated by plasma electrolytic oxidation improve bone healing of simulated femoral fractures on low bone mineral density rats, Mater. Sci. Eng. C. 120 (2021) 111775. https://doi.org/10.1016/j.msec.2020.111775.

[55] H. De Bruyn, V. Christiaens, R. Doornewaard, M. Jacobsson, J. Cosyn, W. Jacquet, S. Vervaeke, Implant surface roughness and patient factors on long-term peri-implant bone loss, Periodontol. 2000. 73 (2017) 218–227. https://doi.org/10.1111/prd.12177.

[56] T. Albrektsson, A. Wennerberg, Oral implant surfaces: Part 1--review focusing on topographic and chemical properties of different surfaces and in vivo responses to them., Int. J. Prosthodont. 17 (2004) 536–43. http://www.ncbi.nlm.nih.gov/pubmed/15543910.

[57] B.D. Boyan, E.M. Lotz, Z. Schwartz, Roughness and Hydrophilicity as Osteogenic Biomimetic Surface Properties, Tissue Eng. Part A. 23 (2017) 1479–1489. https://doi.org/10.1089/ten.tea.2017.0048.

[58] J. Barberi, S. Spriano, Titanium and Protein Adsorption: An Overview of Mechanisms and Effects of Surface Features, Materials (Basel). 14 (2021) 1590. https://doi.org/10.3390/ma14071590.

[59] F. Rupp, L. Liang, J. Geis-Gerstorfer, L. Scheideler, F. Hüttig, Surface characteristics of dental implants: A review, Dent. Mater. 34 (2018) 40–57. https://doi.org/10.1016/j.dental.2017.09.007.

[60] G. Li, Y. Wang, L. Qiao, R. Zhao, S. Zhang, R. Zhang, C. Chen, X. Li, Y. Zhao, Preparation and formation mechanism of copper incorporated micro-arc oxidation coatings developed on Ti-6Al-4V alloys, Surf. Coatings Technol. 375 (2019) 74–85. https://doi.org/10.1016/j.surfcoat.2019.06.096.

[61] T. Beline, I. da S.V. Marques, A.O. Matos, E.S. Ogawa, A.P. Ricomini-Filho, E.C. Rangel, N.C. da Cruz, C. Sukotjo, M.T. Mathew, R. Landers, R.L.X. Consani, M.F. Mesquita, V.A.R. Barão, Production of a biofunctional titanium surface using plasma electrolytic oxidation and glow-discharge plasma for biomedical applications, Biointerphases. 11 (2016) 011013. https://doi.org/10.1116/1.4944061.

[62] A. Wennerberg, T. Albrektsson, Effects of titanium surface topography on bone integration: A systematic review, Clin. Oral Implants Res. 20 (2009) 172–184. https://doi.org/10.1111/j.1600-0501.2009.01775.x.

[63] T. Albrektsson, A. Wennerberg, On osseointegration in relation to implant surfaces, Clin. Implant Dent. Relat. Res. 21 (2019) 4–7. https://doi.org/10.1111/cid.12742.

[64] Y. Zhang, S.E. Chen, J. Shao, J.J.J.P. Van Den Beucken, Combinatorial Surface Roughness Effects on Osteoclastogenesis and Osteogenesis, ACS Appl. Mater. Interfaces. 10 (2018) 36652–36663. https://doi.org/10.1021/acsami.8b10992.

[65] L.P. Qiao, J. Lou, S.F. Zhang, B. Qu, W.H. Chang, R.F. Zhang, The entrance mechanism of calcium and phosphorus elements into micro arc oxidation coatings developed on Ti6Al4V alloy, Surf. Coatings Technol. 285 (2016) 187–196. https://doi.org/10.1016/j.surfcoat.2015.11.041.

[66] H.N. Pantaroto, J.M. Cordeiro, L.T. Pereira, A.B. de Almeida, F.H. Nociti Junior, E.C. Rangel, N.F. Azevedo Neto, J.H.D. da Silva, V.A.R. Barão, Sputtered crystalline TiO2 film drives improved surface properties of titanium-based biomedical implants, Mater. Sci. Eng. C. 119 (2021) 111638. https://doi.org/10.1016/j.msec.2020.111638.

[67] F.G. Oliveira, A.R. Ribeiro, G. Perez, B.S. Archanjo, C.P. Gouvea, J.R. Araújo, A.P.C. Campos, A. Kuznetsov, C.M. Almeida, M.M. Maru, C.A. Achete, P. Ponthiaux, J.P.

Celis, L.A. Rocha, Understanding growth mechanisms and tribocorrosion behaviour of porous TiO 2 anodic films containing calcium, phosphorous and magnesium, Appl. Surf. Sci. 341 (2015) 1–12. https://doi.org/10.1016/j.apsusc.2015.02.163.

[68] A. Jacobs, G. Renaudin, C. Forestier, J.M. Nedelec, S. Descamps, Biological properties of copper-doped biomaterials for orthopedic applications: A review of antibacterial, angiogenic and osteogenic aspects, Acta Biomater. 117 (2020) 21–39. https://doi.org/10.1016/j.actbio.2020.09.044.

[69] M. Hans, A. Erbe, S. Mathews, Y. Chen, M. Solioz, F. Mücklich, Role of Copper Oxides in Contact Killing of Bacteria, Langmuir. 29 (2013) 16160–16166. https://doi.org/10.1021/la404091z.

[70] G. Feng, Y. Cheng, S.-Y. Wang, D.A. Borca-Tasciuc, R.W. Worobo, C.I. Moraru, Bacterial attachment and biofilm formation on surfaces are reduced by small-diameter nanoscale pores: how small is small enough?, Npj Biofilms Microbiomes. 1 (2015) 15022. https://doi.org/10.1038/npjbiofilms.2015.22.

[71] M. Quirynen, C.M.L. Bollen, A. Schotte, M. Marechal, D. van Steenberghe, H.C. van der Mei, G.I. Doornbusch, H.J. Busscher, I. Naert, An in vivo Study of the Influence of the Surface Roughness of Implants on the Microbiology of Supra- and Subgingival Plaque, J. Dent. Res. 72 (1993) 1304–1309. https://doi.org/10.1177/00220345930720090801.

[72] A. Almaguer-Flores, R. Olivares-Navarrete, M. Wieland, L.A. Ximénez-Fyvie, Z. Schwartz, B.D. Boyan, Influence of topography and hydrophilicity on initial oral biofilm formation on microstructured titanium surfaces in vitro, Clin. Oral Implants Res. 23 (2012) 301–307. https://doi.org/10.1111/j.1600-0501.2011.02184.x.

[73] K. Futrega, E. Mosaad, K. Chambers, W.B. Lott, J. Clements, M.R. Doran, Bone marrow-derived stem/stromal cells (BMSC) 3D microtissues cultured in BMP-2 supplemented osteogenic induction medium are prone to adipogenesis, Cell Tissue Res. 374 (2018) 541–553. https://doi.org/10.1007/s00441-018-2894-y.

[74] N. Saulacic, B. Schaller, Prevalence of Peri-Implantitis in Implants with Turned and Rough Surfaces: a Systematic Review, J. Oral Maxillofac. Res. 10 (2019) 1–12. https://doi.org/10.5037/jomr.2019.10101.

2.2 Tailoring Cu^{2+}-loaded electrospun membranes with antibacterial ability for guided bone regeneration#

Jairo M. Cordeiro[ac*], Valentim A. R. Barão[a*], Erica D. de Avila[b], Fang Yang[c], Jeroen J. J. P. van den Beucken[c*]

[a]*Department of Prosthodontics and Periodontology, Piracicaba Dental School, University of Campinas (UNICAMP), Piracicaba, São Paulo, Brazil*
[b]*Department of Dental Materials and Prosthodontics, School of Dentistry at Araraquara, São Paulo State University (UNESP), Araraquara, São Paulo, Brazil*
[c]*Dentistry - Regenerative Biomaterials, Radboudumc, Nijmegen, The Netherlands*

***Corresponding author:**

E-mail addresses: vbarao@unicamp.br (Valentim A.R. Barão), jeroen.vandenbeucken@radboudumc.nl (Jeroen J.J.P. van den Beucken), jairocordeirom@hotmail.com (Jairo M. Cordeiro).

#O artigo será submetido ao periódico *ACS Applied Materials & Interfaces (IF = 9.229).*

Abstract

Copper (Cu)-loaded electrospun membranes were tailored for guided bone regeneration (GBR), targeting the stimulation of innate cells active in bone growth and the prevention of bacterial infections. Functional GBR membranes were produced via an electrospinning set-up using a silk-based solution associated with polyethylene oxide (Silk/PEO - control). Experimental groups were loaded with copper oxide using varying weight percentages (0.05% to 1% of CuO). The morphological, structural, chemical, and mechanical properties of membranes were evaluated. Direct and indirect in vitro cytocompatibility experiments were performed with primary human bone mesenchymal stem cells and primary human umbilical vein endothelial cells. The antibacterial potential of membranes was tested with Staphylococcus aureus biofilm. CuO was successfully incorporated into membranes as clusters without compromising their mechanical properties for clinical applicability. Increased Cu concentrations generated membranes with thinner nanofibers, greater pore areas, and stronger antimicrobial effect ($p<0.01$). Cu^{2+} ion was released from the nanofiber membranes during 1 week, showing higher release in acidic conditions. CuO 0.1% and CuO 0.05% membranes were able to support and stimulate cell adhesion and proliferation ($p<0.05$), and favor angiogenic responses of vascular cells. In addition, detailed quantitative and qualitative analysis determined that amount of the attached biofilm was reduced on the tailored functional Cu^{2+}-loaded GBR membrane. Importantly, these qualities represent a valuable strategy to improve the bone regeneration process and diminish the risk of bacterial infections.

Keywords: Bone regeneration; Copper; Electrospinning; Silk; Biofilm.

Highlights

- Cu^{2+} ion release from electrospun membranes is sustained for up to 7 days and pH-sensitive.
- Cu^{2+}-loaded membranes display appropriate mechanical properties in dry and wet conditions.
- The antibacterial activity of the guided bone regeneration membranes (GBRm) is Cu-concentration dependent.
- Cu^{2+}-loaded membranes have the potential to stimulate cell adhesion, proliferation, and angiogenesis.
- GBRm containing Cu represent a promising approach for bone regeneration and prevention of bacterial infection.

Graphical abstract

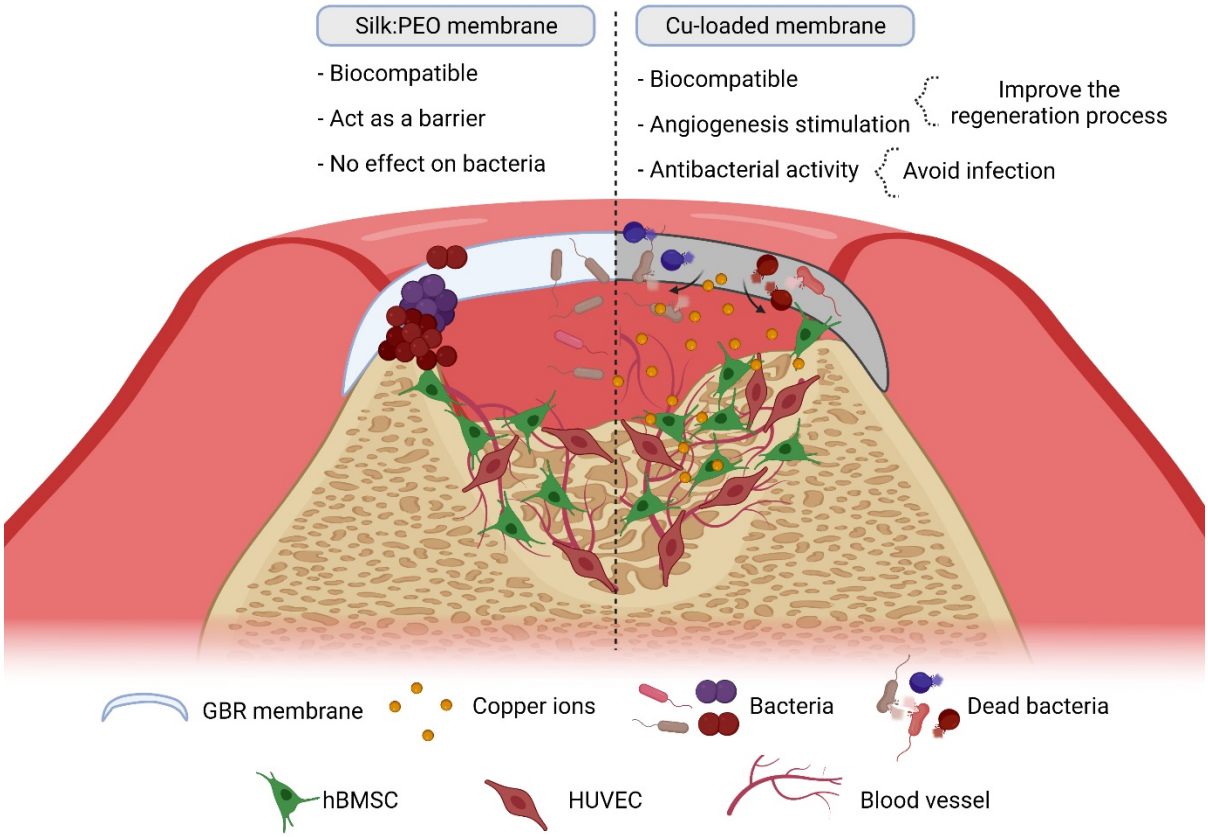

1. INTRODUCTION

Regeneration of vertical alveolar bone deficiencies is one of the most challenging clinical scenarios due to difficulties in regeneration techniques and the presence of anatomical limitations resulting from atrophy, trauma, tumor resection, periodontal and peri-implant diseases.[1] Several approaches have been explored to achieve bone formation/regeneration, which is required for dental implant placement in vertical and/or horizontal defects.[2] Vertical bone regeneration techniques have shown efficiency regarding bone gain and implant survival, especially using guided bone regeneration (GBR) that has been considered as the most predictable technique in terms of bone stability (i.e. smaller bone resorption and lower number of complications after treatment).[2,3]

The GBR technique has been studied since the late 1980s and is based on the application of a resorbable or non-resorbable barrier membrane to stabilize the blood clot and create a secluded space in the wound site to prevent the invasion of soft tissue cells and to favor the proliferation of bone-forming cells.[2,4] The membranes applied in the current clinical practice act as a passive barrier and are not designed to regulate cells participating in bone growth or to avoid infections [5]. Although most of the studies have shown a high success rate of implants placed in GBR augmented ridges (range 90–100%),[2,6] this technique is not free of complications. A systematic review showed that soft tissue complications (e.g., membrane exposure, soft tissue dehiscence, and acute infection/abscess) are present in 16.5% of cases.[7] Specifically, the presence of infection during the healing period reduces the volume of the regenerated bone from 90-100% to 42%-62% of the possible amount of regeneration.[8] In this perspective, multiple methods have been proposed to alter the membranes to create a favorable condition for the healing process, promoting an active role in the regenerative processes by hosting and stimulating the recruited cells in the underlying defect during GBR[9] and protecting the wound from environmental threats and penetration of bacteria.[10]

Inorganic ions, such as Cu^{2+}, have been used to functionalize biomaterials to activate molecular constituents and cells involved in the regeneration process.[11] In fact, Cu has gained attention in bone regeneration due to its broad application regulating many processes involved in angiogenesis, osteogenesis, and bone fracture healing, also avoiding infections.[12,13] *In vivo* studies have shown that bone substitutes doped with Cu present a higher capacity to stimulate bone regeneration and angiogenesis compared to Cu-free ones, as confirmed with increased bone formation and mineralized tissue, and higher new bone volume/total volume.[14] Moreover, incorporating Cu in TiAlV metallic mesh used for GBR significantly inhibited the inflammatory response of non-osteoporotic and osteoporotic bone-related cells.[5] In addition to the potential to regenerate lost bone, the incorporation of Cu can be crucial in clinical applications due to its excellent antibacterial efficacy,[13] since the oral cavity is an area with an abundant presence of bacteria that can increase the risk of infections (e.g. osteomyelitis) and might ultimately impair bone regeneration and lead to implant failure.[5]

To approach the desired biological behavior and reduce dosage-dependent toxicity, the technique used to fabricate the GBR membranes needs to be sufficiently versatile to allow the incorporation and sustained release of ions at desired dosages over time.[11] Electrospinning is a robust, simple technology developed to generate micro- and nanofibers using polymeric solutions or melt polymers.[11,15–17] The nanofibers produced by electrospinning have been applied as a drug delivery system, wound dressing materials, and regenerative medicine scaffolds.[16,18] They have different porosity, topography, and surface area, being densely packed through a sheet-like assembly that may promote cell spreading but prevent cell infiltration into the wound.[19] Interestingly, fiber functionalization can be achieved via supplementation of metallic ions to the polymer solution, enabling their subsequent release.[20–22] In this context, a silk-based solution has been widely used due to its excellent biological

properties as a GBR membrane, supporting osteogenic cell differentiation and proliferation, besides being stably doped with antimicrobial agents.[23]

Recently, the main research focus of biomedical studies using electrospinning techniques is spotlighted on developing bone tissue scaffolds, grafting, and wound dressing.[24–30] However, more efforts should be dedicated to creating functional membranes for GBR that could assist in recruiting and activating endogenous stem cells and support, guide, and stimulate tissue regeneration.[18] Furthermore, the development of functional GBR membranes that could assist in recruiting endogenous stem cells to support bone regeneration and minimize bacteria colonization could overcome the challenges faced in implant rehabilitations, also accelerating the rehabilitation process.[19,31] Consequently, we here tailored a resorbable Cu^{2+}-loaded electrospun membranes for GBR, targeting the stimulation of regenerative and angiogenic cells active in bone formation and the prevention of bacterial infections.

2. EXPERIMENTAL SECTION

2.1. Electrospinning solutions preparation

A silk fibroin-based solution was used for the electrospun membranes. Silk fibroin was extracted as previously reported.[32,33] Briefly, the bombyx mori cocoons were boiled in 0.02 M of sodium carbonate (Na_2CO_3; 99.5% purity; Acros Organics, Belgium) solution for 30 min, followed by washing in distilled water 3 times. Then, degummed fibers were dissolved in a solution containing 9.3 M of lithium bromide (LiBr; 99.0% purity; Acros Organics) at 60 °C for 4 h and dialyzed against distilled water. After dialysis, silk fibroin solution was centrifuged twice at 5000 rpm and adjusted to a concentration of ~7% (w/v), determined by the wet weight methodology.

The solution prepared from 7% silk and 7% polyethylene oxide (PEO; Mv: ~900,000) in a ratio of 4:1 was used as control (Silk:PEO). For experimental groups, a 7% PEO solution

containing CuO (PEO/CuO) was prepared by adding copper oxide (99.9% purity; Sigma Aldrich, The Netherlands) to distilled water and dispersing it under refrigerated condition for 5 min at 50 Hz and 50% amplitude using a UP50H Compact ultrasonic lab homogenizer (50 W, Hielscher-Ultrasound Technology, Germany) before adding PEO powder. Then, 7% silk solution was mixed with PEO/CuO (Silk:PEO = 4:1) and stirred to obtain a final Cu concentration (w/w) into solution of 0.05% (CuO 0.05%), 0.1% (CuO 0.1%), 0.5% (CuO 0.5%), and 1% (CuO 1%).

2.2. Membrane generation

Silk/PEO or Silk/PEO/CuO solutions were electrospun to form nanofiber membranes using electrospinning equipment (Fuence Esprayer ES-2000S, Japan).[33] All parameters were optimized and settled to achieve stable and reproducible spinning: flow rate (20 μL/min), applied voltage (22 kV), and the distance between the tip (21 G) of the syringe and the grounded collector (20 cm). Aluminum foil was used to collect the fibers. Membranes were first water-annealed in a vacuum desiccator to ensure the nanofibrous membranes' mechanical and chemical stability. A sheet-like material was obtained after detaching it from the aluminum foil. Samples of 0.1 ± 0.01 mm of thickness were cut off into discs using a punch of ∅12 mm or ∅6 mm diameter. Samples were sterilized under UV-C light irradiation for 1 h on each side before further testing.

2.3. Morphological and chemical characterization of membranes

Samples were sputtered coated with chromium (~10 nm in thickness) and observed by scanning electron microscopy (SEM; ZEISS Sigma 300, Carl Zeiss Microscopy GmbH, Germany). SEM images were acquired from five random regions and then analyzed by ImageJ 1.53e software (NIH, USA) to measure fibers diameter and pore area of membranes.

Pore surface coverage was calculated by dividing the total pore area by the total area of the image dimension. The membranes' chemical composition was determined by energy-dispersive X-ray (EDX; Bruker, Germany) and X-ray diffraction (XRD; X'pert3 powder; PANalytical, The Netherlands). Cu concentration in membranes was measured by digesting the membranes using 45% nitric acid (HNO_3) for which samples (n = 3) were placed in hermetically closed glass tubes with 10 mL of HNO_3 and kept under continuous stirring until complete digestion. The concentration of Cu was measured from diluted aliquots by inductively coupled plasma optical emission spectrometry (ICP-OES; iCAP 6000, Thermo Fischer Scientific Inc., USA).[34]

2.4. Copper release kinetics of membranes

Cu^{2+} ion release (n = 3) was evaluated in minimum essential medium eagle – alpha modification (Alpha MEM; Gibco™, Life Technologies, The Netherlands) at two pHs: ~8.0 and ~4.0. The acidic pH was adjusted using a sterile-filtered hydrochloric acid solution. Samples were kept in tubes with 3 mL of medium and incubated under agitation (90 rpm) at 37°C. Samples were transferred to a fresh solution at every sampling time point (4 h, 1 day, 2 days, 4 days, and 7 days). Nitric acid 65% Suprapur® (Sigma Aldrich) was used to dilute samples before being analyzed using inductively coupled plasma mass spectroscopy (ICP-MS; X series I, Thermo Fischer Scientific Inc.).[34]

2.5. Mechanical characterization

Mechanical properties of dry and wet electrospun membranes (n = 5) were evaluated using a Universal Testing Machine (LS5, AMETEK Lloyd Instruments Ltd., UK) following the ASTM D-882 protocol. Dumbbell-shaped samples (Figure S1) with a gauge length of 20 mm and cross-sectional areas of approximately 0.1 mm × 4 mm (thickness × width) were punched

from the membranes.[35] Specimens (n = 6) in the wet state were obtained by reaching full hydration with 50 μL of distilled water before the test. A 100 N load cell was employed with a crosshead speed of 2 mm/min and 10 mm/min for the dried and wetted samples, respectively. Young's modulus, tensile strength, and percentage elongation at break were obtained from the corresponding stress/strain data.

2.6. Microbiological assay

Initially, the antibacterial action of membranes was assessed by a direct contact test with the *Staphylococcus aureus* strain (ATCC® 25923™). Bacteria were grown overnight under 10% CO_2 and 37 °C in Mueller Hinton broth (Kasvi, Brazil). Then, 1 mL from the suspension was transferred to a new tube containing 9 mL of fresh medium and incubated for 4 h (exponential growth phase) in the same conditions. The bacterial inoculum was adjusted to a final concentration of 10^7 colony-forming units (CFU) per mL (OD_{630nm} = 0.15) using a 96-well plate spectrophotometer. Next, *S. aureus* suspension was added to the electrospun membranes (3 experiments, n = 3/experiment) to form a biofilm. After 24 h of incubation, membranes were washed twice in sterile saline solution (0.9% NaCl) to remove non-adherent bacteria and transferred to cryogenic tubes containing 2 mL of 0.9% NaCl. The solution was vortexed for 1 min to disaggregate bacteria, followed by serial dilution and plating in Mueller Hinton agar. Plates were incubated in an atmosphere of 10% CO_2 at 37 °C for 24 h, and CFUs were counted. After biofilm formation, additional membranes (n = 2) from each group were washed twice and fixed with Karnovsky solution for 1 h and serially dehydrated with ethanol washes: 50%, 60%, 70%, 80%, 90% for 5 min each, and two washes in 100% solution during 10 min. Then, the membranes were air-dried and gold-sputtered to be evaluated by SEM (JEOL JSM-6010LA, USA).

2.7. Biological assessments

2.7.1. Direct cell biocompatibility

Membrane biocompatibility was assessed by culturing primary human bone mesenchymal stem cells (hBMSCs) isolated and cultured from bone fragments according to an approved ethical protocol (CMO Radboudumc; dossier# 2017-3252). Cells were cultured in minimum essential medium eagle – alpha modification (Alpha MEM; Gibco™, Life Technologies, The Netherlands) supplemented with 10% fetal bovine serum (FBS; Gibco™) and 1% penicillin/streptomycin (Gibco™). In addition, primary human umbilical vein endothelial cells (HUVECs-2; Becton Dickinson Biosciences, The Netherlands) were used for biological assessment. HUVECs were cultured in medium 200 (Gibco™) supplemented with 1% penicillin/streptomycin and a low serum growth supplement (LSGS; Gibco™). Cells were kept in a humidified incubator at 37 °C and 5% CO_2 atmosphere.[34]

Sterilized samples (∅6mm) were seeded at the density of 2×10^4 cells/well for hBMSCs. Before seeding HUVECs cells (4×10^4 cells/well), samples were incubated with 50 µL of FBS for 1 h. Cell metabolic activity (n = 3) was evaluated using the cell counting kit 8 (CCK-8; Abcam plc, China) after 1, 4, and 7 days according to the manufacturer's protocol. The cellular DNA content was quantified (n = 4) in cell lysates by QuantiFluor® dsDNA System (Promega Benelux BV, USA) after 4 and 7 days. Cell lysates were prepared by transferring samples to tubes with demineralized water to be ultrasonicated for 10 min. Three freeze-thaw cycles (-20°C) were performed to disrupt cells before performing the analysis following the manufacturer's instructions. Cell morphology and adhesion onto membranes were verified by SEM (ZEISS Sigma 300, Carl Zeiss Microscopy GmbH, Germany) imaging after 1, 4, and 7 days. Cells were fixed with 4% formaldehyde, dehydrated using a graded series of ethanol, covered with tetramethylsilane (TMS; Sigma-Aldrich, USA), and sputter-coated before observation by SEM.[4]

2.7.2. Indirect cell biocompatibility

For indirect cytotoxicity testing, samples were immersed in the culture medium supplemented as previously described for each cell type, and solutions were collected and replaced with fresh medium on days 1, 4, and 7. Cells were seeded in 96-well plates as mentioned above and then incubated for 24 h. Subsequently, the culture medium was replaced by 200 μL per well of extract medium from each time point. The medium that was incubated without samples and wells treated with methanol for 30 min was used as positive treatment control and negative treatment control, respectively. Cell metabolic activity was verified by CCK-8 assay (n = 3) after 1, 4, and 7 days. Indirect cell viability of hBMSCs and HUVECs after 1 day in contact with extract medium from day 1 was observed using the LIVE/DEAD™ Cell Imaging Kit (Invitrogen™, Life Technologies) following the manufacturer's instructions. Four images from each well were acquired using a fluorescence microscope (Zeiss AxioImager Z.1, Carl Zeiss Microscopy GmbH, Germany). Live and dead cells were counted using ImageJ software.[34]

2.7.3. HUVEC tube formation assay

In vitro angiogenesis was tested by HUVECs tube formation assay according to the manufacturer's instructions. Priorly, sterilized samples were immersed for 24 h in medium 200 supplemented as stated before. Positive control (C+) was tested with medium incubated without samples. Geltrex™ (Gibco™) was thawed out at 4 °C, then added 250 uL of gel solution to prechilled culture chambers. After incubation for 1 h, HUVECs were seeded at $4x10^4$ cells/chamber and left to adhere for 3 h. Then, the culture medium was removed and replaced by the extracted medium. After another 18 h of incubation, samples were stained with Calcein AM (Invitrogen™) for 30 min and evaluated using a fluorescence microscope

(Zeiss AxioImager Z1, Carl Zeiss Inc., Germany).[36] ImageJ was used to measure tube length and dots from five random images.

2.8. Statistical analysis

The Shapiro-Wilk test was used to verify the normality of all dependent variables and the one-way ANOVA was used to analyze the statistically significant differences among the groups. Tukey's Honestly Significant Difference (HSD) test was used for post-hoc comparisons. A significance level of 5% was considered. Tests were performed using IBM SPSS Statistics for Windows (IBM SPSS Statistics for Windows, v.21.0., IBM Corp.; USA), and final graphs were prepared with GraphPad Prism version 8.0.0 for Windows (GraphPad Software).

3. RESULTS AND DISCUSSION

The electrospinning technique is a straightforward and effective strategy for developing a delivery system of functional elements in biological tissues. Herein, electrospun fibers were fabricated and functionalized with Cu^{2+} ion in a facile manner to achieve release for active participation in biological events involved in bone formation and prevent bacterial infections. Our findings clearly demonstrate that incorporating Cu^{2+} ion into GBR membranes is feasible in a facile manner and that fabricated membranes have beneficial effects on bone forming and angiogenic cells, as well as anti-bacterial effects on one of the most prominent pathogenic bacteria (*S. aureus)*.

3.1. Higher concentrations of CuO lead to greater pore areas of GBR membranes

Adequate tissue integration and osteopromotive capacities are intimately related to GBR membranes features, such as surface topography, adequate porosity, relative occlusiveness,

sufficient stiffness, and chemical composition.[37] Herein, uniform and homogenous electrospun membranes were successfully fabricated, showing a network of nanofibers comprising increased amounts of CuO particles depending on the CuO concentration used in the solution (Figure 1). The different amounts of CuO changed the membrane color from off-white to shades of gray (Figure 1a and S1). CuO nanoparticles formed clusters that increased in number with higher concentrations of CuO in the solution (Figure 1b). In general, membranes were defect-free, but the aggregation of nanoparticles in the solution of CuO 1% led to some morphological changes[38] such as the rupture of the nanofiber (Figure S2). Higher concentrations of CuO led to a membrane with greater pore area (Figure 1b) and higher pore surface coverage (Figure 1c), as well as thinner fiber diameter (Figure 1d). This is a result of an increase in solution conductivity by Cu addition that accelerates the liquid jet towards the collector reducing fiber diameter in the electrospinning process.[39] The porosity of membranes for bone regeneration needs to be sufficient to facilitate nutrient uptake and oxygen diffusion for the wound, which is suitable for the regenerative process, but also capable of limiting the invasion of gingival epithelium and connective tissue cells into the wound that can impair the formation of new bone tissue.[19,40] Even though our results indicate an increase in pore size for higher Cu concentrations (i.e., CuO 1% and CuO 0.5%), values were lower than 8 μm and for most pores lower than 3 μm. Besides that, the assembly of multiple layers of nanofibers one on top of each other, densely packed, creates a membrane with an adequate cell-occlusive property (barrier effect) that also could avoid migration of bacteria into, or through, the membrane structure.[41,42]

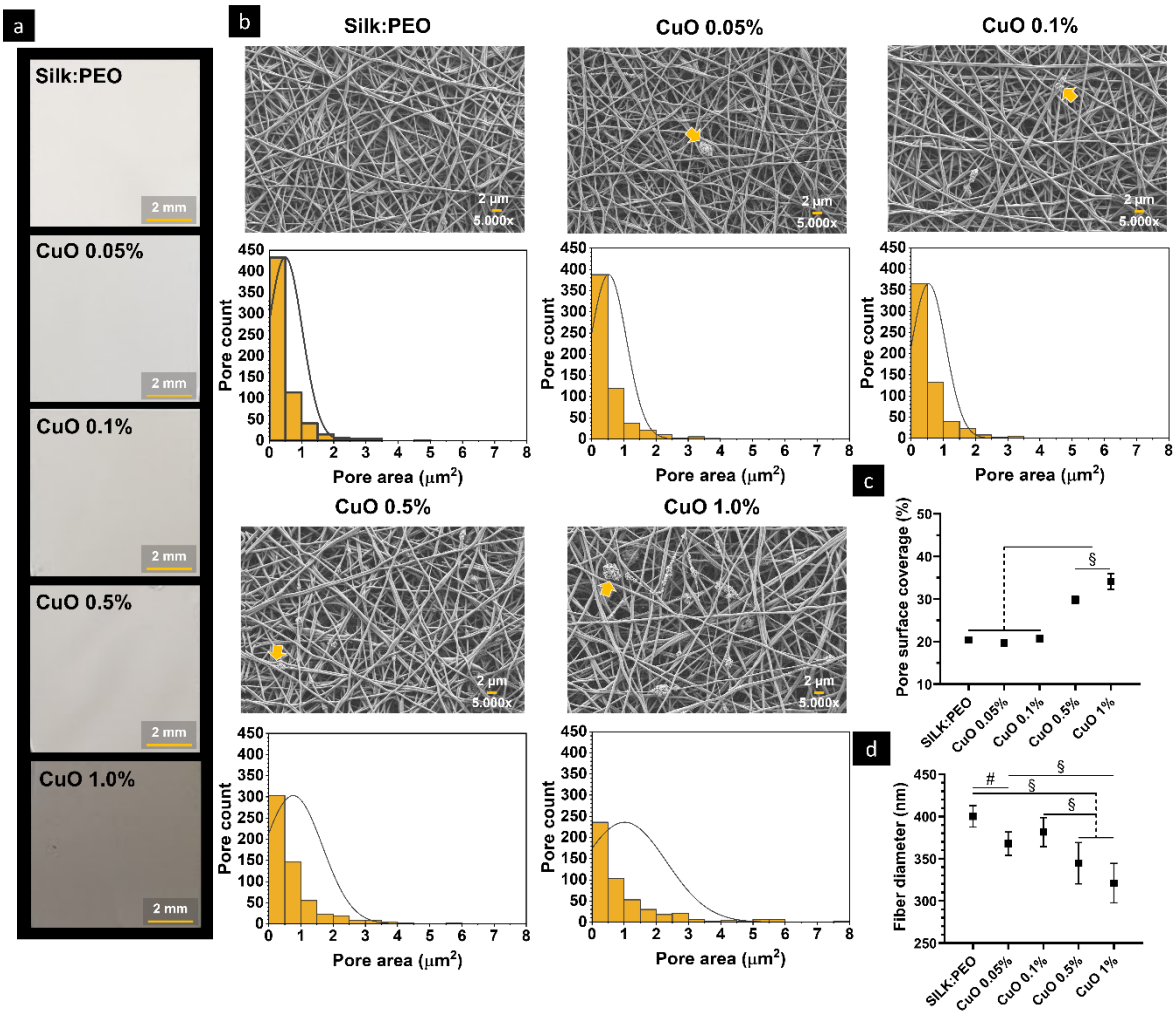

Figure 1. Morphological features of Cu^{2+}-loaded membranes: a) photography of membranes, b) SEM micrographs (top), pore area distribution (bottom), c) percentage of the area covered by pores, and d) fiber diameter. Yellow arrows indicate CuO nanoparticles clusters. Statistically significant differences between groups (n=5) are indicated by symbols: #$p < 0.01$, §$p < 0.001$.

3.2. Acidic environment accelerates and increases the release of Cu^{2+} ion from GBR membranes

It is worth noting that only aqueous solvents and bioresorbable materials were used to avoid toxicity and form an environmentally friendly membrane that follows the concept of green

electrospinning.[43,44] To verify the incorporation of CuO into membranes, samples were investigated by EDX (Figure 2a) and XRD (Figure 2b). Cu was detected in the membranes following the expected at.% concentration and proportionally to CuO amounts (wt. %) in solutions (Table S1). Higher diffraction peaks (2θ = ≈35° and ≈38°) corresponding to (002) and (111) crystal planes of the CuO phase (JCPDS, No. 48-1548) are shown as the concentration of CuO nanoparticles increases in the membrane. Peaks corresponding to silk (2θ = ≈19° and ≈23°) did not change significantly with the increase of Cu into nanofibers.

Cu^{2+} ion was released in culture media with two different pHs (Figure 2c), and the total amount of Cu in membranes (Figure 2d) was investigated by the ICP technique. In an alkaline environment, Cu^{2+} ion was released for up to 7 days showing a sustained release profile, which is instrumental for a prolonged Cu effect within the bone defect. Only ≈5% of Cu was released from CuO 1% and CuO 0.5%, while ≈8% and ≈12% of Cu incorporated into membranes were released from CuO 0.1% and CuO 0.05%, respectively (Figure S3). On the other hand, CuO was released from membranes much faster and completely within 4 days in an acidic environment. This phenomenon may be a consequence of the fast dissolution of PEO from the membrane fibers at a pH of 4 compared to a pH of 8, which accelerates the exposure of CuO nanoparticles to the medium. A more substantial release of Cu in acidic environments can be interesting to overcome the start of acute infections, in which pH decreases may occur due to lactic acid production and oxygen in the wound [45], leaching a higher concentration of Cu to kill pathogenic bacteria.

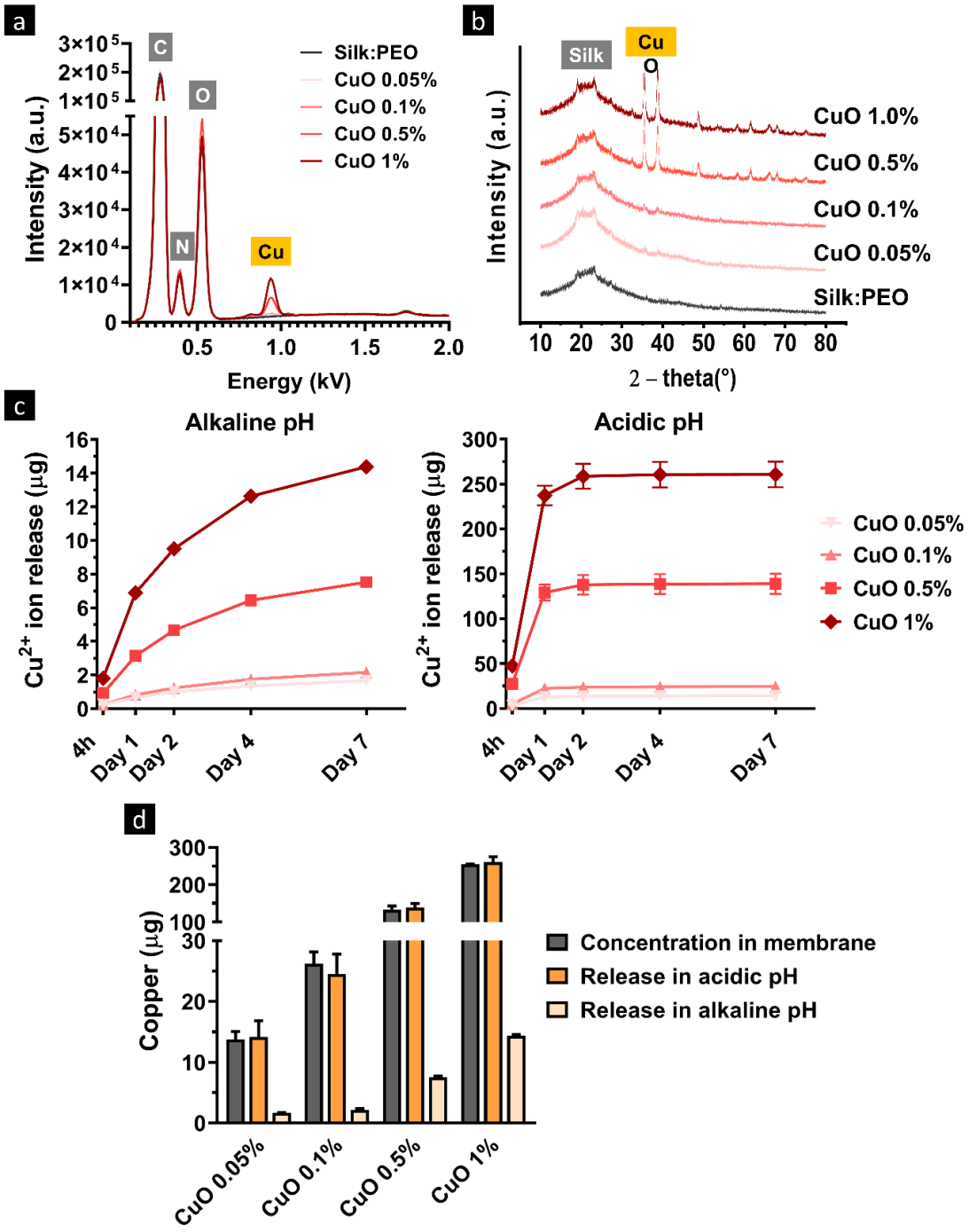

Figure 2. Chemical composition of Cu^{2+}-loaded membranes: a) EDX; b) XRD spectra; c) cumulative Cu^{2+} ion release profile (n = 3) in alkaline and acidic conditions; d) relation between Cu^{2+} total content in membranes and Cu^{2+} ion release.

3.3. Cu^{2+}-loaded GBR membranes demonstrate appropriate mechanical behavior

GBR membranes are responsible for providing timely mechanical support at the implant site until the new bone is able to withstand mechanical load.[46] Membranes were evaluated by mechanical tests to investigate if Cu incorporation into Silk:PEO membranes affect their integrity. Our data showed that Cu incorporation does not change tensile strength and total elongation in a dry condition, but low concentrations of incorporated Cu enhanced Young's modulus (Figure 3). Generally, incorporating nanoparticles into polymeric nanofiber membranes increased their stiffness by a reinforcing effect.[10] However, increasing Cu concentrations led to observable defects in the nanofibers that may affect the mechanical reinforcement for the CuO 1% and CuO 0.5% groups. Under wet conditions, lower tensile strength and total elongation were observed for membranes with low Cu content. It is possible that the swelling evoked by the water, facilitated the leaching of small amounts of Cu from the fibers for these groups, losing their strength. The effect of water in the structure of silk: PEO nanofibers[33] and collagen membranes [47] has been studied before, showing a similar trend as observed here. While the tensile strength is higher for membranes in a dry state, the elongation at break showed greater values for the wet state membranes, indicating a strong ductile behavior of the membranes in humid environments.[33,47] Although Cu^{2+}-loaded membranes displayed slight changes among the groups in terms of fiber diameter, integrity, and porosity, CuO incorporation did not considerably impair the resistance and elasticity of the membranes. In fact, all groups showed mechanical behavior similar to commercially available GBR collagen membranes.[47,48] While Cu^{2+}-loaded membranes showed resistance to break closer to the Bio-Gide® (4.8 MPa), their Young's modulus and elongation were higher than other two collagen membranes (158.5 – 178.9 MPa; 16.9 – 22.1 %, respectively),[48] demonstrating that despite being stiff their fibers are flexible and exhibit stretching ability. Therefore, the silk-based electrospun membranes apparently have appropriate mechanical

properties required to handle and adapt the membrane within a bone defect. It could be applied clinically for space maintenance, also bearing the forces submitted onto the membranes after being placed in position.

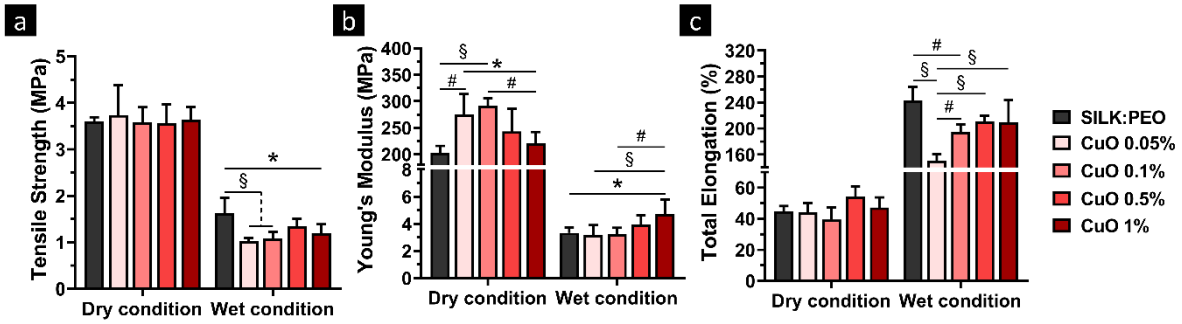

Figure 3. Mechanical properties of Cu^{2+}-loaded membranes in dry and wet conditions: a) tensile strength, b) Young's modulus, and c) percentage of total elongation at break obtained from a universal tensile strength testing machine. Statistically significant differences between groups are indicated by symbols: *$p < 0.05$, #$p < 0.01$, §$p < 0.001$.

3.4. The antibacterial activity of the GBR membranes is Cu-concentration dependent

The antibacterial effect of the Cu^{2+}-loaded GBR membranes was tested against *S. aureus* biofilm grown for 24 h. *S. aureus* is one of the dominant bacteria in bone infections, causing the majority of osteomyelitis cases by the colonization of the bone and expression of a vast array of virulence factors.[49] Once the biofilm is formed, it facilitates the persistence of the infection, delaying the wound healing by inducing inflammatory cell recruitment, decreasing osteoblast activity, increasing osteoclastogenesis, and causing osteoblast death, which impairs osteoblast/osteoclast balance necessary for proper bone formation.[50]

Herein, a less dense *S. aureus* biofilm was observed for Cu^{2+}-loaded membranes with increasing amounts of incorporated CuO (Figure 4a). The CFU counts showed a Cu-concentration-dependent antibacterial effect (Figure 4b). The highest concentration of Cu was

able to reduce ~1.5 logs of CFU ($p < 0.05$), but the lowest CuO amount (i.e. 0.05%) did not show a significant reduction in biofilm formation compared to Cu-free control membranes. These results might be related to the amount of Cu^{2+} ion released from the membranes, which either demonstrates bacterial toxicity or prevents bacterial adhesion and proliferation, mainly by three mechanisms of action: i) electrostatic attraction between *S. aureus* negatively charged cell surface and the positively charged ion (Cu^{2+}) that attaches or enters into bacteria, resulting in cell membrane disruption and loss of cytoplasmic content;[51,52] ii) production of reactive oxygen species (ROS) that lead to apoptosis via damage to lipids, proteins, membrane, and DNA;[51] and iii) impairment of the respiratory chain activity and the gene replication process of the bacteria.[53]

The microbiological assay used in this study only evaluated a single-species microbial biofilm (24 h) for screening purposes. Future research could contemplate more complex biofilm (e.g., polymicrobial and long-term results), co-culture and *in vivo* models to validate these findings. Since implant-related infections of bone tissue are extremely challenging to treat, avoiding bacterial infection from occurring or acting in the primary stage of bacterial infection is key to the treatment.[54] As such, the reduction of bacteria load found herein by the sustained release of Cu can favor the host response to inhibit the progression of the bacterial infection when the immune system is still strong and bacterial levels are relatively low. In this way, it would be possible to prevent the start or progression of the bone infection from an acute to a chronic stage, when a continuous inflammatory process and spreading of bacteria generates the destruction of bone tissues.[54]

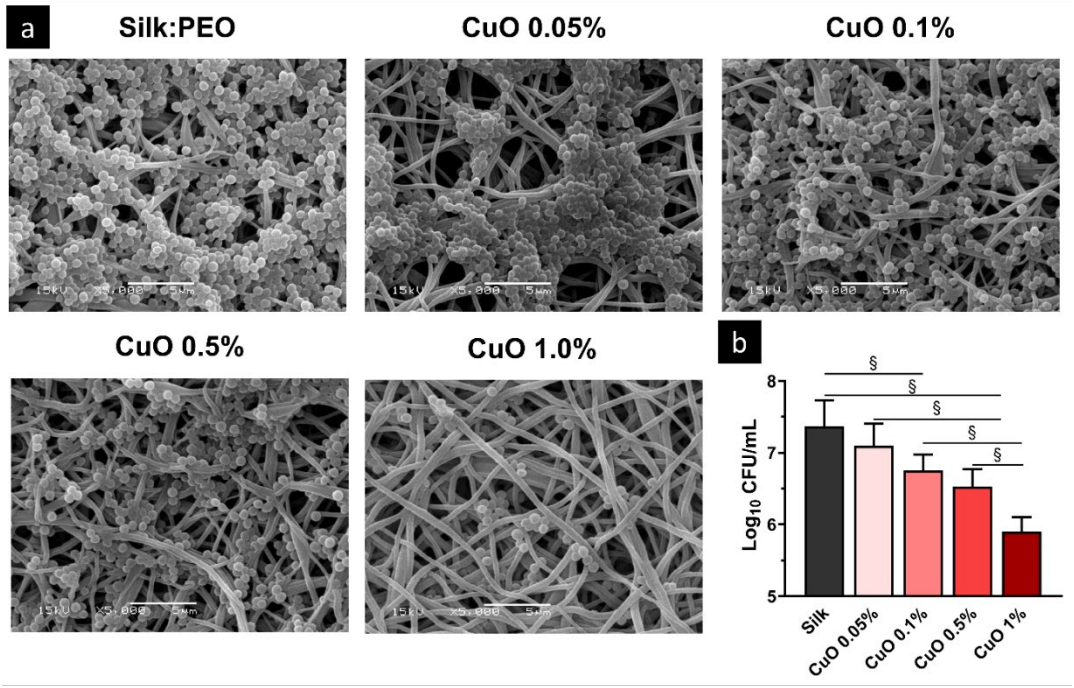

Figure 4. Antibacterial effect of Cu^{2+}-loaded membranes: a) representative SEM micrographs and b) CFU counts after 24 h of *S. aureus* biofilm formation (n = 9). Statistically significant differences between groups are indicated by symbols: §$p < 0.001$.

3.5. CuO 0.1% and 0.05% stimulate the behavior of bone and angiogenic cells

Membrane biocompatibility (Figure 5) was evaluated by culturing two types of primary human cells (hBMSCs and HUVECs) related to the regenerative and wound healing processes. A higher number of cells, i.e. greater DNA content, was observed for membranes with low concentrations of Cu. In fact, CuO 0.05% presented higher DNA content than Silk:PEO after 7 days ($p < 0.01$; Figure 5a,c). In fact, Cu^{2+}-loaded membranes with 0.1 and 0.05% of CuO showed the highest increase in the amount of DNA from day 1, indicating these membranes stimulate cell proliferation. The specific role of Cu^{2+} ion in cell behavior is unclear, but these ions seem to improve the adhesion of cells to the fiber surface of the membranes, which corresponds to the first step in bone formation.[51] While MSCs can migrate to defect sites with a high affinity to differentiate into an osteoblastic lineage, increasing

osteogenesis,[55,56] the endothelial cells are known to form new blood vessel networks,[57] facilitating bone growth. SEM images confirm that CuO 0.1% and 0.05% supported cell adhesion and spreading, displaying cells that almost fully covered membrane surfaces within 7 days of culture. In addition, by culturing the cells on the membrane surface, it was possible to confirm that they did not grow into the membrane, demonstrating an occlusive effect. On the other hand, CuO 1% and 0.5% groups were cytotoxic for hBMSCs and HUVECs, which can be confirmed by the round-shaped cells observed on SEM micrographs (Figure S4). Even though hardly any cells were found for CuO 1% and 0.5% membranes, it was possible to detect cell DNA content for these groups at all time points, possibly due to cells trapped within the nanofibers network after washing.

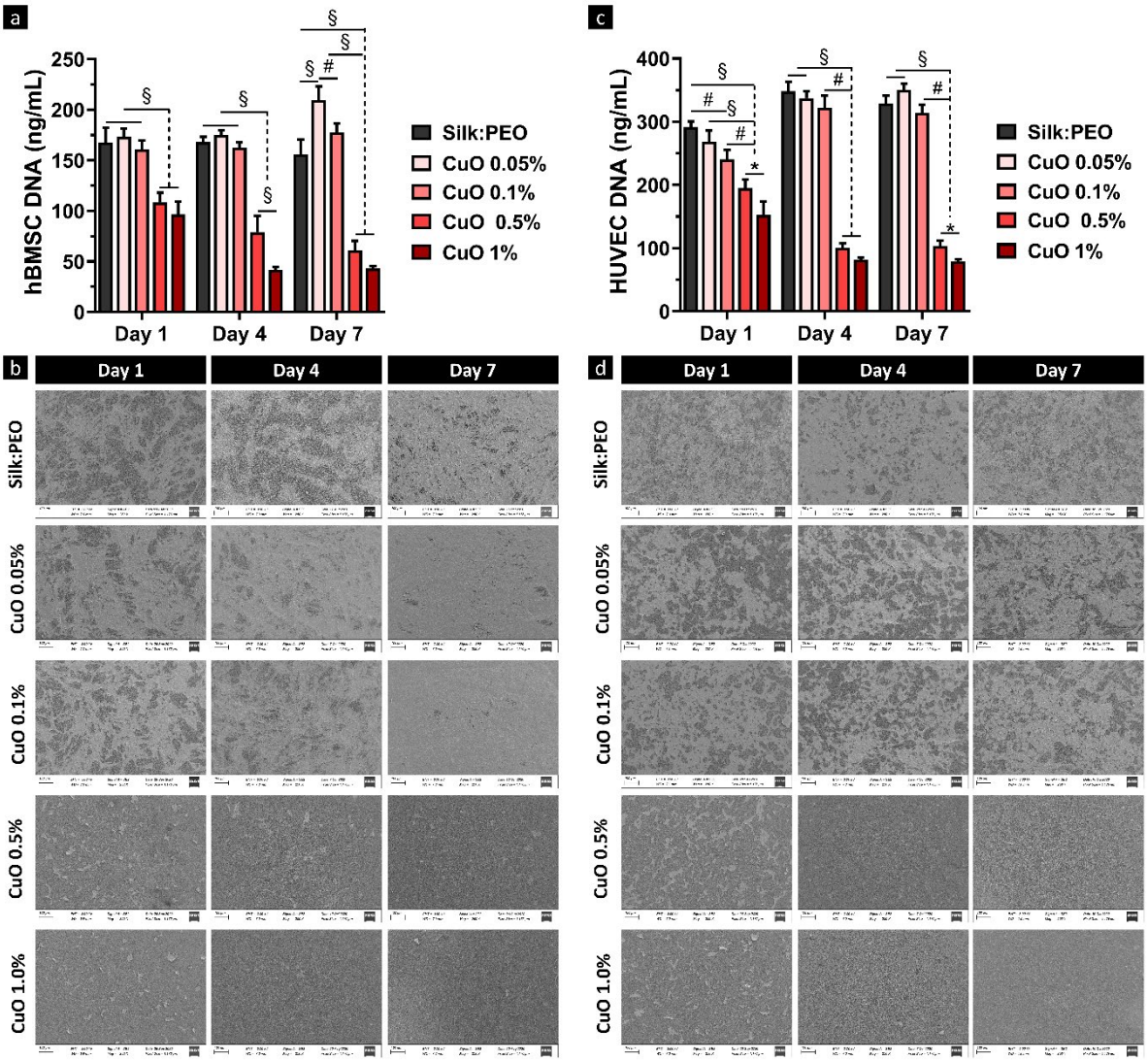

Figure 5. Effect of Cu^{2+}-loaded membranes in the direct cell cultures. DNA content (n = 4) and SEM micrographs of hBMSC (a, b) and HUVEC (c, d). Cells adhered to membranes after 1, 4, and 7 d. Statistically significant differences between groups are indicated by symbols: *p < 0.05, #p < 0.01, §p < 0.001.

In Figure 6, the results from the indirect culture experiments tested with the extract medium containing Cu released after 1, 4, and 7 days of incubation are presented. Cu^{2+} ion released from membranes affected cell metabolic activity measured by CCK-8 assay, especially for membranes with higher concentrations of CuO that diminished cell function (Figure 6a). For hBMSCs, Cu^{2+} ion released from both CuO 0.05 and 0.1% did not change the cell metabolic activity, also presenting practically only live cells in the live/dead experiment (Figure 6b). For HUVEC cells, a more sensitive response to Cu^{2+} ion release was observed. The extract medium collected from CuO 0.1% and 0.05% after 1 day of immersion improved HUVECs metabolic activity compared to Silk:PEO, but media from CuO 1% and 0.5% membranes inhibited cell metabolic activity. Although the amount of Cu^{2+} ion released from the CuO 0.5% membrane showed a cytotoxic effect, cells showed adequate metabolic activity when cultured with the extracted media from days 4 and 7. In fact, the amount of Cu^{2+} ion released within the first day was crucial for compatibility with the tissues. Therefore, controlling the Cu release (concentration and kinetics) from the nanofibers might be an attractive approach to enhance the biological capability of membranes for bone tissue engineering.[58]

When testing the *in vitro* angiogenic effects, endothelial cells assemble into a vascular labyrinth (e.g., vasculogenesis) with subsequent sprouting that ensures expansion of the vascular network, known as angiogenesis.[59] Herein, the extract medium from day 1 was used to culture HUVEC cells on a reduced growth factor basement membrane matrix. CuO 0.1% and 0.05% extracted mediums supported and stimulated angiogenesis, presenting greater tube

length vs. Silk:PEO, demonstrating that Cu has a clear role in forming blood vessels underlying the membrane. Angiogenesis influences cell growth and differentiation by delivering all the essential elements (vascular growth, oxygen, nutrients, cytokines, and several types of cells) needed for osteoblast maturation to form new bone.[51,57] Cu^{2+} ion seem to bind to and interact with several growth factors, proteins, and enzymes involved in blood vessel formation (i.e. VEGF, angiogenin, and matrix metalloproteinases), modulating and coordinating their expression and activity to stimulate the angiogenesis, and hence bone remodeling.[51]

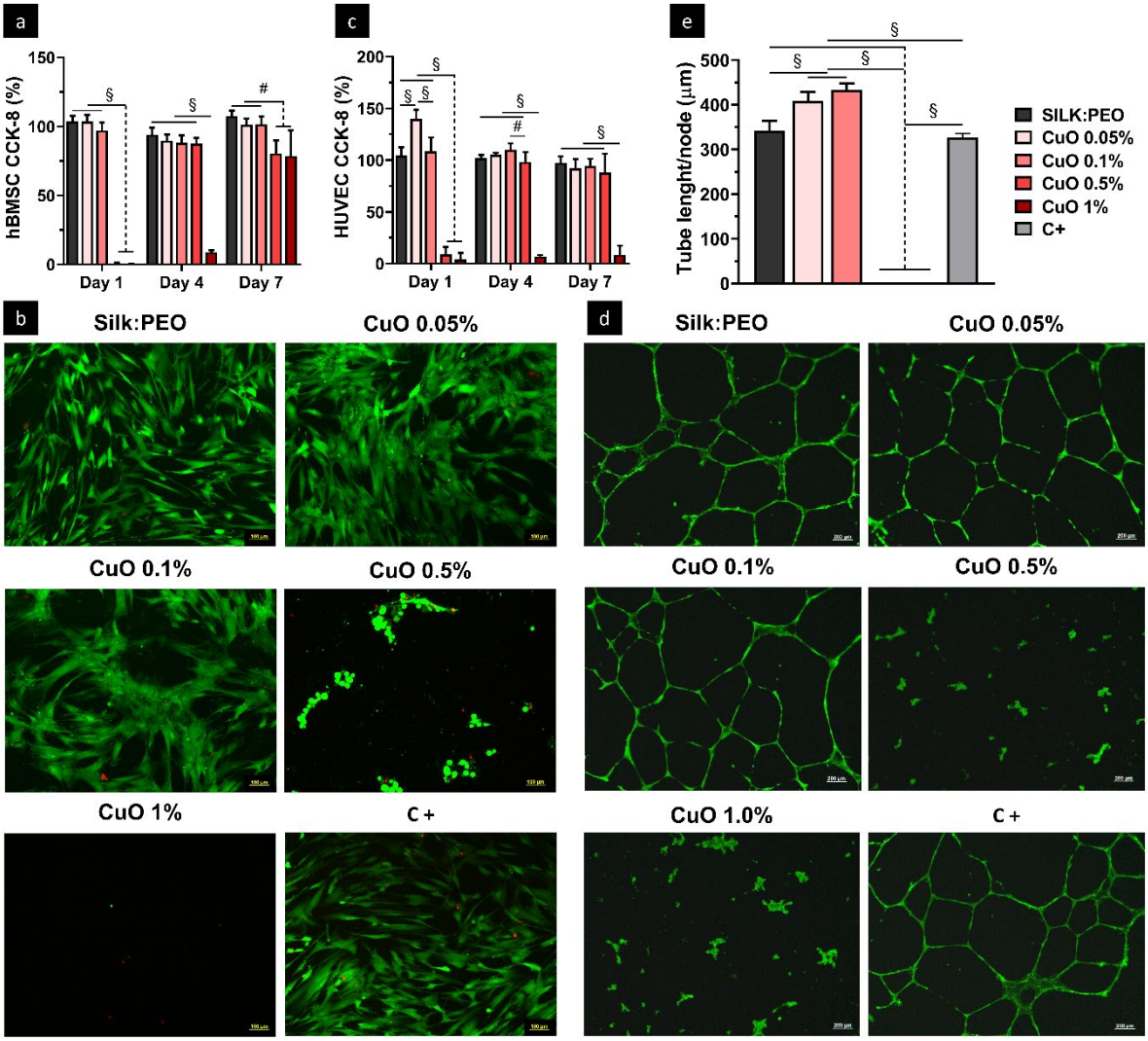

Figure 6. Effect of Cu^{2+}-loaded membranes on the indirect culture of hBMSC and HUVEC: a) hBMSC metabolic activity (%) evaluated by CCK- 8 assay after culturing with extract

medium from 1, 4, and 7 d (n = 3) and b) live/dead analysis after culture with extract medium from day 1 (green for live cells, red for dead cells); c) HUVEC metabolic activity after culture with extract medium from 1, 4, and 7 d (n = 3) and (d) fluorescence images of tube formation assay and e) tube length after 18 h of contact with extract medium from day 1. Statistically significant differences between groups are indicated by symbols: #$p < 0.01$, §$p < 0.001$.

3.6. Clinical relevance and future perspectives

Our results demonstrate, for the first time, the advantage of loading Cu nanoparticles in a silk-based nanofibrous membrane fabricated by electrospinning technique to launch new possibilities for regenerative treatments. Figure 7 summarizes the biological effects of the tailored Cu^{2+}-loaded membranes. Here, we show that using a facile approach to fabricate Cu^{2+}-loaded GBR membranes with tailorable Cu concentration, such GBR membranes improve the regeneration process by supporting the adhesion and proliferation of cells directly and stimulating angiogenesis indirectly, all very important for the formation of blood vessels, bone growth, and hence regeneration of a bone defect. Still, further investigations in comparison to the commercially available materials (gold standards) are necessary to examine their efficacy, advantages, and limitations. Additionally, future studies could address biomolecular mechanisms underlying the effects of Cu on cell responses and evaluate *in vivo* efficacy of Cu^{2+}-loaded GBR membranes.

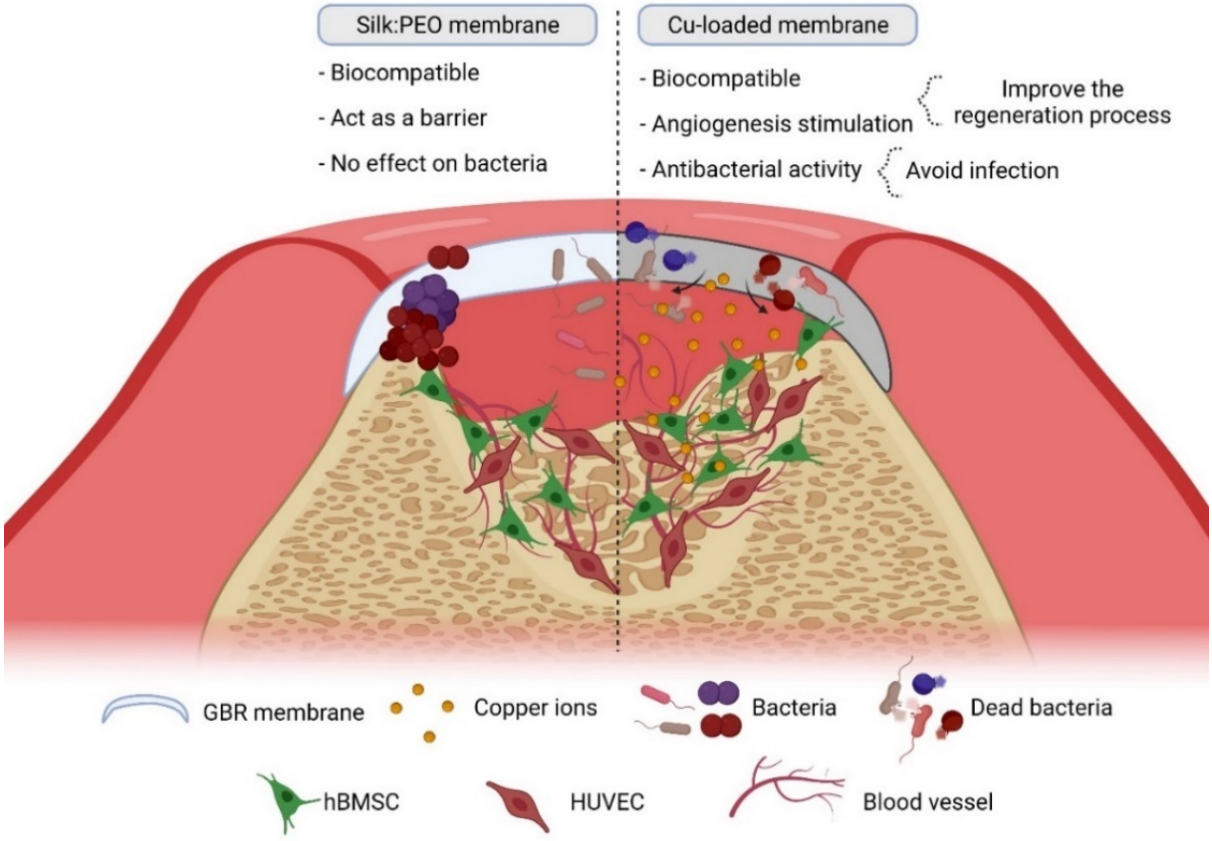

Figure 7. Schematic representation of Cu^{2+}-loaded GBR membrane and its biological effects.

Additionally, these membranes may be a valuable strategy to diminish the risk of infection by a direct killing contact and indirect action of Cu released into the environment. Infections in bone sites are challenging to treat because of their deep localization in the tissue, bacteria immune cell evasion, and protection from antibiotic treatments.[49,51,60] Although the membranes developed here did not eliminate bacteria completely, they reduced the microbial load, facilitating the immune system to fight against bacterial infection. Even though this membrane was developed to be applied for GBR in dental applications, our results also translate toward other rehabilitative procedures in e.g. the orthopedic area. Additionally, GBR membranes can be combined with additional therapeutic approaches, such as bone grafting,

aiming to mitigate or compensate the impact of bone defects, leading to new paths for bone tissue regeneration strategies.[46]

4. CONCLUSIONS

We here successfully synthetized Cu^{2+}-loaded GBR membranes using the electrospinning technique with different Cu concentrations (0.01 – 1 wt.%). Although, the functional Cu^{2+}-loaded GBR membranes with tailorable Cu-amounts exhibited slight antibacterial capacity in the non-cytotoxic concentrations, these results are very encouraging, considering the importance of appropriate mechanical properties, cell adhesion stimulation and proliferation, and angiogenic responses. Consequently, fine-tuning the Cu concentration in fibers may be a valuable strategy to diminish the risk of infections and improve the bone regeneration process in bone defects underneath a GBR membrane, and hence accelerate the rehabilitative treatment providing long-term success.

ACKNOWLEDGMENTS

This work was supported by the São Paulo Research Foundation (FAPESP) – Brazil (grant numbers 2017/01320-0 and 2018/14117-0), the Conselho Nacional de Desenvolvimento Científico e Tecnológico – Brazil (CNPq) (grant number 304853/2018-60), and the Coordenação de Aperfeiçoamento de Pessoal de Nível Superior – Brasil (CAPES) (Finance Code 001). The authors also express their gratitude to the Endodontics Lab at Piracicaba Dental School (UNICAMP) for the microbiology facility and the Regenerative Biomaterials Lab at the Radboud University Medical Center (Radboudumc). Graphical abstract and Fig. 7 were created with BioRender®.

Supplementary material

Figure S1. Dumbbell-shaped samples from membranes used for the mechanical characterization.

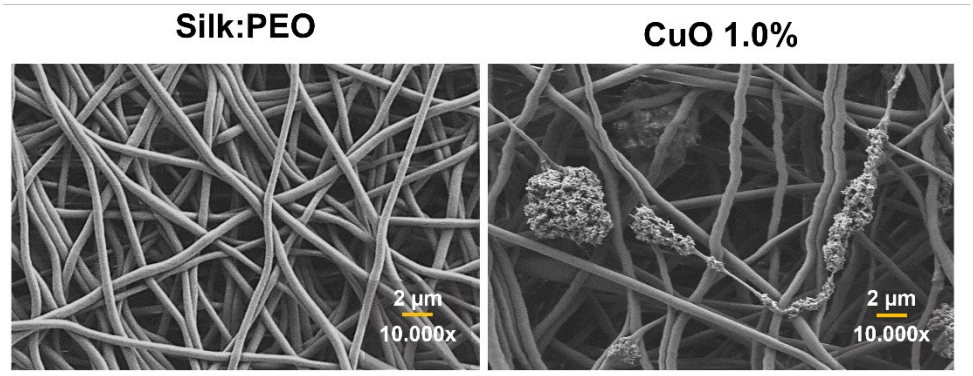

Figure S2. Scanning electron micrographs of Silk:PEO and CuO 1.0% electrospun membranes (10.000 ×).

Table S1. Atomic concentration (at. %) and weight concentration (wt. %) of Cu determined by energy-dispersive X-ray.

	CuO 0.05%	CuO 0.1%	CuO 0.5%	CuO 1%
at. %	0.05 (0.01)	0.09 (0.01)	0.51 (0.02)	1.02 (0.04)
wt. %	4.65 (0.18)	2.57 (0.33)	0.43 (0.06)	0.24 (0,05)

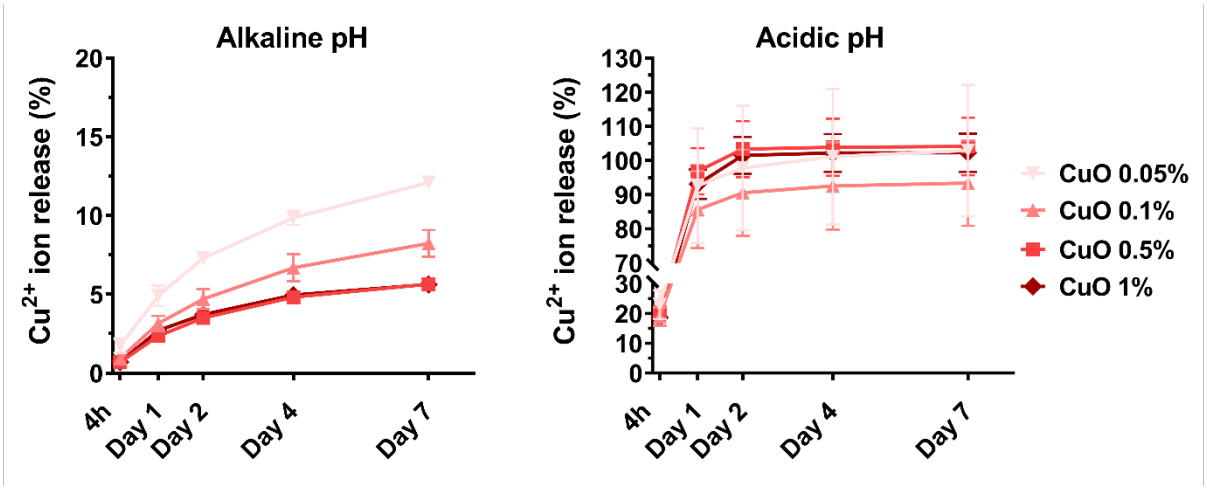

Figure S3. Cumulative Cu^{2+} ion release in alkaline and acidic pH over 7 days expressed in percentage to the total Cu^{2+} concentration in the membranes. Data are expressed as mean ±standard deviation.

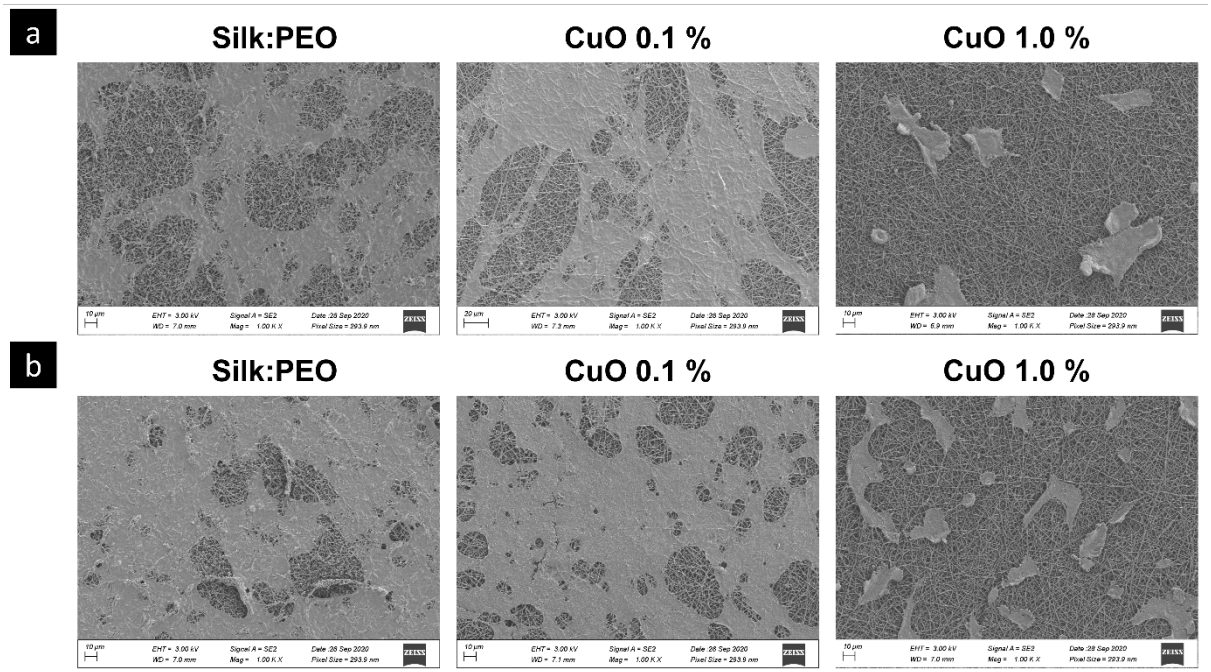

Figure S4. SEM images (n = 2) of hBMSC (a) and HUVEC (b) adhesion to membranes after 1d (1.000 ×).

REFERENCES

(1) D'Mello, S.; Elangovan, S.; Hong, L.; Ross, R. D.; Sumner, D. R.; Salem, A. K. Incorporation of Copper into Chitosan Scaffolds Promotes Bone Regeneration in Rat Calvarial Defects. *J. Biomed. Mater. Res. Part B Appl. Biomater.* **2015**, *103* (5), 1044–1049. https://doi.org/10.1002/jbm.b.33290.

(2) Clementini, M.; Morlupi, A.; Canullo, L.; Agrestini, C.; Barlattani, A. Success Rate of Dental Implants Inserted in Horizontal and Vertical Guided Bone Regenerated Areas: A Systematic Review. *Int. J. Oral Maxillofac. Surg.* **2012**, *41* (7), 847–852. https://doi.org/10.1016/j.ijom.2012.03.016.

(3) Elangovan, S.; Avila-Ortiz, G.; Johnson, G. K.; Karimbux, N.; Allareddy, V. Quality Assessment of Systematic Reviews on Periodontal Regeneration in Humans. *J. Periodontol.* **2013**, *84* (2), 176–185. https://doi.org/10.1902/jop.2012.120021.

(4) Castro, A. G. B.; Diba, M.; Kersten, M.; Jansen, J. A.; van den Beucken, J. J. J. P.; Yang, F. Development of a PCL-Silica Nanoparticles Composite Membrane for Guided Bone Regeneration. *Mater. Sci. Eng. C* **2018**, *85* (August 2017), 154–161. https://doi.org/10.1016/j.msec.2017.12.023.

(5) Xu, X.; Lu, Y.; Yang, X.; Du, Z.; Zhou, L.; Li, S.; Chen, C.; Luo, K.; Lin, J. Copper-Modified Ti6Al4 V Suppresses Inflammatory Response and Osteoclastogenesis While Enhancing Extracellular Matrix Formation for Osteoporotic Bone Regeneration. *ACS Biomater. Sci. Eng.* **2018**, *4* (9), 3364–3373. https://doi.org/10.1021/acsbiomaterials.8b00736.

(6) Elnayef, B.; Monje, A.; Albiol, G.; Galindo-Moreno, P.; Wang, H.-L.; Hernández-Alfaro, F. Vertical Ridge Augmentation in the Atrophic Mandible: A Systematic Review and Meta-Analysis. *Int. J. Oral Maxillofac. Implants* **2017**, *32* (2), 291–312. https://doi.org/10.11607/jomi.4861.

(7) Lim, G.; Lin, G.-H.; Monje, A.; Chan, H.-L.; Wang, H.-L. Wound Healing Complications Following Guided Bone Regeneration for Ridge Augmentation: A Systematic Review and Meta-Analysis. *Int. J. Oral Maxillofac. Implants* **2018**, *33* (1), 51–50. https://doi.org/10.11607/jomi.5581.

(8) Lang, N. P.; Hämmerle, C. H. F.; Brägger, U.; Lehmann, B.; Nyman, S. R. Guided Tissue Regeneration in Jawbone Defects Prior to Implant Placement. *Clin. Oral Implants Res.* **1994**, *5* (2), 92–97. https://doi.org/10.1034/j.1600-0501.1994.050205.x.

(9) Elgali, I.; Omar, O.; Dahlin, C.; Guided, T. P.; Thomsen, P.; Guided, T. P. Guided Bone Regeneration: Materials and Biological Mechanisms Revisited. *Eur. J. Oral Sci.* **2017**, *125* (5), 315–337. https://doi.org/10.1111/eos.12364.

(10) Tonda-Turo, C.; Ruini, F.; Ceresa, C.; Gentile, P.; Varela, P.; Ferreira, A. M.; Fracchia, L.; Ciardelli, G. Nanostructured Scaffold with Biomimetic and Antibacterial Properties for Wound Healing Produced by 'Green Electrospinning.' *Colloids Surfaces B Biointerfaces* **2018**, *172* (August), 233–243. https://doi.org/10.1016/j.colsurfb.2018.08.039.

(11) O'Neill, E.; Awale, G.; Daneshmandi, L.; Umerah, O.; Lo, K. W. H. The Roles of Ions on Bone Regeneration. *Drug Discov. Today* **2018**, *23* (4), 879–890. https://doi.org/10.1016/j.drudis.2018.01.049.

(12) Wang, P.; Yuan, Y.; Xu, K.; Zhong, H.; Yang, Y.; Jin, S.; Yang, K.; Qi, X. Biological Applications of Copper-Containing Materials. *Bioact. Mater.* **2021**, *6* (4), 916–927. https://doi.org/10.1016/j.bioactmat.2020.09.017.

(13) Mitra, D.; Kang, E. T.; Neoh, K. G. Antimicrobial Copper-Based Materials and Coatings: Potential Multifaceted Biomedical Applications. *ACS Appl. Mater. Interfaces* **2020**, acsami.9b17815. https://doi.org/10.1021/acsami.9b17815.

(14) Wang, H.; Zhao, S.; Zhou, J.; Shen, Y.; Huang, W.; Zhang, C.; Rahaman, M. N.; Wang, D. Evaluation of Borate Bioactive Glass Scaffolds as a Controlled Delivery System for Copper Ions in Stimulating Osteogenesis and Angiogenesis in Bone Healing. *J. Mater. Chem. B* **2014**, *2* (48), 8547–8557. https://doi.org/10.1039/c4tb01355g.

(15) Lim, T. C.; Kotaki, M.; Yong, T. K. J.; Yang, F.; Fujihara, K.; Ramakrishna, S. Recent Advances in Tissue Engineering Applications of Electrospun Nanofibers. *Mater. Technol.* **2004**, *19* (1), 20–27. https://doi.org/10.1080/10667857.2004.11753060.

(16) Patil, J. V.; Mali, S. S.; Kamble, A. S.; Hong, C. K.; Kim, J. H.; Patil, P. S. Electrospinning: A Versatile Technique for Making of 1D Growth of Nanostructured Nanofibers and Its Applications: An Experimental Approach. *Appl. Surf. Sci.* **2017**, *423*, 641–674. https://doi.org/10.1016/j.apsusc.2017.06.116.

(17) Zou, Y.; Zhang, L.; Yang, L.; Zhu, F.; Ding, M.; Lin, F.; Wang, Z.; Li, Y. "Click" Chemistry in Polymeric Scaffolds: Bioactive Materials for Tissue Engineering. *J. Control. Release* **2018**, *273* (December 2017), 160–179. https://doi.org/10.1016/j.jconrel.2018.01.023.

(18) Chen, S.; Li, R.; Li, X.; Xie, J. Electrospinning: An Enabling Nanotechnology Platform for Drug Delivery and Regenerative Medicine. *Adv. Drug Deliv. Rev.* **2018**, *132*, 188–213. https://doi.org/10.1016/j.addr.2018.05.001.

(19) Lian, M.; Sun, B.; Qiao, Z.; Zhao, K.; Zhou, X.; Zhang, Q.; Zou, D.; He, C.; Zhang, X. Bi-Layered Electrospun Nanofibrous Membrane with Osteogenic and Antibacterial Properties for Guided Bone Regeneration. *Colloids Surfaces B Biointerfaces* **2019**, *176* (January), 219–229. https://doi.org/10.1016/j.colsurfb.2018.12.071.

(20) Soares, R. M. D.; Siqueira, N. M.; Prabhakaram, M. P.; Ramakrishna, S. Electrospinning and Electrospray of Bio-Based and Natural Polymers for Biomaterials

Development. *Mater. Sci. Eng. C* **2018**, *92* (July), 969–982. https://doi.org/10.1016/j.msec.2018.08.004.

(21) He, M.; Xue, J.; Geng, H.; Gu, H.; Chen, D.; Shi, R.; Zhang, L. Fibrous Guided Tissue Regeneration Membrane Loaded with Anti-Inflammatory Agent Prepared by Coaxial Electrospinning for the Purpose of Controlled Release. *Appl. Surf. Sci.* **2015**, *335*, 121–129. https://doi.org/10.1016/j.apsusc.2015.02.037.

(22) Ji, W.; Yang, F.; Van Den Beucken, J. J. J. P.; Bian, Z.; Fan, M.; Chen, Z.; Jansen, J. A. Fibrous Scaffolds Loaded with Protein Prepared by Blend or Coaxial Electrospinning. *Acta Biomater.* **2010**, *6* (11), 4199–4207. https://doi.org/10.1016/j.actbio.2010.05.025.

(23) Kwon, K. J.; Seok, H. Silk Protein-Based Membrane for Guided Bone Regeneration. *Appl. Sci.* **2018**, *8* (8), 1214. https://doi.org/10.3390/app8081214.

(24) Boda, S. K.; Almoshari, Y.; Wang, H.; Wang, X.; Reinhardt, R. A.; Duan, B.; Wang, D.; Xie, J. Mineralized Nanofiber Segments Coupled with Calcium-Binding BMP-2 Peptides for Alveolar Bone Regeneration. *Acta Biomater.* **2019**, *85*, 282–293. https://doi.org/10.1016/j.actbio.2018.12.051.

(25) He, F. L.; Li, D. W.; He, J.; Liu, Y. Y.; Ahmad, F.; Liu, Y. L.; Deng, X.; Ye, Y. J.; Yin, D. C. A Novel Layer-Structured Scaffold with Large Pore Sizes Suitable for 3D Cell Culture Prepared by near-Field Electrospinning. *Mater. Sci. Eng. C* **2018**, *86*, 18–27. https://doi.org/10.1016/j.msec.2017.12.016.

(26) Zhang, M.; Lin, H.; Wang, Y.; Yang, G.; Zhao, H.; Sun, D. Fabrication and Durable Antibacterial Properties of 3D Porous Wet Electrospun RCSC/PCL Nanofibrous Scaffold with Silver Nanoparticles. *Appl. Surf. Sci.* **2017**, *414*, 52–62. https://doi.org/10.1016/j.apsusc.2017.04.052.

(27) Shrestha, B. K.; Shrestha, S.; Tiwari, A. P.; Kim, J. I.; Ko, S. W.; Kim, H. J.; Park, C. H.; Kim, C. S. Bio-Inspired Hybrid Scaffold of Zinc Oxide-Functionalized Multi-Wall Carbon Nanotubes Reinforced Polyurethane Nanofibers for Bone Tissue Engineering. *Mater. Des.* **2017**, *133*, 69–81. https://doi.org/10.1016/j.matdes.2017.07.049.

(28) Bai, C.; Lu, Z.; Jiang, H.; Yang, Z.; Liu, X.; Ding, H.; Li, H.; Dong, J.; Huang, A.; Fang, T.; Jiang, Y.; Zhu, L.; Lou, X.; Li, S.; Shao, N. Aptamer Selection and Application in Multivalent Binding-Based Electrical Impedance Detection of Inactivated H1N1 Virus. *Biosens. Bioelectron.* **2018**, *110*, 162–167. https://doi.org/10.1016/j.bios.2018.03.047.

(29) Wang, Y.; Cui, W.; Chou, J.; Wen, S.; Sun, Y.; Zhang, H. Electrospun Nanosilicates-Based Organic/Inorganic Nanofibers for Potential Bone Tissue Engineering. *Colloids Surfaces B Biointerfaces* **2018**, *172* (March), 90–97. https://doi.org/10.1016/j.colsurfb.2018.08.032.

(30) Fadaie, M.; Mirzaei, E.; Geramizadeh, B.; Asvar, Z. Incorporation of Nanofibrillated Chitosan into Electrospun PCL Nanofibers Makes Scaffolds with Enhanced Mechanical and Biological Properties. *Carbohydr. Polym.* **2018**, *199* (July), 628–640. https://doi.org/10.1016/j.carbpol.2018.07.061.

(31) Shao, J.; Yu, N.; Kolwijck, E.; Wang, B.; Tan, K. W.; Jansen, J. A.; Walboomers, X. F.; Yang, F. Biological Evaluation of Silver Nanoparticles Incorporated into Chitosan-Based Membranes. *Nanomedicine* **2017**, *12* (22), 2771–2785. https://doi.org/10.2217/nnm-2017-0172.

(32) Rockwood, D. N.; Preda, R. C.; Yücel, T.; Wang, X.; Lovett, M. L.; Kaplan, D. L. Materials Fabrication from Bombyx Mori Silk Fibroin. *Nat. Protoc.* **2011**, *6* (10), 1612–1631. https://doi.org/10.1038/nprot.2011.379.

(33) Serôdio, R.; Schickert, S. L.; Costa-Pinto, A. R.; Dias, J. R.; Granja, P. L.; Yang, F.; Oliveira, A. L. Ultrasound Sonication Prior to Electrospinning Tailors Silk Fibroin/PEO Membranes for Periodontal Regeneration. *Mater. Sci. Eng. C* **2019**, *98* (January), 969–981. https://doi.org/10.1016/j.msec.2019.01.055.

(34) Cordeiro, J. M.; Nagay, B. E.; Dini, C.; Souza, J. G. S.; Rangel, E. C.; da Cruz, N. C.; Yang, F.; van den Beucken, J. J. J. P.; Barão, V. A. R. Copper Source Determines Chemistry and Topography of Implant Coatings to Optimally Couple Cellular Responses and Antibacterial Activity. *Mater. Sci. Eng. C* **2021**, No. November, 112550. https://doi.org/10.1016/j.msec.2021.112550.

(35) Shao, J.; Wang, B.; Li, J.; Jansen, J. A.; Walboomers, X. F.; Yang, F. Antibacterial Effect and Wound Healing Ability of Silver Nanoparticles Incorporation into Chitosan-Based Nanofibrous Membranes. *Mater. Sci. Eng. C* **2019**, *98* (December 2018), 1053–1063. https://doi.org/10.1016/j.msec.2019.01.073.

(36) Ding, Z.; Qiao, Y.; Peng, F.; Xia, C.; Qian, S.; Wang, T.; Sun, J.; Liu, X. Si-Doped Porous TiO2 Coatings Enhanced in Vitro Angiogenic Behavior of Human Umbilical Vein Endothelial Cells. *Colloids Surfaces B Biointerfaces* **2017**, *159*, 493–500. https://doi.org/10.1016/j.colsurfb.2017.08.010.

(37) de Santana, R. B.; de Mattos, C. M. L.; Francischone, C. E.; Van Dyke, T. Superficial Topography and Porosity of an Absorbable Barrier Membrane Impacts Soft Tissue Response in Guided Bone Regeneration. *J. Periodontol.* **2010**, *81* (6), 926–933. https://doi.org/10.1902/jop.2010.090592.

(38) Song, J.; Klymov, A.; Shao, J.; Zhang, Y.; Ji, W.; Kolwijck, E.; Jansen, J. A.; Leeuwenburgh, S. C. G.; Yang, F. Electrospun Nanofibrous Silk Fibroin Membranes

Containing Gelatin Nanospheres for Controlled Delivery of Biomolecules. *Adv. Healthc. Mater.* **2017**, *6* (14), 1700014. https://doi.org/10.1002/adhm.201700014.

(39) Ahire, J. J.; Hattingh, M.; Neveling, D. P.; Dicks, L. M. T. Copper-Containing Anti-Biofilm Nanofiber Scaffolds as a Wound Dressing Material. *PLoS One* **2016**, *11* (3), e0152755. https://doi.org/10.1371/journal.pone.0152755.

(40) Yang, F.; Both, S. K.; Yang, X.; Walboomers, X. F.; Jansen, J. A. Development of an Electrospun Nano-Apatite/PCL Composite Membrane for GTR/GBR Application. *Acta Biomater.* **2009**, *5* (9), 3295–3304. https://doi.org/10.1016/j.actbio.2009.05.023.

(41) Barboza, E. P.; Stutz, B.; Ferreira, V. F.; Carvalho, W. Guided Bone Regeneration Using Nonexpanded Polytetrafluoroethylene Membranes in Preparation for Dental Implant Placements-A Report of 420 Cases. *Implant Dent.* **2010**, *19* (1), 2–7. https://doi.org/10.1097/ID.0b013e3181cda72c.

(42) Naung, N. Y.; Shehata, E.; Van Sickels, J. E. Resorbable Versus Nonresorbable Membranes: When and Why? *Dent. Clin. North Am.* **2019**, *63* (3), 419–431. https://doi.org/10.1016/j.cden.2019.02.008.

(43) Agarwal, S.; Greiner, A. On the Way to Clean and Safe Electrospinning-Green Electrospinning: Emulsion and Suspension Electrospinning. *Polym. Adv. Technol.* **2011**, *22* (3), 372–378. https://doi.org/10.1002/pat.1883.

(44) Chouhan, D.; Mandal, B. B. Silk Biomaterials in Wound Healing and Skin Regeneration Therapeutics: From Bench to Bedside. *Acta Biomater.* **2020**, *103*, 24–51. https://doi.org/10.1016/j.actbio.2019.11.050.

(45) Khan, M. A.; Ansari, U.; Ali, M. N. Real-Time Wound Management through Integrated PH Sensors: A Review. *Sens. Rev.* **2015**, *35* (2), 183–189. https://doi.org/10.1108/SR-08-2014-689.

(46) Aprile, P.; Letourneur, D.; Simon-Yarza, T. Membranes for Guided Bone Regeneration: A Road from Bench to Bedside. *Adv. Healthc. Mater.* **2020**, *9* (19). https://doi.org/10.1002/adhm.202000707.

(47) Raz, P.; Brosh, T.; Ronen, G.; Tal, H. Tensile Properties of Three Selected Collagen Membranes. *Biomed Res. Int.* **2019**, *2019* (c), 1–8. https://doi.org/10.1155/2019/5163603.

(48) Ortolani, E.; Quadrini, F.; Bellisario, D.; Santo, L.; Polimeni, A.; Santarsiero, A.; George, O. Mechanical Qualification of Collagen Membranes Used in Dentistry. *Ann Ist Super Sanità* **2015**, *51* (3), 229–235. https://doi.org/10.4415/ANN_15_03_11.

(49) Muthukrishnan, G.; Masters, E. A.; Daiss, J. L.; Schwarz, E. M. Mechanisms of Immune Evasion and Bone Tissue Colonization That Make Staphylococcus Aureus the Primary Pathogen in Osteomyelitis. *Curr. Osteoporos. Rep.* **2019**, *17* (6), 395–404. https://doi.org/10.1007/s11914-019-00548-4.

(50) Josse, J.; Velard, F.; Gangloff, S. C. Staphylococcus Aureus vs. Osteoblast: Relationship and Consequences in Osteomyelitis. *Front. Cell. Infect. Microbiol.* **2015**, *5* (NOV), 1–17. https://doi.org/10.3389/fcimb.2015.00085.

(51) Jacobs, A.; Renaudin, G.; Forestier, C.; Nedelec, J. M.; Descamps, S. Biological Properties of Copper-Doped Biomaterials for Orthopedic Applications: A Review of Antibacterial, Angiogenic and Osteogenic Aspects. *Acta Biomater.* **2020**, *117*, 21–39. https://doi.org/10.1016/j.actbio.2020.09.044.

(52) Liang, T.; Wang, Y.; Zeng, L.; Liu, Y.; Qiao, L.; Zhang, S.; Zhao, R.; Li, G.; Zhang, R.; Xiang, J.; Xiong, F.; Shanaghi, A.; Pan, H.; Zhao, Y. Copper-Doped 3D Porous Coating Developed on Ti-6Al-4V Alloys and Its in Vitro Long-Term Antibacterial Ability. *Appl. Surf. Sci.* **2020**, *509* (October 2019), 144717. https://doi.org/10.1016/j.apsusc.2019.144717.

(53) Zhang, D.; Han, Q.; Yu, K.; Lu, X.; Liu, Y.; Lu, Z.; Wang, Q. Antibacterial Activities against Porphyromonas Gingivalis and Biological Characteristics of Copper-Bearing PEO Coatings on Magnesium. *J. Mater. Sci. Technol.* **2021**, *61*, 33–45. https://doi.org/10.1016/j.jmst.2020.05.025.

(54) Wen, Q.; Gu, F.; Sui, Z.; Su, Z.; Yu, T. The Process of Osteoblastic Infection by Staphylococcus Aureus. *Int. J. Med. Sci.* **2020**, *17* (10), 1327–1332. https://doi.org/10.7150/ijms.45960.

(55) Oryan, A.; Kamali, A.; Moshiri, A.; Baghaban Eslaminejad, M. Role of Mesenchymal Stem Cells in Bone Regenerative Medicine: What Is the Evidence? *Cells Tissues Organs* **2017**, *204* (2), 59–83. https://doi.org/10.1159/000469704.

(56) Iaquinta, M. R.; Mazzoni, E.; Bononi, I.; Rotondo, J. C.; Mazziotta, C.; Montesi, M.; Sprio, S.; Tampieri, A.; Tognon, M.; Martini, F. Adult Stem Cells for Bone Regeneration and Repair. *Front. Cell Dev. Biol.* **2019**, *7* (November), 1–15. https://doi.org/10.3389/fcell.2019.00268.

(57) Bok, J. S.; Byun, S. H.; Park, B. W.; Kang, Y. H.; Lee, S. L.; Rho, G. J.; Hwang, S. C.; Woo, D. K.; Lee, H. J.; Byun, J. H. The Role of Human Umbilical Vein Endothelial Cells in Osteogenic Differentiation of Dental Follicle-Derived Stem Cells in in Vitro Co-Cultures. *Int. J. Med. Sci.* **2018**, *15* (11), 1160–1170. https://doi.org/10.7150/ijms.27318.

(58) Hoppe, A.; Güldal, N. S.; Boccaccini, A. R. A Review of the Biological Response to Ionic Dissolution Products from Bioactive Glasses and Glass-Ceramics. *Biomaterials* **2011**, *32* (11), 2757–2774. https://doi.org/10.1016/j.biomaterials.2011.01.004.

(59) Carmeliet, P.; Jain, R. K. Molecular Mechanisms and Clinical Applications of Angiogenesis. *Nature* **2011**, *19* (7347), 298–307. https://doi.org/10.1038/nature10144.

(60) Hofstee, M. I.; Muthukrishnan, G.; Atkins, G. J.; Riool, M.; Thompson, K.; Morgenstern, M.; Stoddart, M. J.; Richards, R. G.; Zaat, S. A. J.; Moriarty, T. F. Current Concepts of Osteomyelitis: From Pathologic Mechanisms to Advanced Research Methods. *Am. J. Pathol.* **2020**, *190* (6), 1151–1163. https://doi.org/10.1016/j.ajpath.2020.02.007.

3 DISCUSSÃO

Biomateriais funcionais tem sido cada vez mais adotados como uma solução terapêutica inovadora, uma vez que estes materiais são versáteis e podem ser adaptados para aplicações específicas, como a distribuição farmacêutica direcionada, "*scaffolds*" para regeneração musculoesquelética, cardiovascular e nervosa, ou ainda podem ser empregados como substratos biodegradáveis para a atenuação das respostas do tecido hospedeiro (Castagnola et al., 2021). Segundo Konh (2019), um biomaterial ideal deve satisfazer alguns requisitos quando desenvolvidos: (i) biocompatibilidade e capacidade de reduzir respostas inflamatórias; (ii) capacidade de guiar a fixação e proliferação de células (condutividade); (iii) capacidade de incorporar fatores indutivos para direcionar e aumentar o crescimento de novos tecidos (indutividade); (iv) suportar o crescimento vascular para transporte de oxigênio e biomoléculas; (v) integridade mecânica para suportar cargas; (vi) taxa de degradação controlada, previsível e reproduzível; e (vii) processamento fácil e econômico. Neste trabalho, dois biomateriais voltados para a odontologia foram desenvolvidos na tentativa de suprir os critérios acima citados. Ambos foram funcionalizados com Cu com o intuito de melhorar as respostas biológicas dos implantes dentários e da ROG, bem como garantir uma atividade antimicrobiana importante para se evitar infecções relacionadas ao tratamento reabilitador.

O combate à infecção, inflamação e perda óssea requer uma solução multifuncional por meio do desenvolvimento de biomateriais quem não apenas combatem a inflamação, mas também catalisem a formação óssea (Kohn, 2019). A obtenção de um biomaterial que tenha requisitos biológicos opostos, como ser antimicrobiano *versus* promover a proliferação e diferenciação celular é um dos maiores desafios da atualidade. Neste trabalho, estas propriedades combinadas foram obtidas pelo uso do Cu, um oligoelemento requerido para a saúde do corpo humano que não só possui atividade antimicrobiana de amplo espectro, mas que também tem demonstrado propriedades de estimulação angiogênica e osteogênica favoráveis quando incorporado a um biomaterial (Jacobs et al., 2020; Jin et al., 2016; Vincent et al., 2016; Wang et al., 2021).

O Cu incorporado aos biomateriais e liberado para o ambiente foi responsável por reduzir a formação de biofilme de duas espécies bacterianas, *Streptococcus sanguinis* e *Staphylococcus aureus*, no revestimento para implante dentário e na membrana para ROG, respectivamente. No primeiro caso, o efeito antimicrobiano é importante para prevenir o desenvolvimento de possíveis doenças peri-implantares nos estágios iniciais da

osseointegração em decorrência da formação de biofilme, o que pode ameaçar a durabilidade a longo prazo dos implantes devido uma inflamação grave que está frequentemente associada à perda óssea e, eventualmente, falhas terapêuticas (Huang et al., 2020). Já na ROG, a redução da carga bacteriana é crucial para a diminuição do risco de infecções ósseas, como a osteomielite, que podem impedir o processo regenerativo sob a membrana (Wen et al., 2020).

Um fator crítico no desenvolvimento dos biomateriais antimicrobianos contendo Cu é o seu potencial citotóxico. Em ambos os estudos, foi possível observar que a resposta celular e antimicrobiana é dependente da quantidade de Cu incorporado ao material. Enquanto concentrações mais altas de Cu aumentaram o efeito bactericida e diminuíram a atividade celular, concentrações mais baixas reduziram o efeito inibitório na formação de biofilme, mas foram mais propensas a suportar e promover a fixação e proliferação de células ósseas e endoteliais. De uma forma geral, o Cu gera uma toxicidade distinta em células diferentes, havendo também uma concentração mínima para exibir atividade antibacteriana (Li et al., 2019). Isto foi verificado principalmente com as membranas para ROG, em que foi avaliado o efeito dose-resposta do Cu.

No que diz respeito às reabilitações com implantes dentários, a sua integração ao osso a longo prazo é um objetivo fundamental na implantodontia. Desta forma, o uso de tratamentos de superfície para se obter maiores taxas de sucesso e sobrevivência tem sido uma abordagem frequentemente utilizada. Especificamente, superfícies com propriedades antimicrobianas, com a capacidade de matar as bactérias planctônicas e inibir diretamente a adesão e agregação bacteriana, são idealizadas para superar os problemas relacionados ao biofilme, que podem prejudicar o processo de osseointegração, (Huang et al., 2020). Idealmente, além da capacidade antibacteriana, os revestimentos devem apresentar boa biocompatibilidade. Neste estudo, a avaliação e definição de uma fonte adequada de Cu para a biofuncionalização do Ti mostrou ser crucial para se obter as melhores respostas biológicas: maior atividade antibacteriana e estimulação da proliferação celular.

Com relação às membranas utilizadas na ROG, os biomateriais desenvolvidos com este intuito além de serem biocompatíveis, devem cumprir alguns requisitos específicos: apresentar fácil manuseio e flexibilidade adequada para se adaptar e cobrir de forma ideal um defeito do tecido ósseo, serem resistentes para a manutenção de espaço durante a cicatrização, além de oferecerem função oclusiva e fácil bioativação (Aprile et al., 2020; He et al., 2017). De uma forma geral, as membranas criadas por meio da associação de uma solução de fibroína de seda com o óxido de polietileno tem preenchido estas características ideias para aplicação na ROG (Serôdio et al., 2019; Zheng et al., 2019). Mesmo assim, este estudo propôs

o aprimoramento destas membranas pela incorporação direta do Cu como um composto ativo afim de melhorar os resultados clínicos. De uma forma geral, a membrana funcionalizada com Cu manteve as propriedades mecânicas necessárias para sua aplicação clínica, mas também mostrou funções antimicrobianas e angiogênicas decisivas para os processos regenerativos.

O impacto deste trabalho é maior do que o desenvolvimento e aplicação específica de biomateriais odontológicos antimicrobianos que podem proporcionar o sucesso do tratamento a longo prazo e qualidade de vida ao paciente. Os resultados apresentados podem ainda ser aproveitados para difundir o Cu como um funcionalizador eficiente, bem como as técnicas por PEO e eletrofiação como alternativas no desenvolvimento de novas estratégias de tratamento com implantes dentários em defeitos ósseos. Estudos *in vitro,* como os apresentados aqui, são indispensáveis para compreender as propriedades dos materiais experimentais e verificar se estes alcançaram os requisitos mínimos para a sua aplicação. Estudos *in vivo* em animais e ensaios clínicos randomizado continuam sendo mandatórios para avaliar o potencial e eficcácia do tratamento de superfície para implantes dentários e da membrana para ROG. Além disso, estas pesquisas são decisivas para a validação da segurança para uso na prática clínica.

4 CONCLUSÃO

Os resultados deste trabalho são promissores no que diz respeito ao emprego do Cu como um agente de funcionalização para dois biomateriais diferentes, mas com objetivos similares: melhorar a integração do implante, a formação de novo osso e a prevenção de infecções.

Os revestimentos depositados em Ti contendo Cu para aplicação como implantes dentários foram desenvolvidos por PEO empregando diferentes fontes de Cu, que foram capazes de afetar a morfologia e composição dos revestimentos, também influenciando seu efeito em células humanas e bactérias. A formação de biofilme nos revestimentos experimentais dependeu da concentração de Cu e da rugosidade superficial gerada pelas diferentes fontes utilizadas para funcionalizar o Ti. Uma topografia otimizada do revestimento produzida com acetado de Cu levou à inibição na formação de biofilme e aumento da resposta celular.

As membranas para ROG contendo Cu em diferentes concentrações foram sintetizadas com sucesso pela técnica de eletrofiação. A concentração de Cu foi crucial para as respostas biológicas, em que altas concentrações demonstraram melhor atividade antimicrobiana, mas baixa citocompatibilidade. As membranas com baixa concentração de Cu apresentaram boas propriedades mecânicas, suportando e estimulando a adesão e proliferação de células humanas, bem como a angiogênese.

Ambas as estratégias apresentadas neste trabalho podem ser alternativas valiosas para diminuir o risco de infecções e melhorar o processo de osseointegração e regeneração tecidual, consequentemente, reduzindo o tempo do tratamento reabilitador com implantes dentários.

REFERÊNCIAS*

Ahire JJ, Hattingh M, Neveling DP, Dicks LMT. Copper-containing anti-biofilm nanofiber scaffolds as a wound dressing material. PLoS One 2016;11:e0152755. https://doi.org/10.1371/journal.pone.0152755.

Amna T, Hassan MS, Yang J, Khil M-SS, Song K-DD, Oh J-DD, et al. Virgin olive oil blended polyurethane micro/nanofibers ornamented with copper oxide nanocrystals for biomedical applications. Int J Nanomedicine 2014;9:891–8. https://doi.org/10.2147/IJN.S54113.

Aprile P, Letourneur D, Simon-Yarza T. Membranes for Guided Bone Regeneration: A Road from Bench to Bedside. Adv Healthc Mater 2020;9. https://doi.org/10.1002/adhm.202000707.

Bari A, Bloise N, Fiorilli S, Novajra G, Vallet-Regí M, Bruni G, et al. Copper-containing mesoporous bioactive glass nanoparticles as multifunctional agent for bone regeneration. Acta Biomater 2017;55:493–504. https://doi.org/10.1016/j.actbio.2017.04.012.

Beline T, Marques I da SV, Matos AO, Ogawa ES, Ricomini-Filho AP, Rangel EC, et al. Production of a biofunctional titanium surface using plasma electrolytic oxidation and glow-discharge plasma for biomedical applications. Biointerphases 2016;11:011013. https://doi.org/10.1116/1.4944061.

Bornstein MM, Halbritter S, Harnisch H, Weber H-P, Buser D. A retrospective analysis of patients referred for implant placement to a specialty clinic: indications, surgical procedures, and early failures. Int J Oral Maxillofac Implants 2008;23:1109–16. https://doi.org/10.7892/boris.27149.

Castagnola V, Castagnola E, Bergaud C, Ricci D. Editorial: Short-Term Versus Long-Term Challenges in Functional Biomaterials Interfacing Living Systems: Two Sides of the Coin. Front Bioeng Biotechnol 2021;9:1–4. https://doi.org/10.3389/fbioe.2021.723451.

Castro AGB, Diba M, Kersten M, Jansen JA, van den Beucken JJJP, Yang F. Development of a PCL-silica nanoparticles composite membrane for Guided Bone Regeneration. Mater Sci Eng C 2018;85:154–61. https://doi.org/10.1016/j.msec.2017.12.023.

Clementini M, Morlupi A, Canullo L, Agrestini C, Barlattani A. Success rate of dental

* De acordo com as normas da UNICAMP/FOP, baseadas na padronização do International Committee of Medical Journal Editors - Vancouver Group. Abreviatura dos periódicos em conformidade com o PubMed.

implants inserted in horizontal and vertical guided bone regenerated areas: A systematic review. Int J Oral Maxillofac Surg 2012;41:847–52. https://doi.org/10.1016/j.ijom.2012.03.016.

Clyne TW, Troughton SC. A review of recent work on discharge characteristics during plasma electrolytic oxidation of various metals. Int Mater Rev 2019;64:127–62. https://doi.org/10.1080/09506608.2018.1466492.

Costa RC, Nagay BE, Bertolini M, Costa-Oliveira BE, Sampaio AA, Retamal-Valdes B, et al. Fitting pieces into the puzzle: The impact of titanium-based dental implant surface modifications on bacterial accumulation and polymicrobial infections. Adv Colloid Interface Sci 2021;298:102551. https://doi.org/10.1016/j.cis.2021.102551.

D'Mello S, Elangovan S, Hong L, Ross RD, Sumner DR, Salem AK. Incorporation of copper into chitosan scaffolds promotes bone regeneration in rat calvarial defects. J Biomed Mater Res Part B Appl Biomater 2015;103:1044–9. https://doi.org/10.1002/jbm.b.33290.

Elangovan S, Avila-Ortiz G, Johnson GK, Karimbux N, Allareddy V. Quality Assessment of Systematic Reviews on Periodontal Regeneration in Humans. J Periodontol 2013;84:176–85. https://doi.org/10.1902/jop.2012.120021.

Elnayef B, Monje A, Albiol G, Galindo-Moreno P, Wang H-L, Hernández-Alfaro F. Vertical Ridge Augmentation in the Atrophic Mandible: A Systematic Review and Meta-Analysis. Int J Oral Maxillofac Implants 2017;32:291–312. https://doi.org/10.11607/jomi.4861.

Gérard C, Bordeleau L-J, Barralet J, Doillon CJ. The stimulation of angiogenesis and collagen deposition by copper. Biomaterials 2010;31:824–31. https://doi.org/10.1016/j.biomaterials.2009.10.009.

Gönen SÖ, Erol Taygun M, Küçükbayrak S. Fabrication of bioactive glass containing nanocomposite fiber mats for bone tissue engineering applications. Compos Struct 2016;138:96–106. https://doi.org/10.1016/j.compstruct.2015.11.033.

Gutiérrez MF, Alegría-Acevedo LF, Méndez-Bauer L, Bermudez J, Dávila-Sánchez A, Buvinic S, et al. Biological, mechanical and adhesive properties of universal adhesives containing zinc and copper nanoparticles. J Dent 2019;82:45–55. https://doi.org/10.1016/j.jdent.2019.01.012.

He M, Jiang H, Wang R, Xie Y, Zhao C. Fabrication of metronidazole loaded poly (ε-caprolactone)/zein core/shell nanofiber membranes via coaxial electrospinning for guided tissue regeneration. J Colloid Interface Sci 2017;490:270–8. https://doi.org/10.1016/j.jcis.2016.11.062.

He M, Xue J, Geng H, Gu H, Chen D, Shi R, et al. Fibrous guided tissue regeneration membrane loaded with anti-inflammatory agent prepared by coaxial electrospinning for the purpose of controlled release. Appl Surf Sci 2015;335:121–9. https://doi.org/10.1016/j.apsusc.2015.02.037.

Hoppe A, Güldal NS, Boccaccini AR. A review of the biological response to ionic dissolution products from bioactive glasses and glass-ceramics. Biomaterials 2011;32:2757–74. https://doi.org/10.1016/j.biomaterials.2011.01.004.

Howe MS, Keys W, Richards D. Long-term (10-year) dental implant survival: A systematic review and sensitivity meta-analysis. J Dent 2019;84:9–21. https://doi.org/10.1016/j.jdent.2019.03.008.

Hu C, Ashok D, Nisbet DR, Gautam V. Bioinspired surface modification of orthopedic implants for bone tissue engineering. Biomaterials 2019;219:119366. https://doi.org/10.1016/j.biomaterials.2019.119366.

Huang DN, Wang J, Ren KF, Ji J. Functionalized biomaterials to combat biofilms. Biomater Sci 2020;8:4126–40. https://doi.org/10.1039/d0bm00526f.

Huang Q, Li X, Elkhooly TA, Liu X, Zhang R, Wu H, et al. The Cu-containing TiO2 coatings with modulatory effects on macrophage polarization and bactericidal capacity prepared by micro-arc oxidation on titanium substrates. Colloids Surfaces B Biointerfaces 2018;170:242–50. https://doi.org/10.1016/j.colsurfb.2018.06.020.

Jacobs A, Renaudin G, Forestier C, Nedelec JM, Descamps S. Biological properties of copper-doped biomaterials for orthopedic applications: A review of antibacterial, angiogenic and osteogenic aspects. Acta Biomater 2020;117:21–39. https://doi.org/10.1016/j.actbio.2020.09.044.

Jin S, Li J, Wang J, Jiang J, Zuo Y, Li Y, et al. Electrospun silver ion-loaded calcium phosphate/ chitosan antibacterial composite fibrous membranes for guided bone regeneration.

Int J Nanomedicine 2018;13:4591–605. https://doi.org/10.2147/IJN.S167793.

Jin S, Ren L, Yang K. Bio-Functional Cu Containing Biomaterials: a New Way to Enhance Bio-Adaption of Biomaterials. J Mater Sci Technol 2016;32:835–9. https://doi.org/10.1016/j.jmst.2016.06.022.

Kharaghani D, Khan MQ, Tamada Y, Ogasawara H, Inoue Y, Saito Y, et al. Fabrication of electrospun antibacterial PVA/Cs nanofibers loaded with CuNPs and AgNPs by an in-situ method. Polym Test 2018;72:315–21. https://doi.org/10.1016/j.polymertesting.2018.10.029.

Kohn DH. Multi-functional Biomaterials with Clinical Utility. Matter 2019;1:1114–5. https://doi.org/10.1016/j.matt.2019.09.010.

Kullar AS, Miller CS. Are There Contraindications for Placing Dental Implants? Dent Clin North Am 2019;63:345–62. https://doi.org/10.1016/j.cden.2019.02.004.

Kumar S, Nehra M, Kedia D, Dilbaghi N, Tankeshwar K, Kim KH. Nanotechnology-based biomaterials for orthopaedic applications: Recent advances and future prospects. Mater Sci Eng C 2020;106:110154. https://doi.org/10.1016/j.msec.2019.110154.

Kunrath MF, Muradás TC, Penha N, Campos MM. Innovative surfaces and alloys for dental implants: What about biointerface-safety concerns? Dent Mater 2021;37:1447–62. https://doi.org/10.1016/j.dental.2021.08.008.

Li J, Zhai D, Lv F, Yu Q, Ma H, Yin J, et al. Preparation of copper-containing bioactive glass/eggshell membrane nanocomposites for improving angiogenesis, antibacterial activity and wound healing. Acta Biomater 2016;36:254–66. https://doi.org/http://dx.doi.org/10.1016/j.actbio.2016.03.011.

Li K, Xia C, Qiao Y, Liu X. Dose-response relationships between copper and its biocompatibility/antibacterial activities. J Trace Elem Med Biol 2019;55:127–35. https://doi.org/10.1016/j.jtemb.2019.06.015.

Lian M, Sun B, Qiao Z, Zhao K, Zhou X, Zhang Q, et al. Bi-layered electrospun nanofibrous membrane with osteogenic and antibacterial properties for guided bone regeneration. Colloids Surfaces B Biointerfaces 2019;176:219–29. https://doi.org/10.1016/j.colsurfb.2018.12.071.

Lim G, Lin G-H, Monje A, Chan H-L, Wang H-L. Wound Healing Complications Following

Guided Bone Regeneration for Ridge Augmentation: A Systematic Review and Meta-Analysis. Int J Oral Maxillofac Implants 2018;33:51–50. https://doi.org/10.11607/jomi.5581.

Lim TC, Kotaki M, Yong TKJ, Yang F, Fujihara K, Ramakrishna S. Recent advances in tissue engineering applications of electrospun nanofibers. Mater Technol 2004;19:20–7. https://doi.org/10.1080/10667857.2004.11753060.

Liu W, Cheng M, Wahafu T, Zhao Y, Qin H, Wang J, et al. The in vitro and in vivo performance of a strontium-containing coating on the low-modulus Ti35Nb2Ta3Zr alloy formed by micro-arc oxidation. J Mater Sci Mater Med 2015;26:203. https://doi.org/10.1007/s10856-015-5533-0.

Lu X, Mohedano M, Blawert C, Matykina E, Arrabal R, Kainer KU, et al. Plasma electrolytic oxidation coatings with particle additions – A review. Surf Coatings Technol 2016;307:1165–82. https://doi.org/10.1016/j.surfcoat.2016.08.055.

Luo J, Guo S, Lu Y, Xu X, Zhao C, Wu S, et al. Cytocompatibility of Cu-bearing Ti6Al4V alloys manufactured by selective laser melting. Mater Charact 2018;143:127–36. https://doi.org/10.1016/j.matchar.2017.12.003.

Marques I da SV, Barão VAR, Cruz NC da, Yuan JC-C, Mesquita MF, Ricomini-Filho AP, et al. Electrochemical behavior of bioactive coatings on cp-Ti surface for dental application. Corros Sci 2015;100:133–46. https://doi.org/10.1016/j.corsci.2015.07.019.

Nagay BE, Dini C, Cordeiro JM, Ricomini-Filho AP, de Avila ED, Rangel EC, et al. Visible-Light-Induced Photocatalytic and Antibacterial Activity of TiO 2 Codoped with Nitrogen and Bismuth: New Perspectives to Control Implant-Biofilm-Related Diseases. ACS Appl Mater Interfaces 2019;11:18186–202. https://doi.org/10.1021/acsami.9b03311.

O'Neill E, Awale G, Daneshmandi L, Umerah O, Lo KWH. The roles of ions on bone regeneration. Drug Discov Today 2018;23:879–90. https://doi.org/10.1016/j.drudis.2018.01.049.

Ojha NK, Zyryanov G V., Majee A, Charushin VN, Chupakhin ON, Santra S. Copper nanoparticles as inexpensive and efficient catalyst: A valuable contribution in organic synthesis. Coord Chem Rev 2017;353:1–57. https://doi.org/10.1016/j.ccr.2017.10.004.

Patil J V., Mali SS, Kamble AS, Hong CK, Kim JH, Patil PS. Electrospinning: A versatile technique for making of 1D growth of nanostructured nanofibers and its applications: An experimental approach. Appl Surf Sci 2017;423:641–74. https://doi.org/10.1016/j.apsusc.2017.06.116.

Polo TOB, da Silva WP, Momesso GAC, Lima-Neto TJ, Barbosa S, Cordeiro JM, et al. Plasma Electrolytic Oxidation as a Feasible Surface Treatment for Biomedical Applications: an in vivo study. Sci Rep 2020;10:10000. https://doi.org/10.1038/s41598-020-65289-2.

Prinz C, Elhensheri M, Rychly J, Neumann HG. Antimicrobial and bone-forming activity of a copper coated implant in a rabbit model. J Biomater Appl 2017;32:139–49. https://doi.org/10.1177/0885328217713356.

Sedelnikova MB, Komarova EG, Sharkeev YP, Ugodchikova A V., Mushtovatova LS, Karpova MR, et al. Zn-, Cu- or Ag-incorporated micro-arc coatings on titanium alloys: Properties and behavior in synthetic biological media. Surf Coatings Technol 2019;369:52–68. https://doi.org/10.1016/j.surfcoat.2019.04.021.

Serôdio R, Schickert SL, Costa-Pinto AR, Dias JR, Granja PL, Yang F, et al. Ultrasound sonication prior to electrospinning tailors silk fibroin/PEO membranes for periodontal regeneration. Mater Sci Eng C 2019;98:969–81. https://doi.org/10.1016/j.msec.2019.01.055.

Shao J, Yu N, Kolwijck E, Wang B, Tan KW, Jansen JA, et al. Biological evaluation of silver nanoparticles incorporated into chitosan-based membranes. Nanomedicine 2017;12:2771–85. https://doi.org/10.2217/nnm-2017-0172.

Spriano S, Yamaguchi S, Baino F, Ferraris S. A critical review of multifunctional titanium surfaces: New frontiers for improving osseointegration and host response, avoiding bacteria contamination. Acta Biomater 2018;79:1–22. https://doi.org/10.1016/j.actbio.2018.08.013.

Van Steenberghe D, Jacobs R, Desnyder M, Maffei G, Quirynen M. The relative impact of local and endogenous patient-related factors on implant failure up to the abutment stage. Clin Oral Implants Res 2002;13:617–22. https://doi.org/10.1034/j.1600-0501.2002.130607.x.

Tamayo L, Azócar M, Kogan M, Riveros A, Páez M. Copper-polymer nanocomposites: An excellent and cost-effective biocide for use on antibacterial surfaces. Mater Sci Eng C 2016;69:1391–409. https://doi.org/10.1016/j.msec.2016.08.041.

Vincent M, Hartemann P, Engels-Deutsch M. Antimicrobial applications of copper. Int J Hyg Environ Health 2016;219:585–91. https://doi.org/10.1016/j.ijheh.2016.06.003.

Wang H, Zhao S, Zhou J, Shen Y, Huang W, Zhang C, et al. Evaluation of borate bioactive glass scaffolds as a controlled delivery system for copper ions in stimulating osteogenesis and angiogenesis in bone healing. J Mater Chem B 2014;2:8547–57. https://doi.org/10.1039/c4tb01355g.

Wang P, Yuan Y, Xu K, Zhong H, Yang Y, Jin S, et al. Biological applications of copper-containing materials. Bioact Mater 2021;6:916–27. https://doi.org/10.1016/j.bioactmat.2020.09.017.

Wang X, Dong H, Liu J, Qin G, Chen D, Zhang E. In vivo antibacterial property of Ti-Cu sintered alloy implant. Mater Sci Eng C 2019;100:38–47. https://doi.org/10.1016/j.msec.2019.02.084.

Wen Q, Gu F, Sui Z, Su Z, Yu T. The process of osteoblastic infection by staphylococcus aureus. Int J Med Sci 2020;17:1327–32. https://doi.org/10.7150/ijms.45960.

Weng L, Boda SK, Teusink MJ, Shuler FD, Li X, Xie J. Binary Doping of Strontium and Copper Enhancing Osteogenesis and Angiogenesis of Bioactive Glass Nanofibers while Suppressing Osteoclast Activity. ACS Appl Mater Interfaces 2017;9:24484–96. https://doi.org/10.1021/acsami.7b06521.

Wojcieszak D, Mazur M, Kalisz M, Grobelny M. Influence of Cu, Au and Ag on structural and surface properties of bioactive coatings based on titanium. Mater Sci Eng C 2017;71:1115–21. https://doi.org/10.1016/j.msec.2016.11.091.

Wu C, Zhou Y, Xu M, Han P, Chen L, Chang J, et al. Copper-containing mesoporous bioactive glass scaffolds with multifunctional properties of angiogenesis capacity, osteostimulation and antibacterial activity. Biomaterials 2013;34:422–33. https://doi.org/10.1016/j.biomaterials.2012.09.066.

Xu X, Lu Y, Li S, Guo S, He M, Luo K, et al. Copper-modified Ti6Al4V alloy fabricated by selective laser melting with pro-angiogenic and anti-inflammatory properties for potential guided bone regeneration applications. Mater Sci Eng C 2018a;90:198–210. https://doi.org/10.1016/j.msec.2018.04.046.

Xu X, Lu Y, Yang X, Du Z, Zhou L, Li S, et al. Copper-Modified Ti6Al4 V Suppresses Inflammatory Response and Osteoclastogenesis while Enhancing Extracellular Matrix Formation for Osteoporotic Bone Regeneration. ACS Biomater Sci Eng 2018b;4:3364–73. https://doi.org/10.1021/acsbiomaterials.8b00736.

Yao X, Zhang X, Wu H, Tian L, Ma Y, Tang B. Microstructure and antibacterial properties of Cu-doped TiO 2 coating on titanium by micro-arc oxidation. Appl Surf Sci 2014;292:944–7. https://doi.org/10.1016/j.apsusc.2013.12.083.

Zhang J, Wu H, He F, Wu T, Zhou L, Ye J. Concentration-dependent osteogenic and angiogenic biological performances of calcium phosphate cement modified with copper ions. Mater Sci Eng C 2019;99:1199–212. https://doi.org/10.1016/j.msec.2019.02.042.

Zhang X, Li J, Wang X, Wang Y, Hang R, Huang X, et al. Effects of copper nanoparticles in porous TiO2 coatings on bacterial resistance and cytocompatibility of osteoblasts and endothelial cells. Mater Sci Eng C 2018;82:110–20. https://doi.org/10.1016/j.msec.2017.08.061.

Zheng Z, Zhang K, Wu B, Yang H, Wang M, Dong T, et al. Green electrospun nanocuprous oxide–poly(ethylene oxide)–silk fibroin composite nanofibrous scaffolds for antibacterial dressings. J Appl Polym Sci 2019;136:47730. https://doi.org/10.1002/app.47730.

Zhou Z, Li X, Li Q, Zhao Y, Pang H. Copper-based materials as highly active electrocatalysts for the oxygen evolution reaction. Mater Today Chem 2019;11:169–96. https://doi.org/10.1016/j.mtchem.2018.10.008.

Zou Y, Zhang L, Yang L, Zhu F, Ding M, Lin F, et al. “Click” chemistry in polymeric scaffolds: Bioactive materials for tissue engineering. J Control Release 2018;273:160–79. https://doi.org/10.1016/j.jconrel.2018.01.023.

ANEXOS

Anexo 1 – Comprovante de publicação do artigo 1

ARTICLE IN PRESS

Materials Science & Engineering C xxx (xxxx) xxx

Contents lists available at ScienceDirect

Materials Science & Engineering C

journal homepage: www.elsevier.com/locate/msec

Copper source determines chemistry and topography of implant coatings to optimally couple cellular responses and antibacterial activity

Jairo M. Cordeiro [a,e,*], Bruna E. Nagay [a], Caroline Dini [a], João G.S. Souza [b,c], Elidiane C. Rangel [d], Nilson C. da Cruz [d], Fang Yang [e], Jeroen J.J.P. van den Beucken [e,**,1], Valentim A.R. Barão [a,**,1]

[a] Department of Prosthodontics and Periodontology, Piracicaba Dental School, University of Campinas (UNICAMP), Piracicaba, São Paulo 13414-903, Brazil
[b] Faculdade de Ciências Odontológicas (FCO), Montes Claros, Minas Gerais 39401-303, Brazil
[c] Dental Research Division, Guarulhos University, Guarulhos, São Paulo 07023-070, Brazil
[d] Laboratory of Technological Plasmas, Institute of Science and Technology, São Paulo State University (UNESP), Sorocaba, São Paulo 18087-180, Brazil
[e] Regenerative Biomaterials, Dentistry, Radboudumc, 6500 HB Nijmegen, the Netherlands

ARTICLE INFO

Keywords:
Titanium
Microarc oxidation
Dental implant
Biomimetic material
Osseointegration
Biofilm

ABSTRACT

Implant-related infections at the early healing period are considered one of the main risk factors in implant failure. Designing coatings that control bacterial adhesion and have cell stimulatory behavior remains a challenging strategy for dental implants. Here, we used plasma electrolytic oxidation (PEO) to produce antimicrobial coatings on commercially pure titanium (cpTi) using bioactive elements (calcium and phosphorus) and different copper (Cu) sources: copper acetate (CuAc), copper sulfate (CuS), and copper oxide (CuO); coatings containing only Ca and P (CaP) served as controls. Cu sources drove differential physical and chemical surface features of PEO coatings, resulting in tailorable release kinetics with a sustained Cu ion release over 10 weeks. The antibacterial effects of Cu-containing coatings were roughness-dependent. CuAc coating exhibited optimal properties in terms of its hydrophilicity, pores density, and limited surface roughness, which provided the most robust antibacterial activity combined with appropriate responses of human primary stem cells and angiogenic cells. Our data indicate that Cu source selection largely determines the functionality of Cu-containing PEO coatings regarding their antibacterial efficacy and cytocompatibility.

1. Introduction

Designing implants with specific biology-related physical and chemical surface properties has attracted attention for the application in the biomedical field. Coating technologies have been applied in dental implantology to create bioactive surfaces similar to the bone in terms of topography and composition, which can improve cellular responses or the growth of new natural bone on and around the implant surface, increasing implant stability and osseointegration [1–3]. In fact, surface modifications for dental implants enable steering desired biological responses by activating specific molecular pathways and cells involved in bone healing and remodeling. For example, several biomaterials have aimed at stimulating angiogenesis due to their key roles in repairing tissues, supporting the delivery of nutrients and signaling factors, and removing bioproducts, thus promoting neotissue formation [4].

Even with the ongoing advances in the biomedical field, titanium (Ti) implants still undergo some undesirable biological responses and treatment failure, such as implant-related infections, which also impair the osseointegration due to the challenging physiological environment established by the biofilm accumulation and inflammatory process [5]. Commercially available implants have shown improved osseointegration and success rates by tuning their surface chemistry and topography [1,6]. On the other hand, no Ti dental implants currently exist in the market with proven reliable antimicrobial properties for clinical use [7].

* Correspondence to: J. M. Cordeiro, Department of Prosthodontics and Periodontology, Piracicaba Dental School, University of Campinas (UNICAMP), Piracicaba, São Paulo 13414-903, Brazil.
** Corresponding authors.
E-mail addresses: jairocordeirom@hotmail.com (J.M. Cordeiro), jeroen.vandenbeucken@radboudumc.nl (J.J.J.P. van den Beucken), vbarao@unicamp.br (V.A.R. Barão).
[1] Valentim A. R. Barão and Jeroen J. J. P. van den Beucken should be considered a joint senior author.

https://doi.org/10.1016/j.msec.2021.112550
Received 23 August 2021; Received in revised form 16 October 2021; Accepted 10 November 2021
Available online 15 November 2021
0928-4931/

Anexo 2 – Certificação do Comitê de Ética

UNICAMP - FACULDADE DE ODONTOLOGIA DE PIRACICABA DA

PARECER CONSUBSTANCIADO DO CEP

DADOS DO PROJETO DE PESQUISA

Título da Pesquisa: Desenvolvimento de uma superfície bioativa e antibacteriana contendo Cu2O para implantes dentários

Pesquisador: JAIRO MATOZINHO CORDEIRO

Área Temática:

Versão: 2

CAAE: 79224917.0.0000.5418

Instituição Proponente: Faculdade de Odontologia de Piracicaba - Unicamp

Patrocinador Principal: Financiamento Próprio

DADOS DO PARECER

Número do Parecer: 2.387.521

Apresentação do Projeto:

Trata-se de estudo laboratorial, longitudinal, com tratamento, que utilizará como insumo em uma das etapas saliva total humana, obtida de dois voluntários, alunos de pós-graduação da FOP, com idades entre 18 e 30 anos e sem distinção de sexo. Serão incluídos estudantes que apresentam boa saúde geral e bucal, com o consentimento da doação de saliva para o estudo, de acordo com as normas de coleta. Serão excluídos indivíduos que apresentem saúde geral e/ou bucal comprometida, ou façam o uso de medicamentos como antibióticos, antifúngicos ou que reduzem o fluxo salivar são excluídos. Discos de Ticp (15 mm de diâmetro e 2 mm de espessura) serão submetidos a diferentes modificações de superfície: usinado (superfície I - controle); modificada por PEO com solução de cálcio e fosfato (superfície II); modificada por PEO com solução de cálcio, fosfato e nanopartículas de Cu2O (superfície III). As superfícies das amostras serão caracterizadas quanto a rugosidade de superfície (Ra, Rq, Rt, Rz), microscopia de força atômica, microscopia eletrônica de varredura (MEV), espectroscopia de energia dispersiva, espectroscopia de fotoelétrons excitados por raios X, difratometria de raios-X, molhabilidade e energia livre de superfície. Ensaio eletroquímico com testes padrões (potencial de circuito aberto, espectroscopia de impedância eletroquímica e teste potenciodinâmico) serão conduzidos em solução de fluido corpóreo (pH 7,4) com a finalidade de se compreender a cinética de corrosão e investigar as propriedades do filme de óxido formado na superfície dos discos. Para os testes biológicos, será utilizada a linhagem celular pré-osteoblásticas MC3T3E1. A estrutura e morfologia celular serão

Endereço: Av.Limeira 901 Caixa Postal 52
Bairro: Areião **CEP:** 13.414-903
UF: SP **Município:** PIRACICABA
Telefone: (19)2106-5349 **Fax:** (19)2106-5349 **E-mail:** cep@fop.unicamp.br

avaliadas por MEV. A reação quantitativa de cadeia de transcriptase polimerase reversa (qRT-PCR) será utilizada para determinar os níveis de expressão de genes osteogênicos. O ensaio de MTT será realizado para avaliar a viabilidade celular. Para o teste microbiológico, biofilme composto por Streptococcus sanguinis será formado na superfície dos discos. Serão quantificadas as unidades formadoras de colônia (log UFC) e a análise estrutural do biofilme será realizada através da MEV. A influência do tratamento de superfície sobre a adsorção de proteínas do soro sanguíneo (albumina, fibrinogênio e fibronectina) será determinada. Os dados quantitativos serão submetidos à análise estatística mais apropriada com nível de significância de 5%. O número de espécimes para cada ensaio será determinado após o estudo piloto. Quanto aos locais de realização do estudo, foi descrito o seguinte: a modificação com PEO, assim como a caracterização de superfície (MFA, MEV, EDS, XPS, XRD, rugosidade, molhabilidade e energia de superfície) serão realizadas no Laboratório de Plasmas Tecnológicos, UNESP (Campus Sorocaba); os testes biológicos serão realizados nos laboratórios da área de Periodontia da FOP-UNICAMP; o ensaio microbiológico nos Laboratórios da área de Bioquímica da FOP-UNICAMP e a preparação dos discos de Ti, ensaio eletroquímico e demais etapas na área de Prótese Total da FOP-UNICAMP. O cronograma da pesquisa, presente no projeto de pesquisa informa que a pesquisa será realizada em 36 meses (os valores anotados no quadro não permitem conclusão). Já o cronograma disposto na PB indica que a pesquisa será iniciada em 11/10/2017 (etapas preliminares), em 11/06/2018 (estudo piloto) e concluída em 11/11/2020. A capa do projeto, a declaração dos pesquisadores e a PB indicam como pesquisadores Jairo Matozinho Cordeiro (Cirurgião Dentista, doutorando pelo PPG em Clínica Odontológica da FOP, Pesquisador responsável) e Valentim Adelino Ricardo Barão (Cirurgião Dentista, área de Prótese Total da FOP, Orientador).

Objetivo da Pesquisa:

O presente projeto tem como objetivo geral o desenvolvimento e avaliação de superfícies antibacterianas e bioativas contendo Cu2O em discos de Ticp por meio da oxidação por plasma eletrolítico. Os objetivos específicos desse estudo são: (1) Caracterizar a superfície dos discos de Ticp quanto à sua topografia, rugosidade, energia de superfície e composição química e cristalinas; (2) Compreender a cinética de corrosão e investigar as propriedades do filme de óxido formado na superfície dos discos de Ticp através da espectroscopia de impedância eletroquímica (EIE) e das curvas de polarização potenciodinâmica; (3) Avaliar a biocompatibilidade das superfícies através da análise da morfologia celular, ensaio de viabilidade celular e expressão gênica; (4) Entender como o tratamento de superfície influencia a adsorção de proteínas do soro sanguíneo (albumina, fibrinogênio e fibronectina); (5) Avaliar os efeitos da adição de Cu2O no tratamento por

PEO na formação de biofilme de S. sanguinis quanto às unidades formadoras de colônias (UFC). A hipótese do presente estudo é que o tratamento de superfície contendo Cu2O apresentará ação antibacteriana superior à superfície usinada e sem Cu2O. Além disso, é hipotetizado que os tratamentos de superfície alterarão as características de superfície de forma a influenciar as propriedades eletroquímicas e biológicas, elevando a resistência à corrosão, aumentando a absorção de proteínas, a adesão e proliferação celular.

Avaliação dos Riscos e Benefícios:

Os pesquisadores informaram que "os voluntários que aceitarem participar do estudo precisarão coletar saliva, o desconforto previsto para este procedimento é apresentar jejum de 1 hora e meia. Para evitar constrangimento durante as coletas, estas serão realizadas em uma sala fechada, para que o voluntário sinta-se confortável, e em casos de ânsia, o voluntário pode parar a coleta a qualquer momento". Informaram também que "não há benefícios diretos aos sujeitos da pesquisa. O benefício científico esperado será desenvolver um tratamento de superfície para implantes que apresente ação antibacteriana e seja bioativo, podendo ser utilizados no futuro para reabilitações orais".

Comentários e Considerações sobre a Pesquisa:

Quanto ao modo de obtenção do TCLE, os pesquisadores informaram que "os indivíduos serão abordados, de forma sutil e educada, evitando qualquer constrangimento. Nesta abordagem será explicado todo o procedimento que será realizado, qualquer dúvida sobre os procedimentos será esclarecida, e o voluntário terá completa liberdade e direito para aceitar ou recusar sua participação no estudo. Além disso, será explicado ao voluntário que, caso preciso, ele pode cancelar sua participação sem nenhum prejuízo". Os participantes serão abordados pelo pesquisador Jairo Matozinho Cordeiro de forma sutil e educada na Faculdade de Odontologia de Piracicaba, sendo que os alunos envolvidos sob mesma orientação ou até mesmo em aula com docentes envolvidos não serão abordados, para evitar possíveis constrangimentos. Os pesquisadores não propuseram métodos de redução de risco/desconforto, pois os mesmos não estão previstos na pesquisa. Os pesquisadores garantiram o sigilo da identidade dos participantes. Os pesquisadores não propuseram ressarcimento na pesquisa pois não há previsão de gastos pelos participantes. Não há previsão de indenização na pesquisa pois não há risco previsível pela participação na pesquisa. Não foram propostos critérios de suspensão ou encerramento precoce da pesquisa. Pendência 1 (atendida)– Em resposta de 10/11/17 os pesquisadores justificaram a participação de grupo vulnerável na pesquisa (alunos da instituição que promove a pesquisa) afirmando que "A participação de alunos da instituição em que se realiza a pesquisa é justificada

pela comodidade dos alunos já estarem próximos ao local de coleta, não sendo necessário o deslocamento desses alunos, evitando gastos com transporte e também o desconforto da locomoção".

Considerações sobre os Termos de apresentação obrigatória:

A FR foi apresentada, preenchida e assinada pelo pesquisador responsável e pelo Diretor da FOP, Prof. Guilherme Elias P. Henriques, assinalados 2 participantes e não havendo patrocinador. A capa do arquivo projeto conta com os dados dos pesquisadores. Foi apresentada a declaração dos pesquisadores, a declaração da instituição, a autorização de acesso e uso dos laboratórios da área de Periodontia, a autorização de acesso e uso dos laboratórios da área de Bioquímica e a autorização de acesso e uso do Laboratório de Plasmas Tecnológicos – LaPTec da Universidade Estadual Paulista Júlio de Mesquita – Campus de Sorocaba. O orçamento presente na PB informa que a pesquisa terá financiamento próprio dos pesquisadores e custará R$ 10.000,00. Pendência 2 (atendida)– Em resposta de 10/11/17 os pesquisadores apresentaram o modelo de carta de envio atualizada. Pendência 3 (atendida)– Em resposta de 10/11/17 os pesquisadores apresentaram o modelo ajustado de TCLE a ser utilizado na pesquisa.

Recomendações:

RECOMENDAÇÃO 1- Após a aprovação do protocolo de pesquisa os pesquisadores devem atentar para a necessidade de envio de relatórios parciais de atividade (no mínimo um a cada 12 meses) e do relatório final de atividade (ao término da pesquisa). RECOMENDAÇÃO 2- Reforça-se a necessidade do registro, na forma de Biorrepositórios ou Biobancos, dos materiais biológicos coletados que venham a ser estocados para uso futuro, tanto no projeto quanto na declaração dos pesquisadores e de registrar a intenção no TCLE que será assinado pelo participante. RECOMENDAÇÃO 3- Os pesquisadores devem atentar para a necessidade de aplicação de TCLE para coleta de amostras a serem estocadas em Biobancos e Biorrepositórios e para a necessidade de aplicação de novo TCLE quando da realização de novas pesquisas com o material estocado. RECOMENDAÇÃO 4- Pesquisas com dentes doados por profissionais de saúde ainda são toleradas em hipótese pelo CEP-FOP, mas os pesquisadores devem estar cientes de que esta solução dista do ideal ético de consulta direta ao participante por meio de TCLE específico da pesquisa ou da obtenção dos dentes a partir de um Biobanco de dentes e que estas últimas situações deveriam ser escolhidas em substituição à primeira. RECOMENDAÇÃO 5- Destaca-se que o parecer consubstanciado é o documento oficial de aprovação do sistema CEP/CONEP e os certificados emitidos pela secretaria do CEP-FOP, a pedido, após a aprovação final do protocolo, só têm valor simbólico e devem ser evitados. RECOMENDAÇÃO 6- Intercorrências e eventos adversos devem ser

relatados ao CEP-FOP por meio da PB. RECOMENDAÇÃO 7- Eventuais mudanças pretendidas no protocolo devem ser comunicadas como emendas ao CEP por meio da PB. RECOMENDAÇÃO 8- O parecer do CEP-FOP é fortemente baseado nos textos do protocolo encaminhado pelos pesquisadores e pode conter inclusive trechos transcritos literalmente do projeto ou de outras partes do protocolo. Trata-se, ainda assim, de uma interpretação do protocolo. Caso algum trecho do parecer não corresponda ao que efetivamente foi proposto no protocolo, os pesquisadores devem se manifestar sobre esta discrepância. A não manifestação dos pesquisadores será interpretada como concordância com a fidedignidade do texto do parecer no tocante à proposta do protocolo.

Conclusões ou Pendências e Lista de Inadequações:

Não há mais pendências por resolver.

Considerações Finais a critério do CEP:

Parecer de aprovação de Protocolo emitido "ad referendum" conforme autorização do Comitê na reunião de 05/04/2017. Será submetido para homologação na reunião de 06/12/2017.

Este parecer foi elaborado baseado nos documentos abaixo relacionados:

Tipo Documento	Arquivo	Postagem	Autor	Situação
Informações Básicas do Projeto	PB_INFORMAÇÕES_BÁSICAS_DO_PROJETO_1012917.pdf	10/11/2017 10:47:41		Aceito
Outros	Respostaparecer.pdf	10/11/2017 10:47:09	JAIRO MATOZINHO CORDEIRO	Aceito
Outros	2Cartadeenvio.pdf	10/11/2017 10:44:05	JAIRO MATOZINHO CORDEIRO	Aceito
TCLE / Termos de Assentimento / Justificativa de Ausência	5TCLE.pdf	10/11/2017 10:42:36	JAIRO MATOZINHO CORDEIRO	Aceito
Outros	CEPcompleto.pdf	23/10/2017 11:19:13	Leny Cecilia Faro Pereira	Aceito
Declaração de Instituição e Infraestrutura	64DecInfra.pdf	23/10/2017 09:49:49	JAIRO MATOZINHO CORDEIRO	Aceito
Declaração de Instituição e Infraestrutura	62DecInst.PDF	23/10/2017 09:49:27	JAIRO MATOZINHO CORDEIRO	Aceito
Declaração de Pesquisadores	61DecPesq.PDF	23/10/2017 09:48:59	JAIRO MATOZINHO CORDEIRO	Aceito

UNICAMP - FACULDADE DE ODONTOLOGIA DE PIRACICABA DA

Continuação do Parecer: 2.387.521

Outros	4comentarios.pdf	23/10/2017 09:48:08	JAIRO MATOZINHO CORDEIRO	Aceito
Projeto Detalhado / Brochura Investigador	3Projeto.pdf	23/10/2017 09:47:03	JAIRO MATOZINHO CORDEIRO	Aceito
Folha de Rosto	1Folhaderosto.PDF	23/10/2017 09:44:47	JAIRO MATOZINHO CORDEIRO	Aceito

Situação do Parecer:
Aprovado

Necessita Apreciação da CONEP:
Não

PIRACICABA, 20 de Novembro de 2017

Assinado por:
jacks jorge junior
(Coordenador)

Endereço: Av.Limeira 901 Caixa Postal 52
Bairro: Areião **CEP:** 13.414-903
UF: SP **Município:** PIRACICABA
Telefone: (19)2106-5349 **Fax:** (19)2106-5349 **E-mail:** cep@fop.unicamp.br

Anexo 3 – Verificação de originalidade e prevenção de plágio

Tese_Doutorado

ORIGINALITY REPORT

22%	16%	14%	5%
SIMILARITY INDEX	INTERNET SOURCES	PUBLICATIONS	STUDENT PAPERS

PRIMARY SOURCES

1	repositorio.unicamp.br Internet Source	6%
2	Jairo M. Cordeiro, Bruna E. Nagay, Caroline Dini, João G.S. Souza et al. "Copper source determines chemistry and topography of implant coatings to optimally couple cellular responses and antibacterial activity", Materials Science and Engineering: C, 2021 Publication	5%
3	Ricardo Serôdio, Sónia L. Schickert, Ana R. Costa-Pinto, Juliana R. Dias, Pedro L. Granja, Fang Yang, Ana L. Oliveira. "Ultrasound sonication prior to electrospinning tailors silk fibroin/PEO membranes for periodontal regeneration", Materials Science and Engineering: C, 2019 Publication	1%
4	Submitted to Universidade Estadual de Campinas Student Paper	1%
5	link.springer.com	